Eastern Mediterranean University

Department of Mechanical Engineering

Capstone Team Project

MECT 411

Name of Project: Gyrobike

Group Members:

18700707 Ahmed Hammouda

16701818 Hamza Katout

17701019 Mohammad Said

18701528 Mahmoud Al-Zamel

17700094 Rayan Darwiche

Supervisor: Assist. Prof. Dr. Babak Safaei

Semester: Spring 2020-2021

Submission Date: June 7, 2021

Abstract

The Gyrobike is unlike any other electric bike, as it is unique in an exemplary way. It includes an autonomous control system that allows the bike to maintain its upright posture regardless of whether the vehicle is moving or not. This is only possible through the rotation of a reaction wheel at the center of the bike, which uses angular acceleration for angle correction. The system is best represented as an underactuated, nonlinear mechanical system where the bike assumes the form of an inverted pendulum. Even though the Gyrobike can be modified to become a road motorcycle and function autonomously along with similar vehicles, its actual importance comes when dealing with similar nonlinear, electromechanical systems that depend on reaction wheels for balancing, such as satellites and humanoid robots. This report explains in detail the mechanical design, different operating subsystems, the standards followed, and a detailed cost analysis of the project.

Both the mechanical design and the control system are developed to optimize the response speed of the angular correction, making the main scope of this project revolve around the performance of the bike. Although the bike did manage to maintain its balance and reject some minor disturbances, the system was expected to handle higher forces in magnitude and more intense disturbance. This was due to inaccuracies in the mechanical design as well as the mathematical model which the control system was based on. Finally, the future work on the system would be to test the control system on models that assume the form of an inverted pendulum other than the gyrobike, such as satellites or drones.

Table of Contents

List of Figures

List of Tables

List of Symbols/Acronyms/Abbreviations

IMU: Inertial Measurement Unit

DC: Direct Current

RC: Remote Control

EMF: Electromotive Force

P: Proportional

PID: Proportional Integral Differential

MDF: Medium-Density Fiberwood

RHS: Right Hand Side

LHS: Left Hand Side

USD: United States Dollars

TX: Transmit

RX: Receive

PLA: Polylactic Acid

ABS: Acrylonitrile Butadiene Styrene

SAE: Society of Automotive Engineers

ISO: International Organization for Standardization

CNC: Computer Numerical Control

IEEE: Institute of Electrical and Electronics Engineers

LQR: Linear Quadratic Regulator

DIN: Deutsches Institut für Normung

Chapter 1

Introduction

1.1 Defining the Gyrobike

The gyrobike is a two-wheeled vehicle much like any other motorcycle. However, its name derives from its ability to maintain its upright balance at all times, regardless of the vehicle's speed. Even if the bike is parked and with a passenger on board, it will be capable of maintaining its posture using the autonomous control system built into the motorcycle. Figure 1 shows the entire vehicle along with the control system.

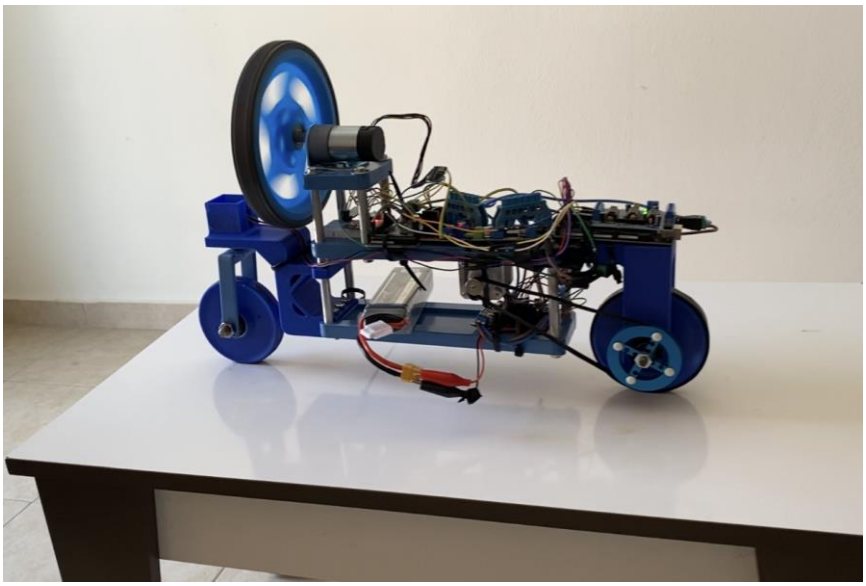

Figure 1: The Gyrobike

The gyrobike includes two main systems that function simultaneously in order to achieve its purpose. The first is the control system, which comprises the reaction wheel, the encoder DC motor, an Arduino microcontroller, and the Inertial Measurement Unit (IMU). Simply put, the IMU is an electronic device that measures and reports a body's specific force, angular rate, and sometimes the orientation of the body, using a combination of accelerometers, gyroscopes, and

sometimes magnetometers [1]. So, its pickup angle-tilt readings and signals the microcontroller that the bike is falling over. The Arduino then performs the necessary calculations and indicates the appropriate torque that the motor must provide in order for the reaction wheel to correct the angle error. The second subsystem in the vehicle is the Remote Control (RC) system Radio-controlled cars (or RC cars for short) are miniature model cars or trucks that can be controlled from a distance using a specialized transmitter or remote [2], which is responsible for moving and steering the bike. This system consists of two permanent magnet DC motors which is a class of rotary electrical motors that converts direct current electrical energy into mechanical energy [3]. (one for power and the other for steering), another Arduino microcontroller, and a Bluetooth module for wireless connectivity. The remote control would be used to communicate with the Bluetooth module mounted on the microcontroller to move the bike and steer it.

1.2 Significance of the Project

The success of a project such as the gyrobike strongly impacts our much autonomous world. Bikers all around the world are more susceptible to accidents than passengers of any other type of vehicle. The gyrobike's control system that prevents it from falling can protect bikers from hundreds of road surprises and hazards. It would allow for sharper turns, quicker bike acceleration, and any other maneuver that would lead to the driver falling off a traditional motorcycle. Furthermore, the applications don't stop there. By further modifying the gyrobike to make a complete robot (meaning that it would function without any human interaction), the vehicle could be used to transport both goods and non-driving passengers.

Besides these traditional uses of the project, the gyrobike is part of something much greater and much more important. The control of the bike is best represented as balancing an

inverted pendulum, only now the pendulum is in constant motion along with steering. This project serves as a leap in nonlinear, underactuated mechanical systems that use reaction wheels for control. Other examples of such control systems that can be modified using models from the gyrobike are satellites, humanoid robots, and submarines. Figure 2 shows a reaction wheel system that is used for controlling the satellite's attitude in its orbit around Earth.

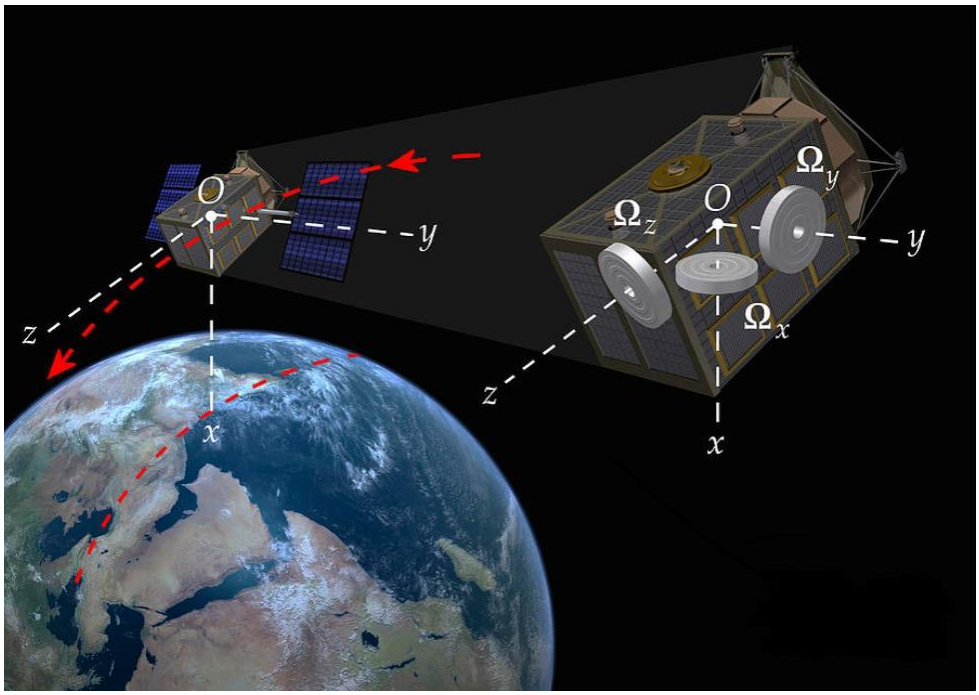

Figure 2: Reaction Wheels in Satellite Attitude Control

1.3 Project Objectives

1.3.1 Design for Performance:

The main objective of this project is to control the gyroscopic balance of a bike using a DC motor and a reaction wheel as the system actuators. This control system should not only serve to keep the motorcycle upright, but should also do so in the least amount of time with the lowest overshoot possible. In order to do so, different controllers such as proportional (P) controller, proportional integral differential (PID) controller which is an instrument used in

industrial control applications to regulate temperature, flow, pressure, speed and other process variables. PID (proportional integral derivative) controllers use a control loop feedback mechanism to control process variables and are the most accurate and stable controller [4], and a full-state feedback controller would be used to monitor factors such as the rise time and settling time of the system.

1.3.2 Design for Cost:

Even though the main objective of this project is to optimize the performance of the gyrobike, many cutbacks had to be made to make the financial requirements meet the budget. These reductions even affected the efficiency of the control system. However, most reductions were done in the mechanical design as topology optimization to save materials, money, and even reduce the mass of the bike and boost control. These factors definitely make the bike's design a reduction of costs and a partial optimization of performance.

1.4 Constraints

Constraints are always present on any engineering project, but they are even more so on a student lead project. There are multiple limitations that had to be taken into account:

1.4.1 Financial Constraints

All engineering projects have financial constraints that limit the performance that could be achieved, much more in a student-lead project. However, proving just the concept of the gyrobike includes only building a small model, which includes a budget of around 800 USD.

1.4.2 Environmental Constraints

One of the gyrobike's outstanding qualities is its ability to function without the use of fuel like a traditional bike. Even though much of the chassis is made of polymers, recycling any broken parts along with other plastics makes the gyrobike an eco-friendly vehicle.

1.4.3 Availability Constraints

The materials and manufacturing processes that were selected for this project were chosen while taking into consideration the availability of such processes in Northern Cyprus. Even though they are not the most common, PLA, MDF, and CNC milling are all available in Cyprus.

1.4.4 Health and safety Constraints

One of the safety concerns in the project is the high current that is required to deliver high torque through the reaction DC motor. Electrical circuits must be safely concealed and out of reach while the vehicle is running.

1.4.5 Reliability Constraints

The gyrobike is a fairly new concept that is still being introduced into the engineering world. Along with the fact that it is an underactuated, highly nonlinear mechanical system, the vehicle might not be as reliable as other vehicles that have been around for decades. Plenty of research must still be carried out in the field of inverted pendulums to increase the system's reliability.

1.4.6 Manufacturability Constraints

The mechanical workshop is the optimal place to assemble the vehicle once it has been manufactured. The production will mostly involve 3D printing, wood trimming, and screwing. All processes are readily available and can be adequately carried out.

1.5 Report Organization

This report includes a detailed explanation of the mechanical design, the control system, the remote control system, the manufacturing process, and the cost analysis of the gyrobike. Chapter 2 is the literature review, and gathers most of the previous work done in the control of underactuated mechanical systems in the form of inverted pendulums. Chapter 3 gathers the details of both subsystems along with the detailed mechanical design of the bike. It also includes all the project calculations, the engineering standards integrated in this project, and the cost analysis of the components and the manufacturing of the bike.

Chapter 4 revolves around the manufacturing process used and the steps taken to produce and assemble the gyrobike. These steps include the Pugh criteria matrix for material selection. Finally, chapter 5 includes the steps that should be taken in the future in order to verify the performance of the vehicle. More so, it includes what tests should be carried out to ensure that the engineering standards indicated in this report have been followed adequately.

Chapter 2

Literature Review

This chapter introduces some background information on inverted pendulums and describes the previous work done in controlling reaction wheels. These reaction wheels are used precisely in order to manage systems that assume the form of inverted pendulums and are susceptible to instability.

2.1 Background Information

The problem of balancing an inverted pendulum is not new in control theory, as it has been a benchmark for testing control strategies over the previous century. This problem that engineers and mathematicians have been dealing with for decades is quite simple to understand. It includes maintaining an inverted pendulum upside down at an upright position and overcoming any disturbance forces that might lead the pendulum to fall over. As simple as it may seem, there has not been an optimal solution to this problem to this day. The classical solution to the problem usually involves a cart or an arm in the case of a Furuta pendulum [5]. However, the introduction of the reaction wheel to this common problem helps shed a new light on control laws in optimal control theory. The reaction wheel can help balance most systems that are susceptible to instability, and has already been a crucial part in the functioning of satellites and drones for stability without requiring fuel. This phenomenon is best described by the system in Figure 3.

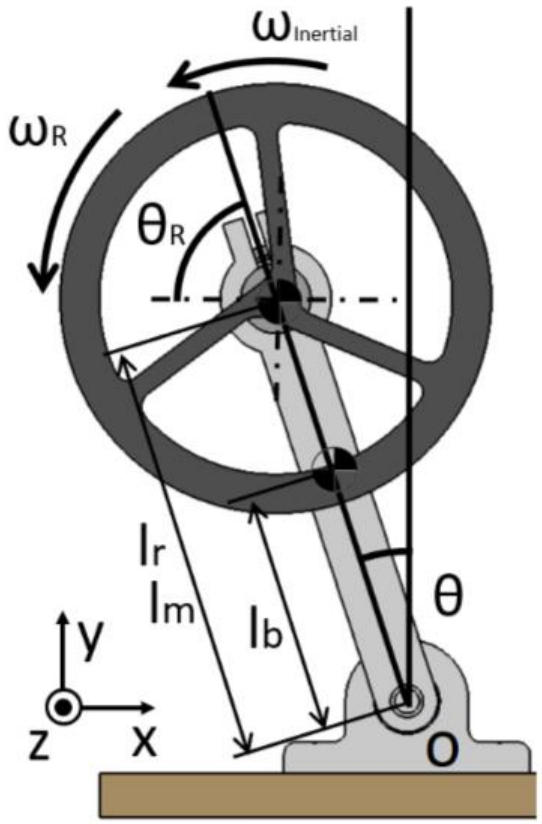

Figure 3: The inertia wheel pendulum

2.2 Concurrent Solutions

2.2.1 Balancing an Inverted Pendulum on a cart

In 2017, four professors from Tokyo University by the names of Murata, Moran, Hayase and Mat-suno observed the nonlinear characteristics of an inverted pendulum mounted on a cart [6]. As portrayed in Figure 4, the correction of any disturbances to the posture of the pendulum were corrected using the movement of the cart in the respective direction, and the cart's motion could be controlled by DC motors located either at the wheels of the cart or controlling a belt attached to the cart. However, after observing the nonlinear characteristics of the system, the researchers discovered that the slipping of the cart's wheels lead to inaccuracies in the relative

position of the cart in the assumed position of the cart relative to its actual position. This problem applies only to pendulum-balancing using linear carts.

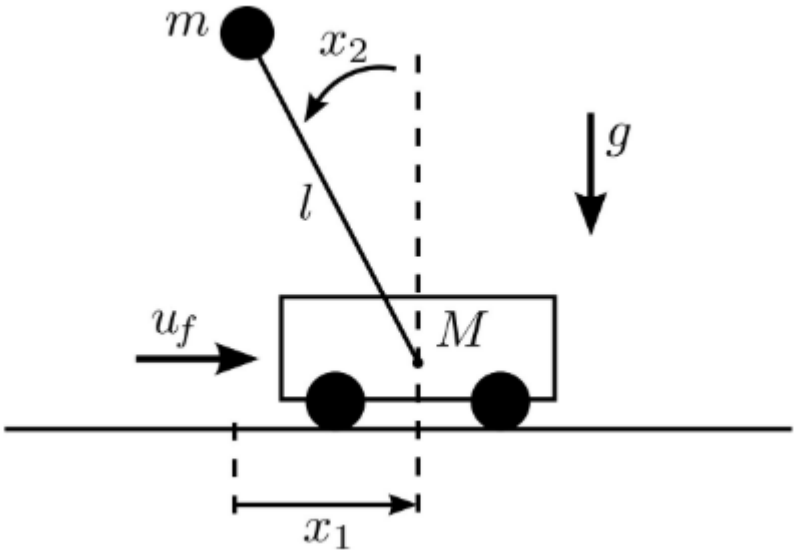

Figure 4: Inverted pendulum mounted on a car

2.2.2 Balancing an Inverted Pendulum in a cube form

Ramm and Sjostedt explored the applicability of using a reaction flywheel in balancing an inverted pendulum in the form of a cube [7]. However, the scope of the project was not to achieve the balance of the pendulum, but to investigate the different potential positions of the inertial measurement unit (IMU) to reduce the error to a minimum. The designed structure was one degree of freedom system that included an Arduino-controlled permanent magnet DC motor that acts upon readings gathered from the IMU. Figure 5 shows the complete system. After observing six different positions of the IMU, Alexander and Mikael concluded that the best possible location for the sensor was the furthest away from the motor and flywheel. They explained this concept by stating that the closer the IMU was to the front frame of the cube and the motor, the more the induced magnetic field contributed to the noise read by the sensor. Therefore, the optimal location of the IMU that provided the pair with the most accurate readings

was position B in Figure 6; the furthest away from the DC motor. Nevertheless, Alexander and Mikael had complete freedom over placing the sensor in different locations since the cube would not move in a second plane, making their design of an inverted pendulum somewhat limited.

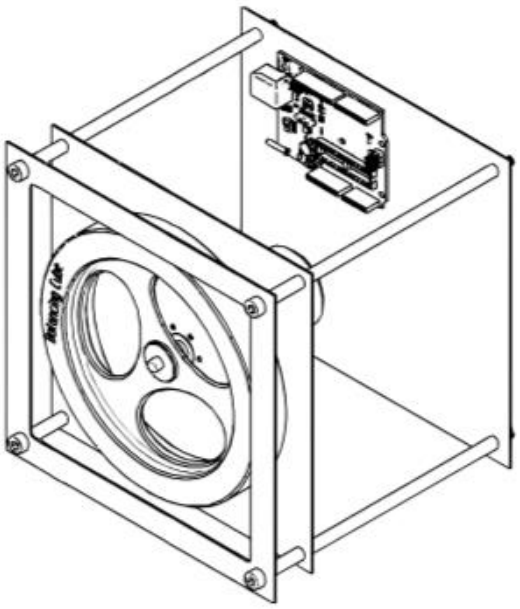

Figure 5: Cube-Form Inverted Pendulum

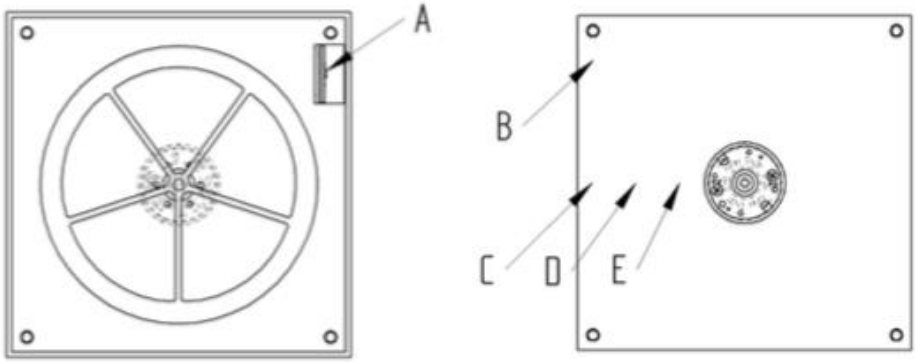

(a) IMU placement, front

(b) IMU placement, back

Figure 6: IMU Placement

2.2.3 The Furuta Pendulum

In their research paper “On the Dynamics of the Furuta Pendulum,” Cazzolato and Prime observed the third way of controlling and stabilizing inverted pendulums [8]. The Furuta pendulum consists of a driven arm which rotates in the horizontal plane and a pendulum attached to that arm which is free to rotate in the vertical plane [9], demonstrated in Figure 7. The pendulum was first developed at the Tokyo Institute of Technology by Furuta and his colleagues. Since then, dozens, possibly hundreds of papers and these have used the system to demonstrate linear and nonlinear control laws. However, new studies are currently being conducted on how to embed the concept of machine learning in order to stabilize the pendulum using nonlinear control laws. Anyhow, the problem with the Furuta pendulum arises when the arm along with the pendulum accumulates a heavy mass. The DC motor must be powerful enough to overcome both weights and force the horizontal arm into motion, which will then stabilize the vertical arm.

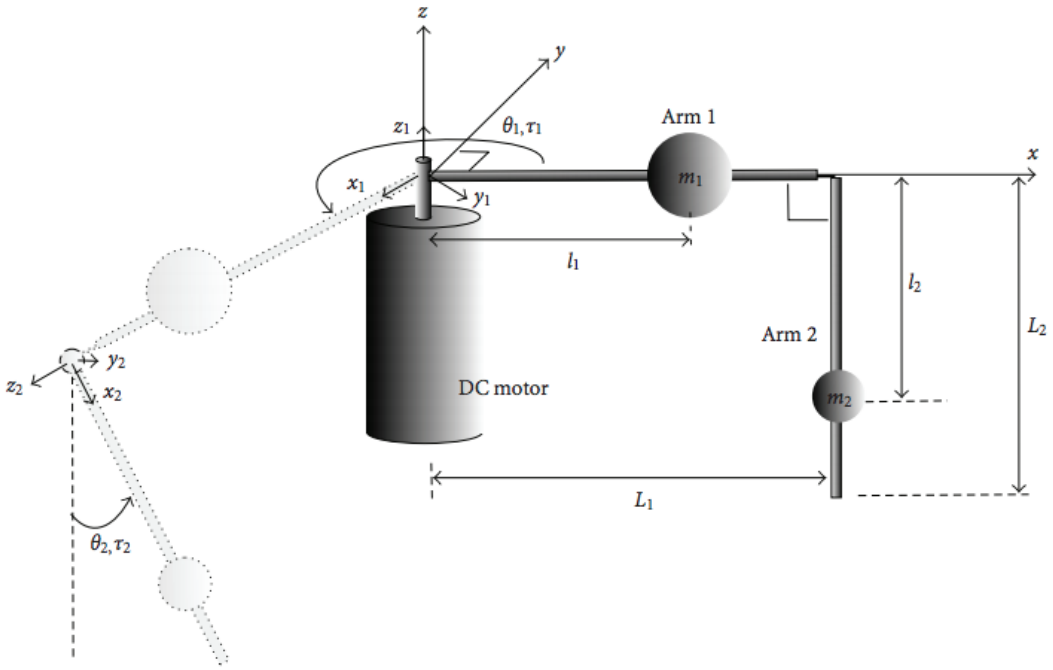

Figure 7: The furuta pendulum

2.3 Comparison of Concurrent Solutions

In this subchapter, the different forms of pendulum stabilization techniques are compared and analyzed. Even though the cart and Furuta pendulum prove efficient in systems that experience high disturbance force magnitudes, the reaction wheel pendulum is most accurate with angle corrections if the proper control system is used. In addition, the reaction wheel pendulum can be embedded into systems that are already in motion, for instance the Gyrobike. Since the cart pendulum already requires linear motion as part of its control mechanism, it is almost impossible to include as part of a bigger dynamic system. This contrast is summarized in table 1. In conclusion, using a reaction to stabilize the Gyrobike is perhaps the most efficient and accurate method in controlling the system.

Table 1: Comparison of Concurrent Solutions

Pendulum\Property	Motion	System Type	System State
Inertia Wheel Pendulum	Rotary	Can be embedded into almost any inverted pendulum	The entire system can be in motion
Furuta Pendulum	Rotary	Can be embedded into any pendulum around fixed point	System must have a fixed point
Cart Pendulum	Linear	Can only be embedded if the entire pendulum is in motion	System must have a fixed point

2.4 Engineering Standards of Concurrent Solutions

The following engineering standards are those that apply to all control systems of inverted pendulums regardless of the method of control.

- ISO 21940-31:2013 Mechanical Vibration — Rotor Balancing
- ISO 2953:1985 Balancing Machines — Description and Evaluation

- ISO 17409 Electrical Propelled vehicles –Connection to an external electric power supply – Safety requirements

Chapter 3

Design and Analysis

3.1 Proposed Design

3.1.1 Mechanical Design

The mechanical design of the gyrobike consists of four main parts: the front wheel, the balance/reaction wheel, the base, and the back wheel. This applies not only to the final design, but also to the preliminary design configurations included in this report. The final design is displayed in Figure 8.

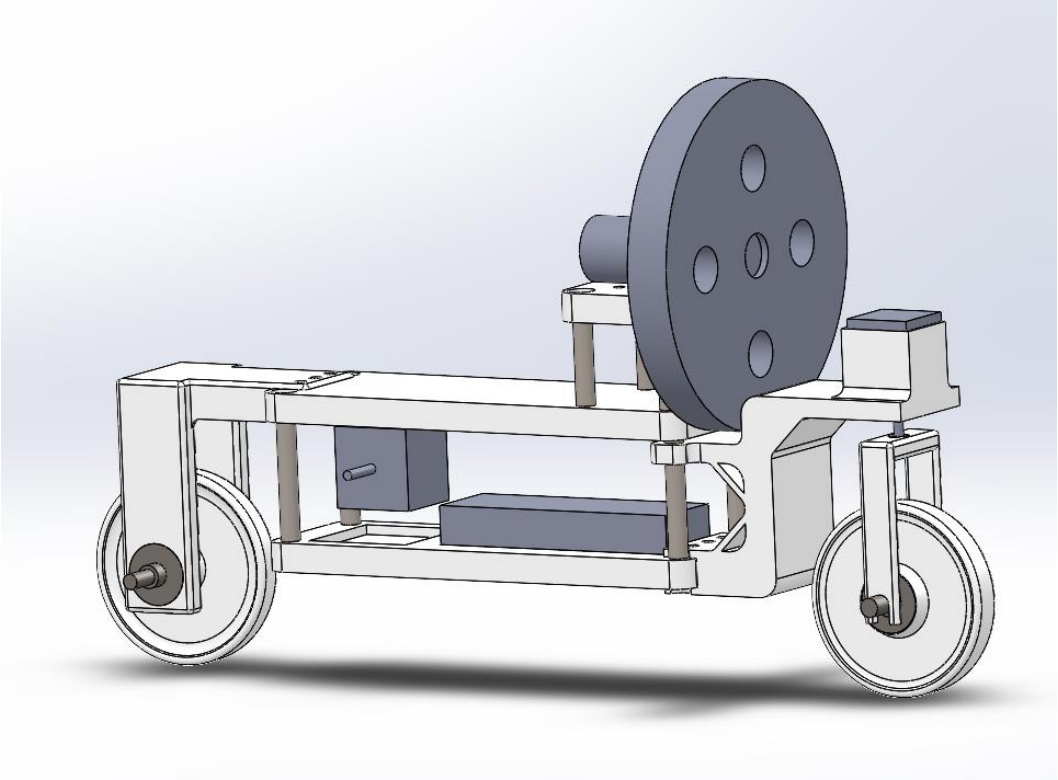

Figure 8: Final Design

3.1.1.1 The Base

The base consists of three main shelves (or planks). The first and lowest shelf in Figure 9 is used to carry the battery.

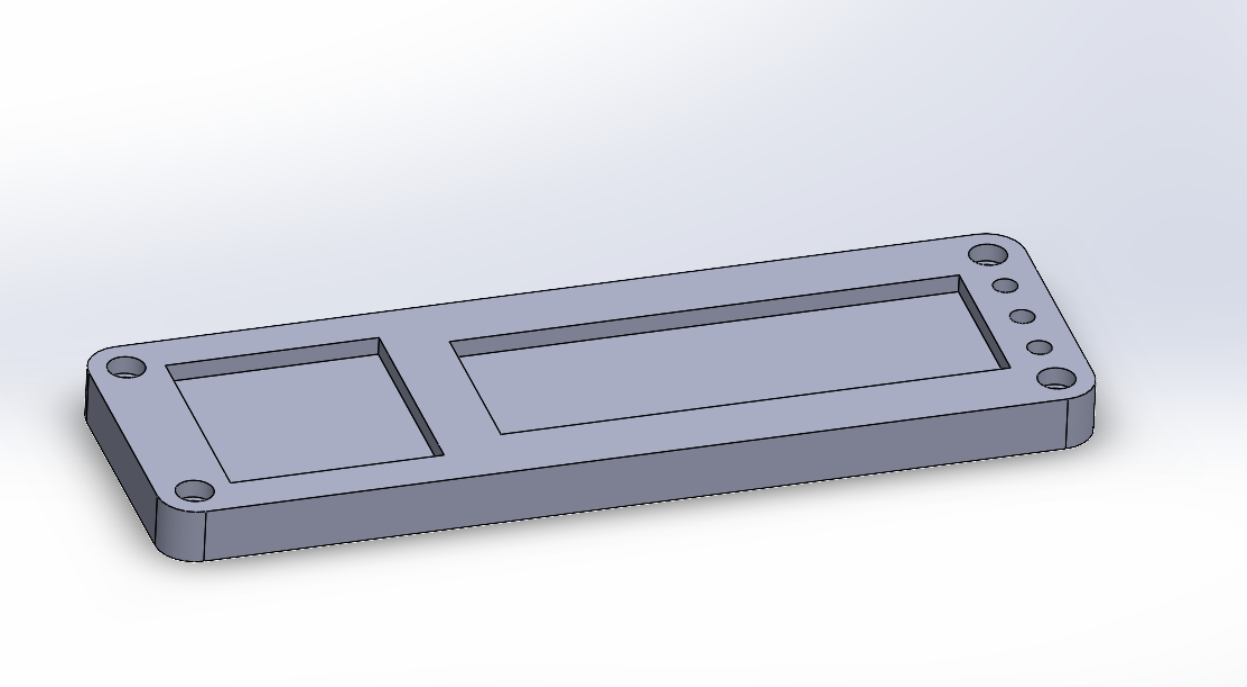

Figure 9: Battery Shelf

The battery shelf takes the shape of a thin long rectangle with the dimensions of 80x250mm and thickness of 15mm on the top of the shelf there are two smaller sockets with dimensions of 57x57x5mm and 136x45x5mm , that are made to hold the battery an the stepper motor respectively however since the stepper motor was changed after the design was printed the second socket is used to hold the motor driver, in addition to that there are holes with diameter of 10 to hold the support beams on each corner and on the front side there are screw holes to connect it to the front wheel.

Figure 10 shows the second shelf is used to carry the rest of the electrical components, and is where most of the wiring in the system will be done. Similar to the first shelf, this one also has the same dimension but without the sockets since it was not necessary, in addition to that

there are the support beam holders on the front while on the back corners there are the screw holders for the support beams of the first shelf that is used to make the design sturdier and the screw holes in between them that is used to connect the main base to the back wheel.

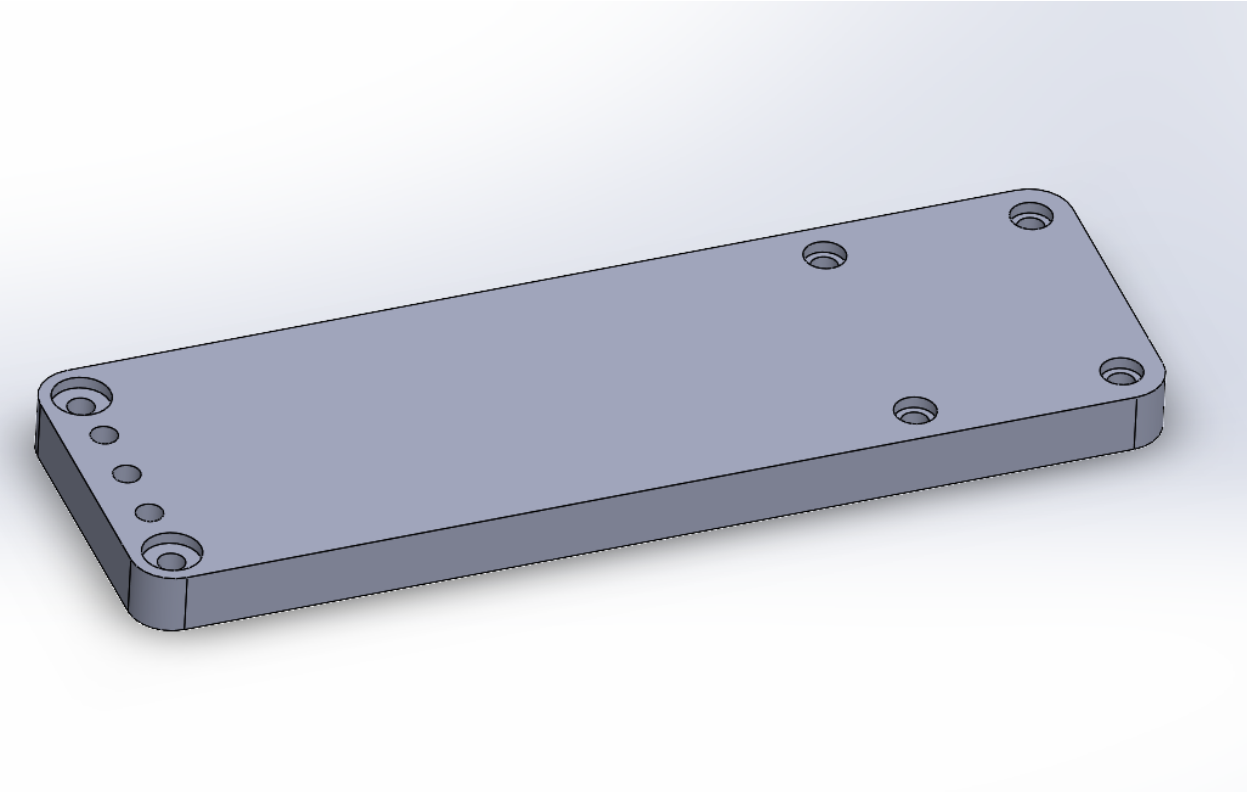

Figure 10: Breadboard Shelf

Since the shape of the motor that is used to spin the balance wheel is different from the shape of the batteries and the breadboard, the team had to design a different support system for it, as portrayed in Figure 11.

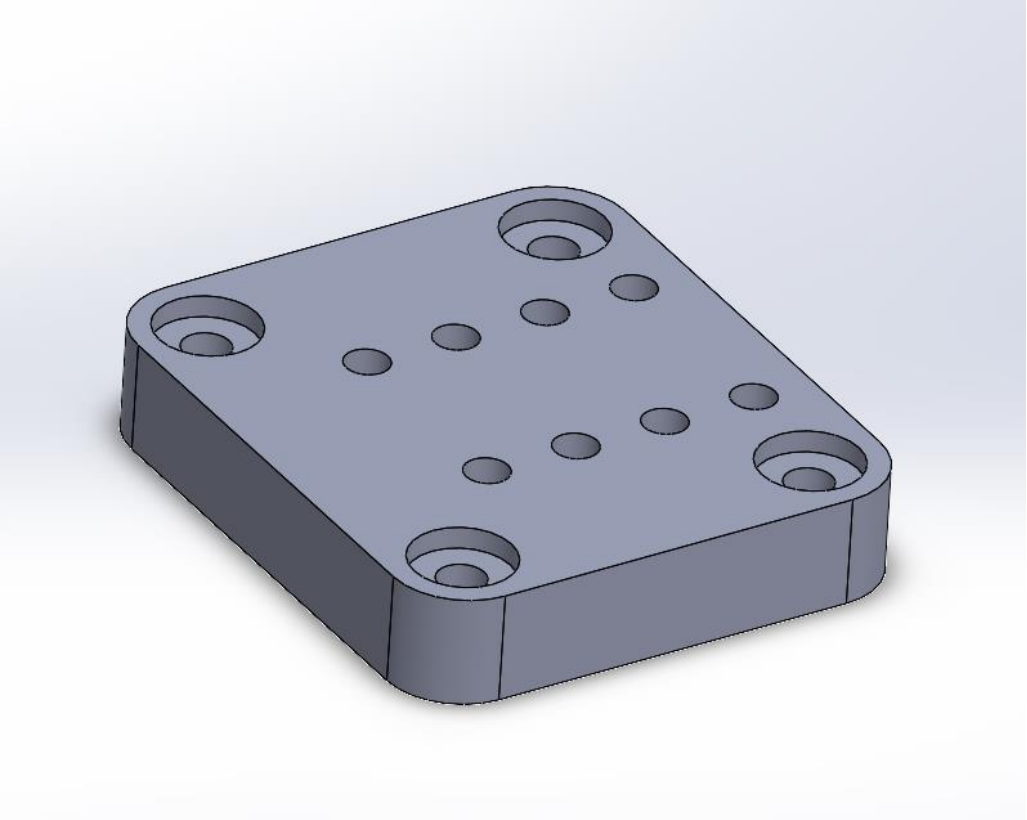

Figure 11: Motor Shelf

The dimensions of the motor shelf is 80x70x15mm which is considerably smaller than the other two shelves since it's only holds the motor that connects to the balance wheel so in addition to the support beam holes on each corner there are smaller screw holes in the middle to stabilize the motor holder to the shelf.

Between the each of the three shelves is places a set of four beams, as shown in Figure 12.

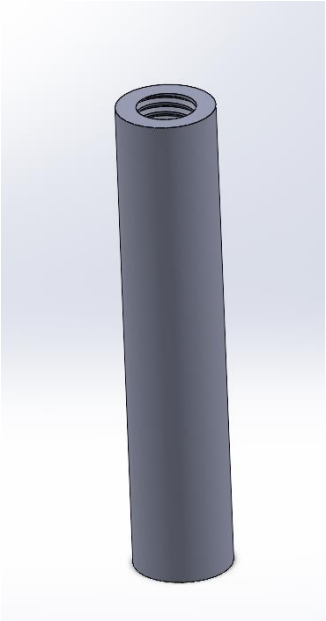

Figure 12: Beam

The dimensions of the beams that are placed between the base and components shelf are 10 mm in diameter and 70 mm in length with a M6 Tapped hole on both sides that has a diameter of 6 mm and length of 25 mm and between the components to the shelf the dimensions are also 10mm diameter but with 50mm in length and similarly to the first set it also has an M6 tapped hole on both sides with a diameter of 6mm but it has 15mmin length.

3.1.1.2 Balance Wheel

The balance wheel is the simplest yet probably one of the most important parts of this vehicle, since it is the one that will do the actual balancing. Its size of 180mm outer diameter and 5mm inner diameter to hold the shaft and weighing 270g respectively are the two most essential parameters that relate directly to the control system. Figure 13 shows a simple wheel design that

was used and is connected directly to the DC motor from one side and to the optical encoder from the second side.

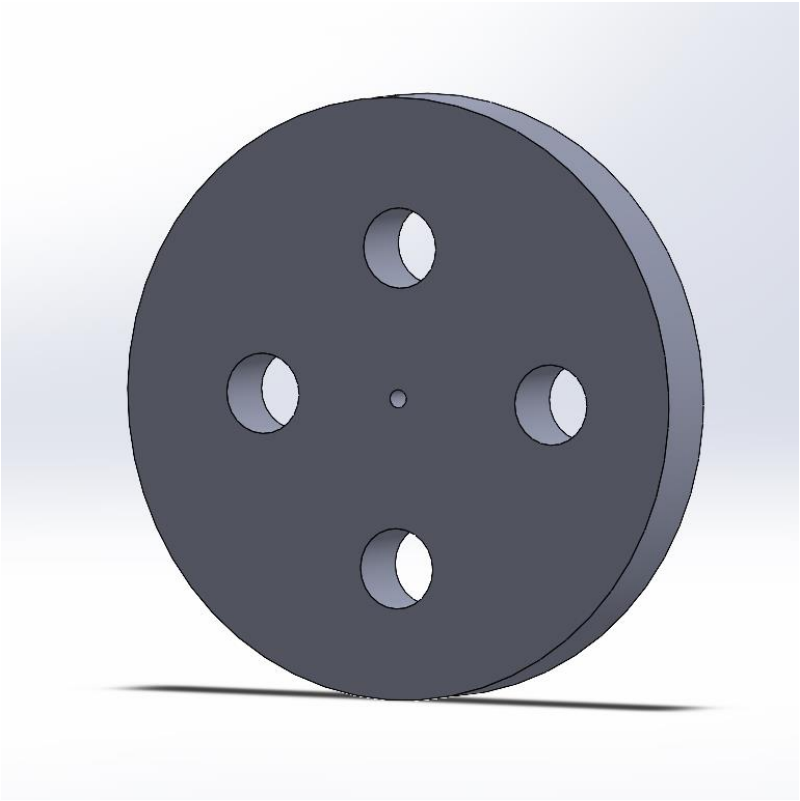

Figure 13: Balance Wheel

3.1.1.3 Front Wheel

The front-wheel consists of four main parts: the first is the front wheel connection which is used to connects the pieces between the base and the rest of the front wheel system, the second is the wheel holder that connects the front connector to the wheel and shaft, the third is the front shaft which is used to hold the front wheel to the wheel holder and finally the fourth is the wheel itself. The attachment is established using the connector in Figure 14.

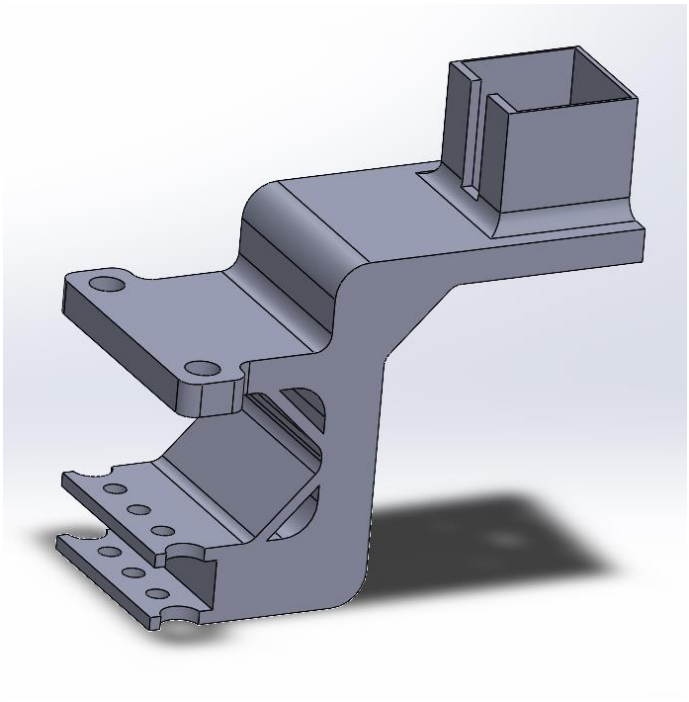

Figure 14: Front Wheel Connection

The connection fragment is used to connect the front wheel with the main base. This part is connected to the battery shelf of the base on one end, to the stepper motor that is connected to the front wheel on another end, in addition to that there is an extra shelf to support the connector and stop it from bending that connects to the front support beams of the system

The connector had to be carefully designed in order to avoid interfering with the reaction wheel. It includes a housing in order to insert the stepper motor that is used for turning the front wheel. Finally, the connector also has a few slots for screws in the battery shelf as well as the breadboard shelf to ensure it would not be detached from the main bike while it is moving.

The front wheel of the Gyrobike is a standard wheel with the connection in Figure 15 that allows the motor to twist the entire part along with the wheel for steering.

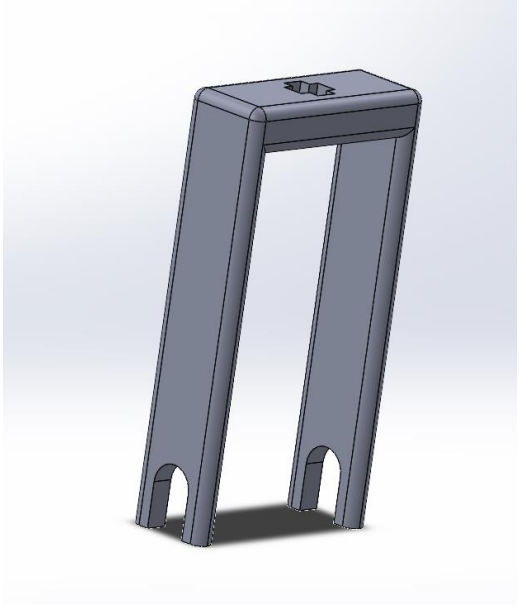

Figure 15: Front connector

The piece was designed with the dimension of the wheel and front shaft in mind in order to make sure that it will not interfere with the movement of the wheel, in addition to that there is a "keyhole" on the top of the piece that allows the stepper motor to be able to steer the front wheel, the "key" is shown in Figure 16.

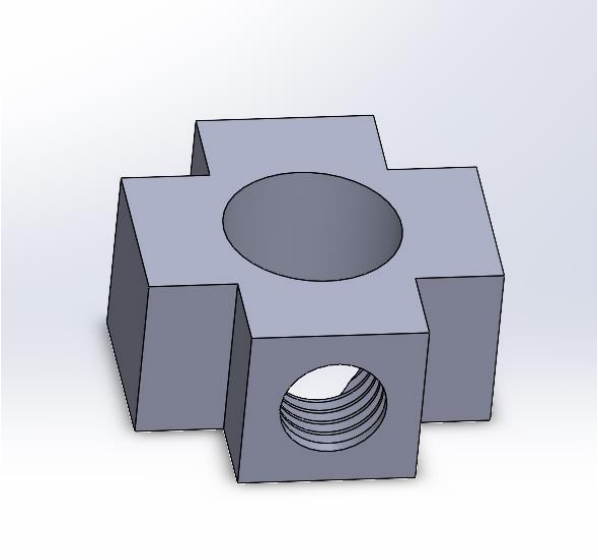

Figure 16 Key

The key was simply designed to fit between the stepper motor and the front wheel holder in order to make the steering from the small shaft of the stepper motor possible. Additionally, on one side there was a 3mm hole inserted with a #M Tapping to allow the set screw to enter.

In order to make it possible for the wheel holder piece to hold and move the wheel as intended it was essential that a wheel shaft to be designed and the front shaft can be seen in Figure 17.

Figure 17: Front shaft

The dimensions of the shaft were made in order to allow it to enter the open sides of the wheel holder and be able to fit the inner diameter of the wheel perfectly in order to make the wheel move in a stable way and on each of the sides a M10 threading was made along the shaft.

The front wheel is made with a simple design with an outer diameter of 100mm and an inner diameter of 21mm with a holder of the 6002RS bearing in the center of the wheel, the front wheel can be seen in Figure 18.

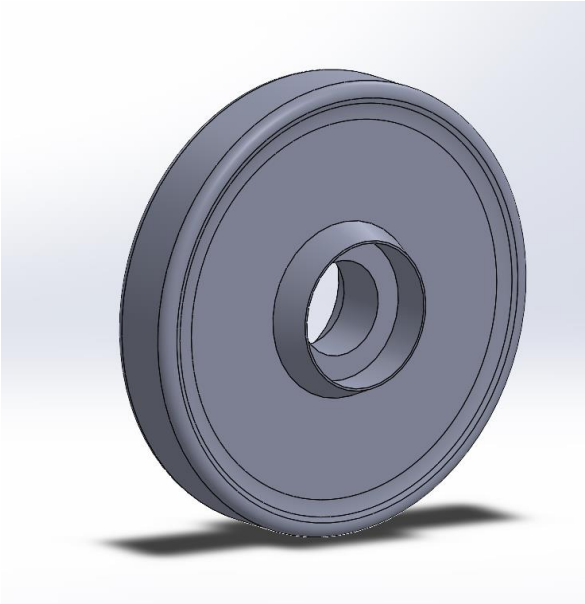

Figure 18: Front Wheel

3.1.1.4 Back Wheel

The back wheel section is divided into three main parts, which are: the back wheel connector, the back shaft and the wheel itself. The first of these pieces can be seen in Figure 19.

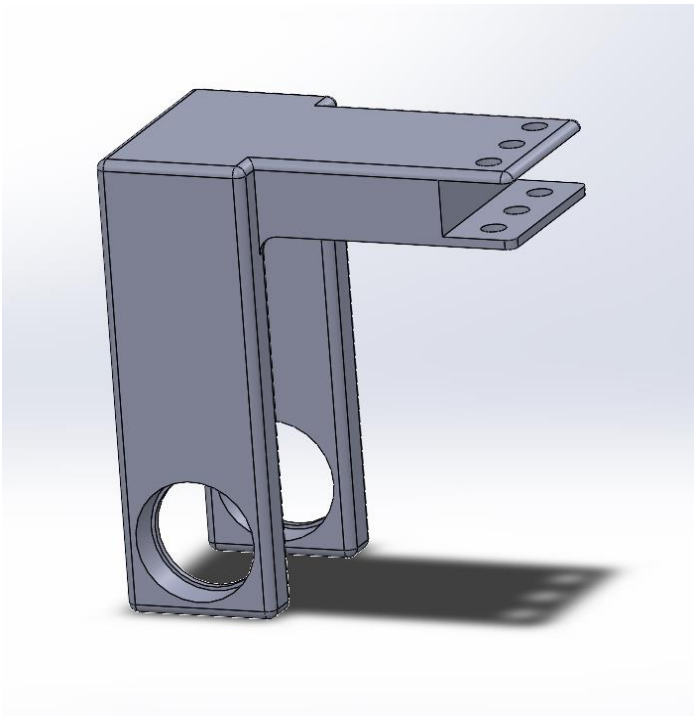

Figure 19: Back Wheel connector

The connector was designed to connect the component shelf from Figure 9 to the back wheels it also has two slots to fit the 6201 bearings in order to help the shaft spin easily and make the wheel turn for movement, also in order to ensure smooth movement the connector was designed to have enough space for the wheel and shaft to fit inside of it, and the shaft can be seen in Figure 20.

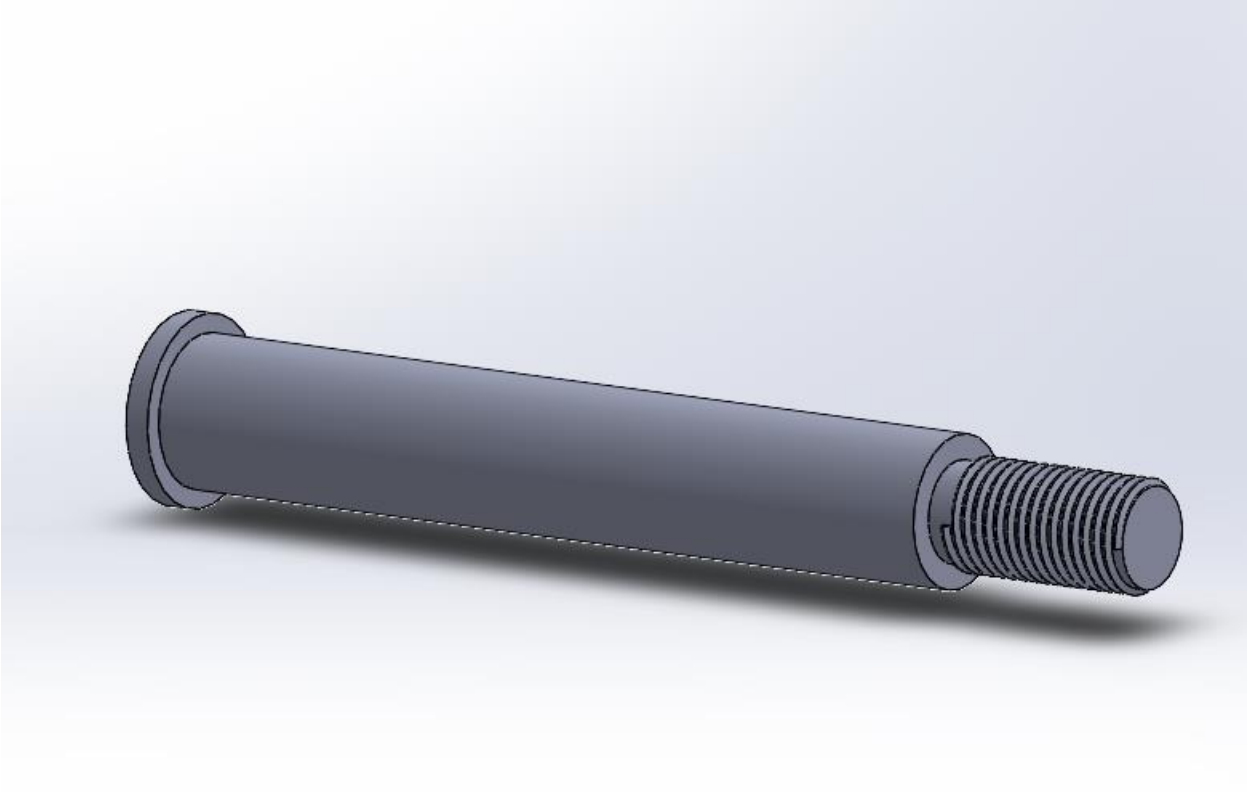

Figure 20: Back Shaft

The back shaft was designed with the purpose of allowing the back wheel to be able to move easily and steadily, this was done by making it fit perfect into the inner diameter of the wheel that is shown in Figure 21and the two bearings, the design also includes one tip that pops out of the back connector from the side in order to connect it to the belt that is attached to the stepper motor from the main base to allow it to move forwards or backwards, on the other tip a safety measure was placed in order to not have the shaft go through all the way and get disconnected, in addition to that a M8 threading was added to the side to help the belt holder to not fall off and allow the bike to move.

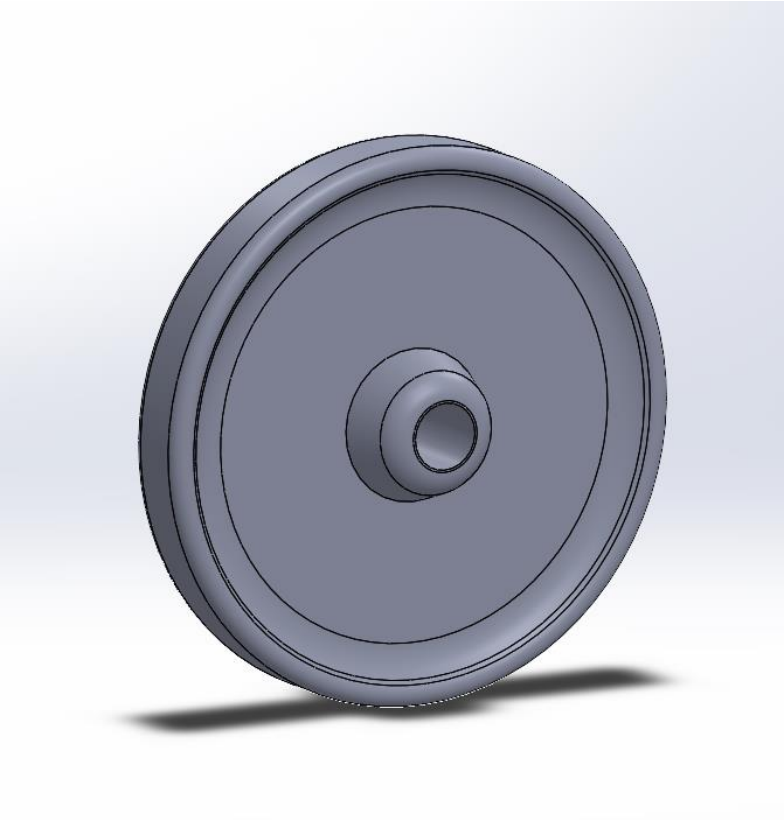

Figure 21: Back Wheel

The back wheel has one of the simplest designs in this project with an outer diameter of 100mm and an inner diameter of 12 mm.

3.1.1.5 Design Configuration 1

As for the first design configuration, the final design of this configuration is demonstrated in Figure 22.

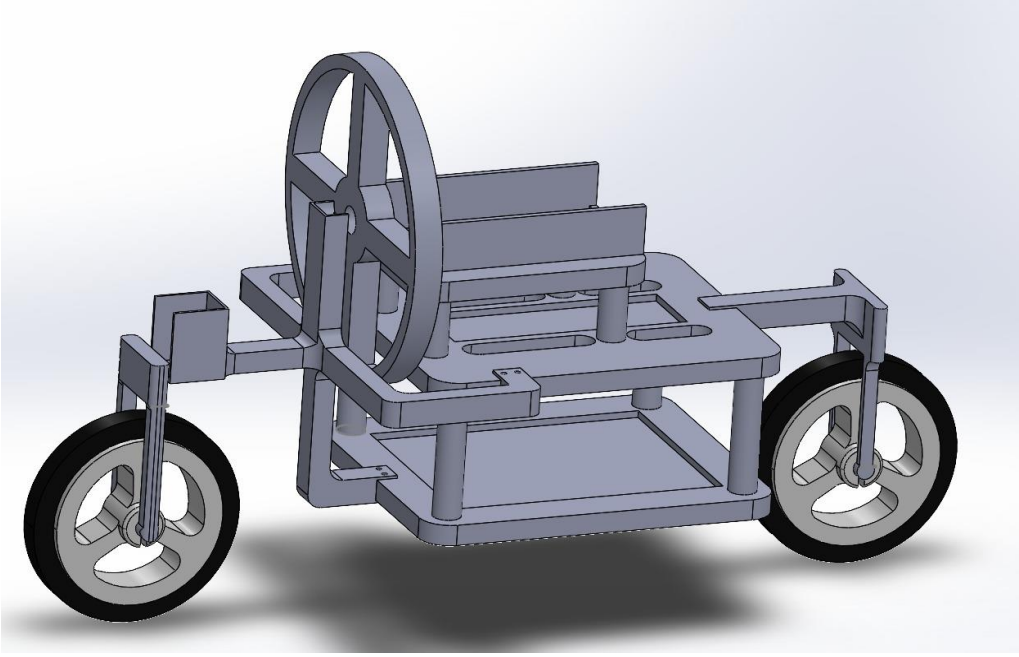

Figure 22: Design Configuration 1

3.1.1.6 First Configuration - The Base

The base consists of three main shelves (or planks). The first and lowest shelf in Figure 23 is used to carry the batteries.

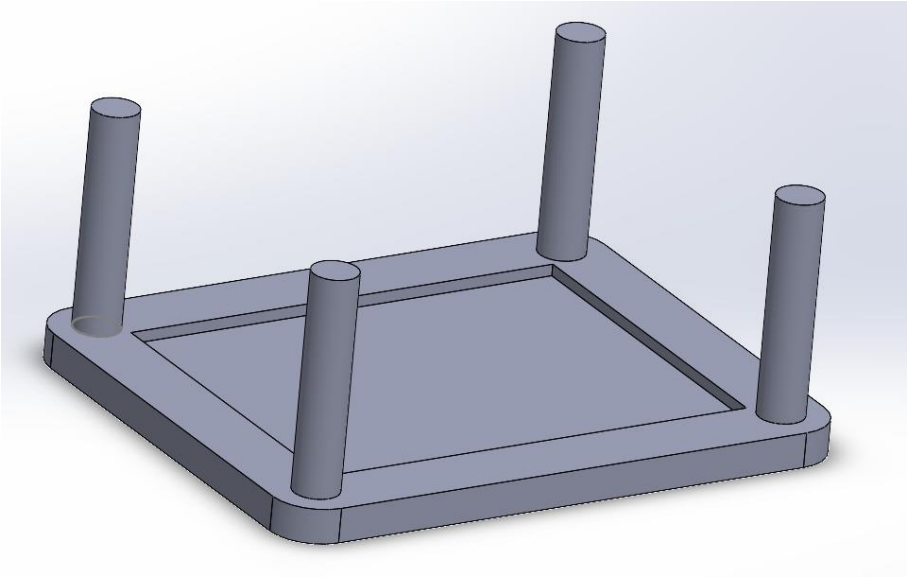

Figure 23: First Configuration - Battery Shelf

The battery shelf consists of two rectangles, one for carrying the batteries and one that works as a frame and helps hold the entire vehicle together. The inner rectangle has a size of 196x150mm, which is the size of two 12V batteries laid next to each other. As for the size of the frame, it is 216x171 mm and has a 10 mm radius circle on each of its four corners where the support beams are placed to carry the rest of the components. In addition, the battery and beams' support have a cut with the size of 5mm in order to help keep everything stable and in check, while the bike is moving around.

Figure 24 shows the second shelf is used to carry the breadboard, and is where most of the wiring in the system will be done. Similar to the first shelf, this one also consists of a breadboard holder and a frame, so the breadboard holder has a size of 55x170 mm while the outer frame also has a size of 171x216 mm and the same support system around the inner frame.

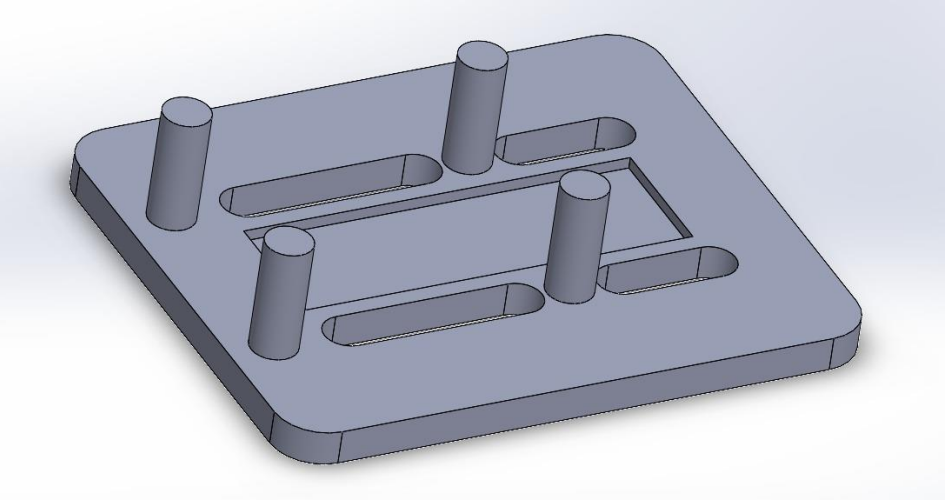

Figure 24: First Configuration - Breadboard Shelf

One of the main differences between the first and second planks is that there are pockets on the lower side of the shelf for the support beams extending from the first shelf to be placed in. In addition, four different holes are engraved into the plank to allow wires coming from the battery and encoder to pass through to the breadboard.

Since the shape of the motor that is used to spin the balance wheel is different from the shape of the batteries and the breadboard, the team had to design a different support system for it, as portrayed in Figure 25.

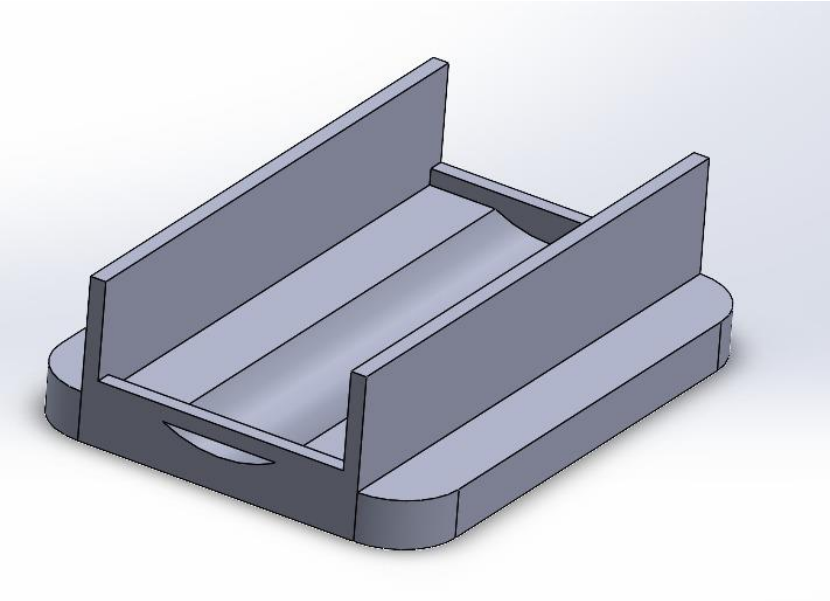

Figure 25: First Configuration - Motor Shelf

The same concept as before was applied as in having the frame engraved and the piece placed inside of it to help with stability. However, additional support shelves had to be added on the side to make sure that motor would not just roll off the sides as the machine is moving around, while also placing smaller supports on the front and the back to make sure that the motor would not fall off when the machine is navigating an inclined or a declined surface. Similarly, the other two shelves of the frame part have a size of 90x170 mm. Unlike the other two, this one only has the support beam pockets on the lower side since there is no need for it to be on top as well.

3.1.1.7 First Configuration - Balance Wheel

The balance wheel is the simplest yet probably one of the most important parts of this vehicle, since it is the one that will do the actual balancing. Its size and mass are the two most essential parameters that relate directly to the control system. Figure 26 shows a simple wheel design that was used and is connected directly to the DC motor from one side and to the optical encoder from the second side.

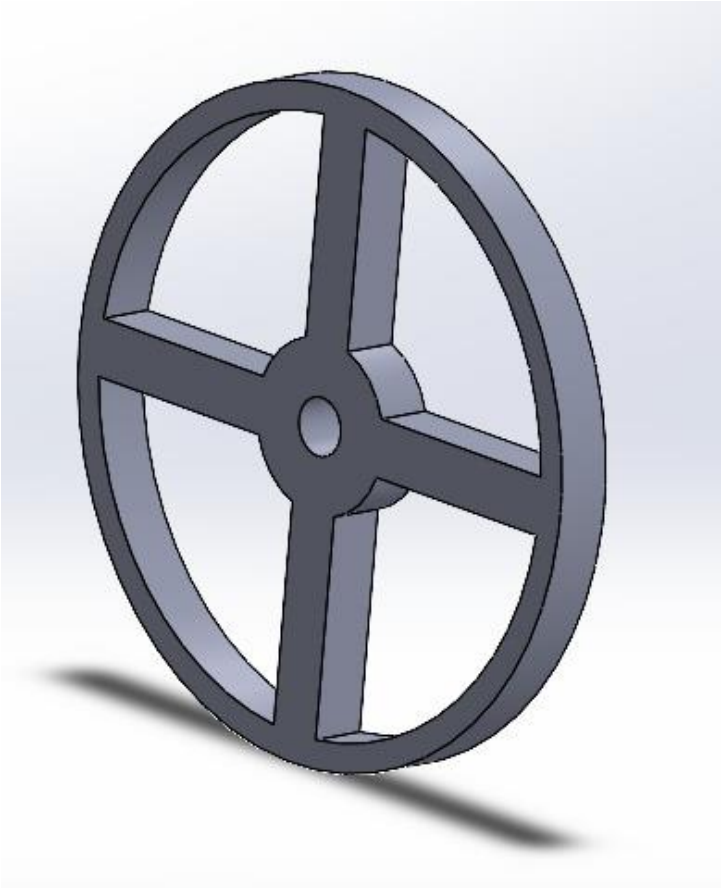

Figure 26: First Configuration - Balance Wheel

3.1.1.8 First Configuration - Front Wheel

The front-wheel consists of two main parts: the first is the connecting piece between the wheel and the base, and the second is the wheel itself. The attachment is established using the connector in Figure 27.

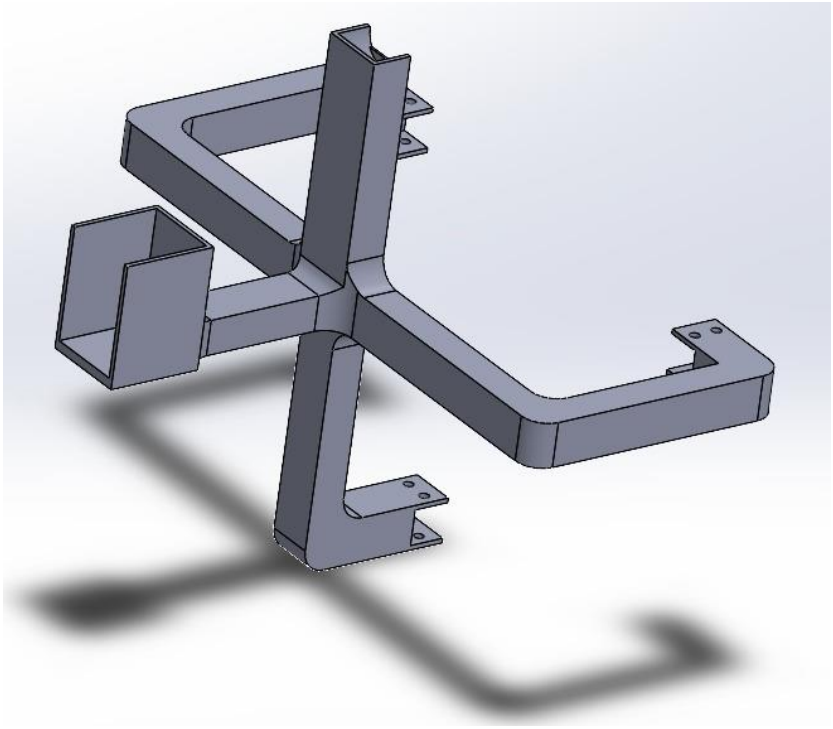

Figure 27: First Configuration - Front Wheel Connection

The connection fragment is used to connect the front wheel with the main base. This part is connected to the battery shelf of the base on one end, to the stepper motor that is connected to the front wheel on another end, to the optical encoder at the top of the vehicle at a third end, and to the breadboard shelf through two support arms.

The connector had to be carefully designed in order to avoid interfering with the reaction wheel. It includes a housing in order to insert the stepper motor that is used for turning the front wheel. Finally, the connector also has a couple of slots for screws in the battery shelf as well as the breadboard shelf to ensure it would not be detached from the main bike while it is moving.

The front wheel of the Gyrobike is a standard wheel with the connection in Figure 28 that allows the motor to twist the entire part along with the wheel for steering.

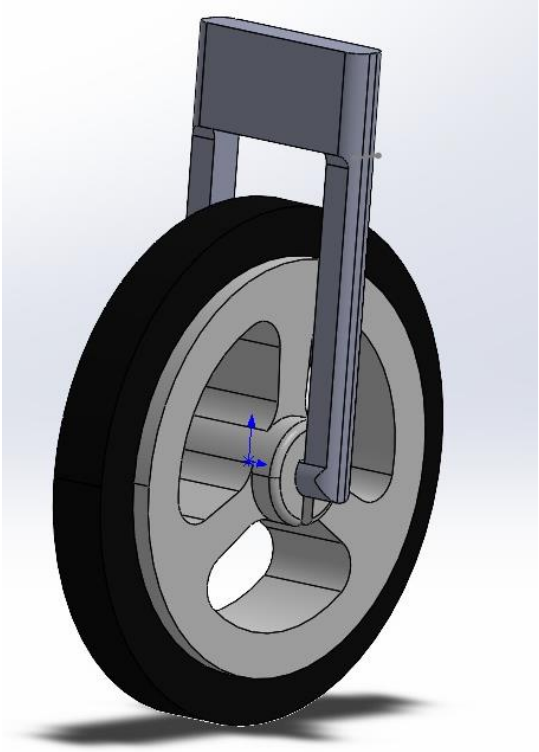

Figure 28: First Configuration - Front Wheel

3.1.1.9 First Configuration - Back Wheel

Similar to the front wheel, Figure 28 shows the back wheel that also consists of two main parts: the connector and the wheel itself.

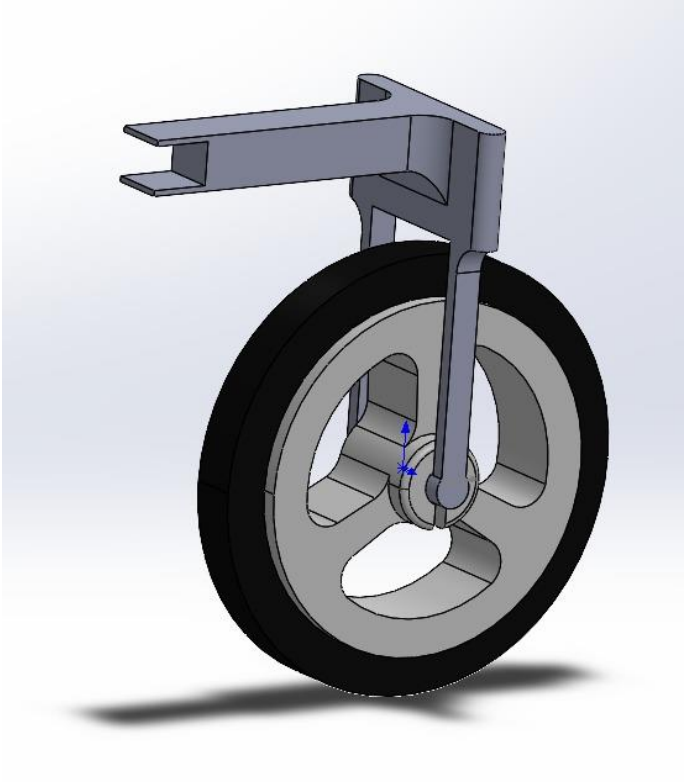

Figure 29: First Configuration - Back Wheel

The wheels themselves are identical in design. However, the connector of the back wheel is much simpler than that of the front wheel since it only needs to support the back wheel without worrying about interfering with the balance wheel. The connector also does not need to house the encoder as the front connector does. Therefore, a much more efficient “T” shape was used.

3.1.1.10 Design Configuration 2

Figure 30 portrays the design configuration which was initially chosen as the final design for the Gyrobike. However, complexities like embedding the encoder and supporting the front wheel connector called for minor changes in this configuration.

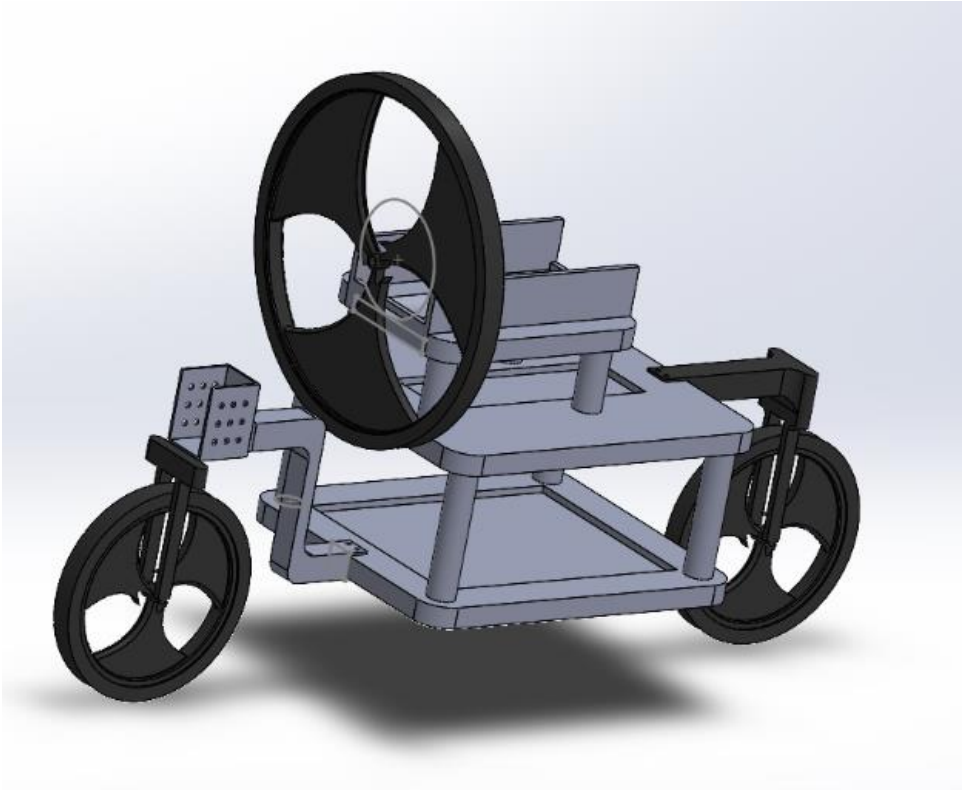

Figure 30: Design Configuration 2

In contrast to the final design's breadboard shelf, the plank in Figure 31 did not include holes for the wiring in the system as well as the pillars that would support the motor shelf. Adding these aspects to the final design improved the bike greatly.

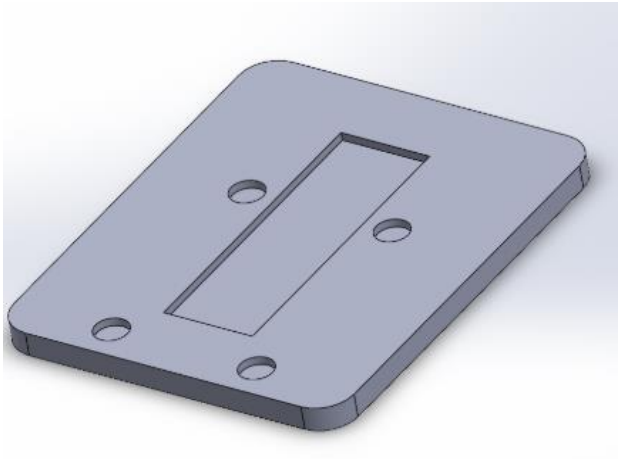

Figure31: Second Configuration - Breadboard Shelf

The reaction wheel in the first design configuration in Figure 32 was somewhat problematic as it is not symmetric. This asymmetry is due to the tiny propulsions near the wheel's center. Furthermore, using this wheel for balancing would have caused unbalance and micro vibrations in the entire system at high rotation speeds.

Figure 32: Second Configuration - Balance Wheel

Perhaps the biggest change to one part between the final design and this configuration was done to the front wheel connector in Figure 33. After realizing the need for an optical encoder near the top motor shelf, an arm was extended to support that encoder. However, the connector would then have been unstable since the only support it has is its connection to the battery shelf. As a solution, two extension arms were added to the final connector to solve that issue.

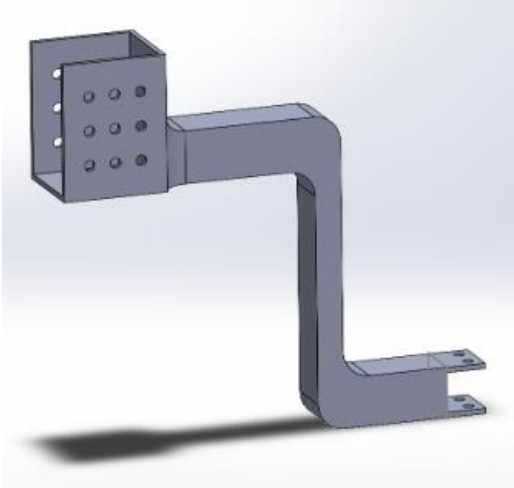

Figure 33: Second Configuration - Front Wheel Connector

Figures 34 and 35 show the front and back wheels that were quite similar to that of the final design's wheels. Only the dimensions and the wheel type were modified for optimization.

Figure 34: Second Configuration - Front Wheel

Figure 35: Second Configuration - Back Wheel

3.1.1.11 Design Configuration 3 (Preliminary Design Concept)

The original design in Figure 36 consisted of two boxes with holes in the middle to reduce the weight and give space for wire connectivity. The two boxes would have the top open layer covered by the housing in Figure 37, which then acts as a base for the motor on top.

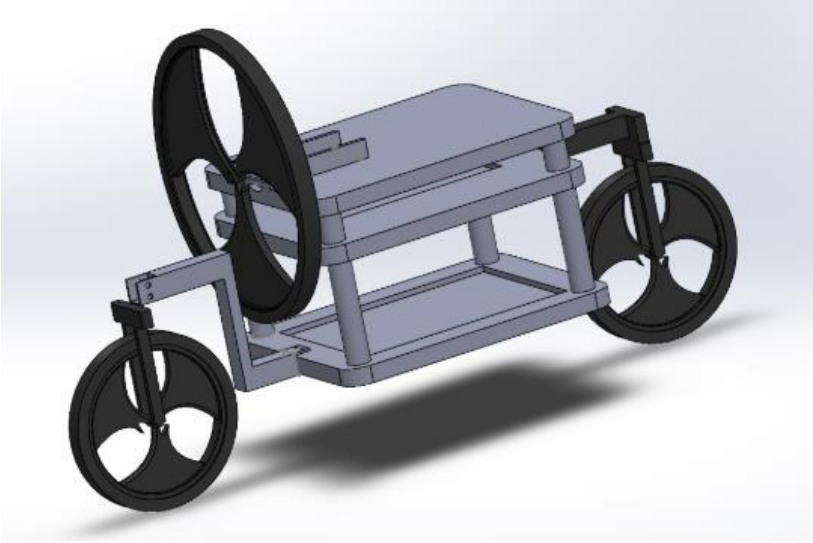

Figure 36: Design Configuration 3

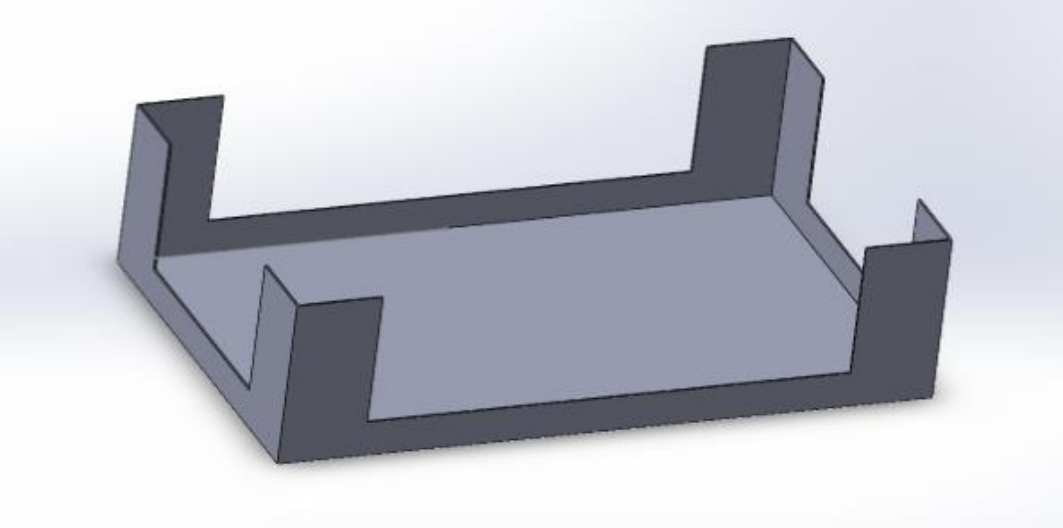

Figure 37: Third Configuration - Battery Shelf

The size of the design was the same size of two 12V batteries lying next to each other. The design included another identical shelf to carry the breadboard, with a plank on top for the motor. Since this design could not support heavy loads, it was a bit difficult to connect the wheels to the base. In addition, due to some limitations in 3D printing, it was best not to use this design concept as it would further complicate matters during the manufacturing process.

The preliminary design is somewhat similar to design configuration 1. However, there are a few main differences in the motor shelf, the breadboard shelf, and the connectors.

The main differences between this design and the final design is that the final design's motor plank is noticeably smaller, as displayed in Figure 38. It is difficult to have a proper grasp on the power needed for the motor to efficiently function early on in the project, which resulted in some overestimation of the motor size. The second difference is that the final design includes a large cutoff of the area from the former design of the motor plank. This can be considered as topology optimization, as all of the unused material both saves money and increases efficiency.

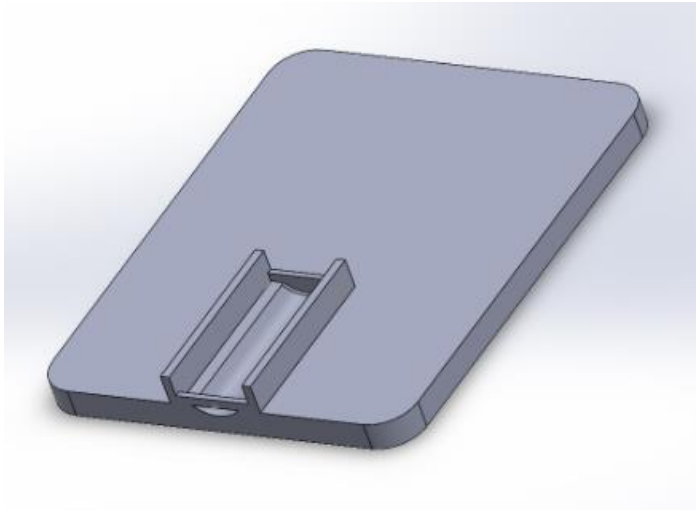

Figure 38: Third Configuration - Motor Shelf

One of the most substantial differences between the designs is in the breadboard shelves. The location of the support beams in Figure 39 significantly changed as the size of the motor shelf changed as well.

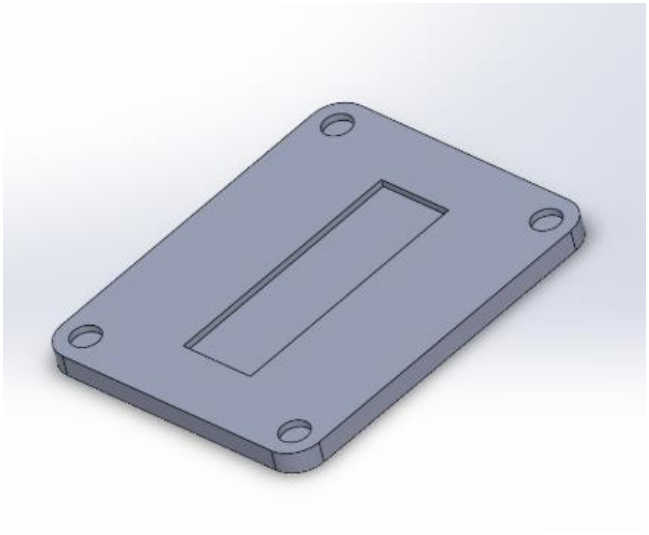

Figure 39: Third Configuration - Breadboard Shelf

As for the front wheel connector in Figure 40, similar to the motor shelf, the dimension used to hold the motor was not accurate early on in the project. Thus, the size of the motor pocket was off. Another difference is that in the initial design the connector had rough corners and angles that were later chamfered in the first design configuration. The adjusted fillets and chamfers both increase the strength of the part and ease the manufacturing process of the connector.

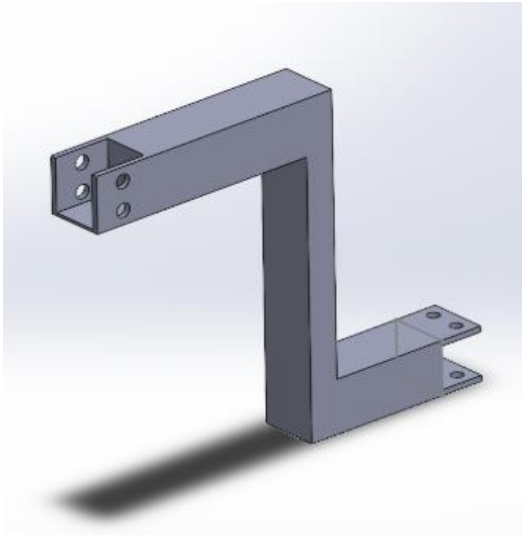

Figure 40: Third Configuration - Front Wheel Connector

Similar to the front wheel connector, the edges of the back wheel connector in Figure 41 were smoothed out and connected to the back wheel in a similar manner.

Figure 41: Third Configuration - Back Wheel

3.1.2 Remote Control (RC) System

The Arduino controls and manipulates the components while adding different buttons, switches, and sensors to assist in controlling it. Furthermore, another way is controlling the Arduino wirelessly from a smartphone. Aside from a smartphone and the Arduino, the rest of the requirements include a method to link the system [10]. To do that, a Bluetooth module will be used along with a 12V battery, a breadboard, and connecting wires. The Bluetooth module setup is automatic once it is plugged in, and the pins on it are labeled as power, ground, the receiver and the transmitter. After connecting the Arduino with the module, the power pin must connect to the 5-volt, while connecting the ground pin. The correct connection of the transmitter and receiver are RX to the TX pin and TX to the RX pin. This should finally establish Bluetooth connectivity. The entire system and its wiring is portrayed in Figure 42.

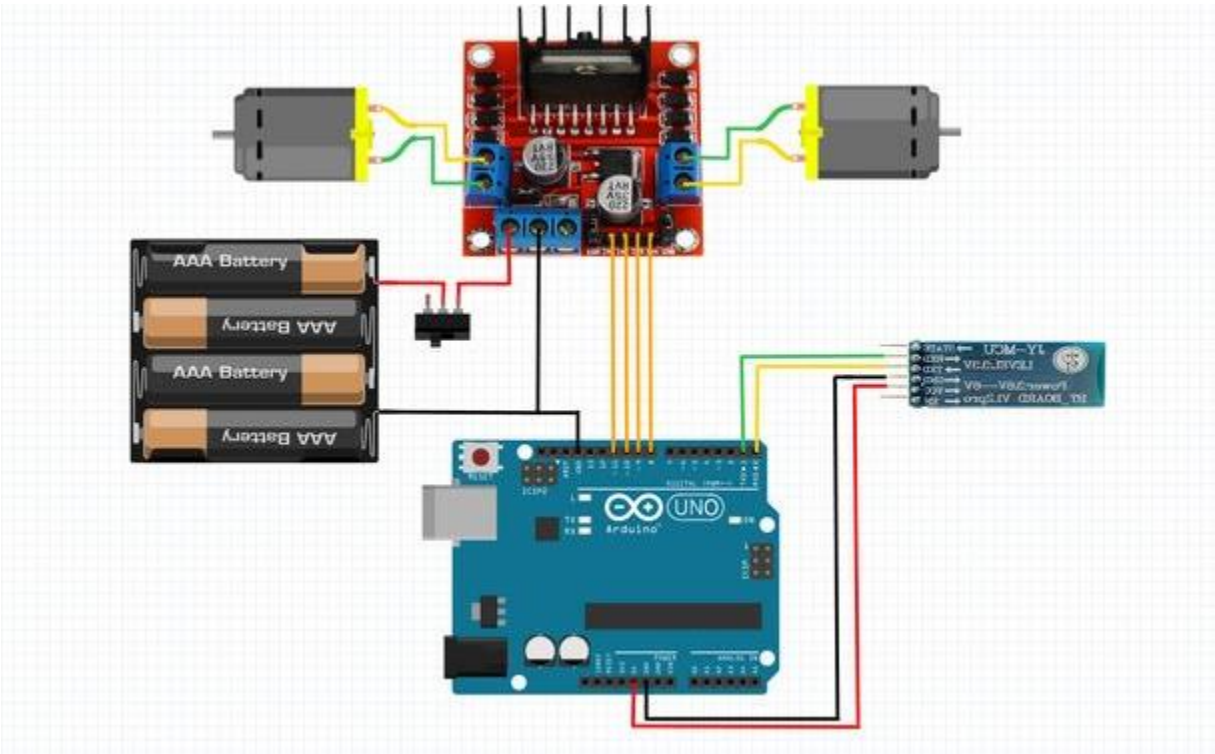

Figure 42: Remote Control System

3.2 Engineering Standards

The Gyrobike in its entirety must follow a lot of engineering standards in order to be accepted as a safe, functioning vehicle. Some of these standards can be classified as the following.

1. In order for the Gyrobike to become an authorized road vehicle in the future, it must obey:
    - ISO 8856:2014 Road vehicles - Electrical performance of starter motors - Test methods and general requirements
    - IEC 61851-21 Ed. 1.0 b:2001 Electric vehicle conductive charging system connection to an A.C./D.C. supply
    - SAE J 2561:2016-11-08 Bluetooth TM Wireless Protocol for Automotive Applications
2. The Gyrobike is a balancing machine, and must adhere to the standards for balancing equipment:
    - ISO 21940-31:2013 Mechanical Vibration and Rotor Balancing
    - ISO 2953:1985 Balancing Machines — Description and Evaluation
3. Since the bike is battery operated:
    - IEEE 1561-2019 Optimizing the Performance of Lead-Acid Batteries in Remote Power Systems
    - ISO 13064-2:2012 Battery-electric mopeds and motorcycles
4. As for the manufacturing standards of the Gyrobike:
    - SAE J 1739:2009-01-15 Potential Failure Mode and Effects Analysis in Design (Design FMEA).

- ISO/IEC CD 23510 3D Printing and scanning — Framework for Additive Manufacturing Service Platform (AMSP)

3.3 Design Calculations (The Control System)

This subchapter is concerned with the primary aim of this project; the use of a reaction wheel to balance a bike. The bike can be best represented as an inverted pendulum that requires balancing in a single plane and will be treated as such in the control system.

3.3.1 Mathematical Model of Permanent Magnet DC Motor

The DC motor is the only actuator involved in the gyroscopic control of the two degrees of freedom bike, making this a nonlinear, underactuated, and highly unstable mechanical system. Permanent magnet DC motors can be modeled mathematically using their armature circuits, such as the one shown in Figure 43.

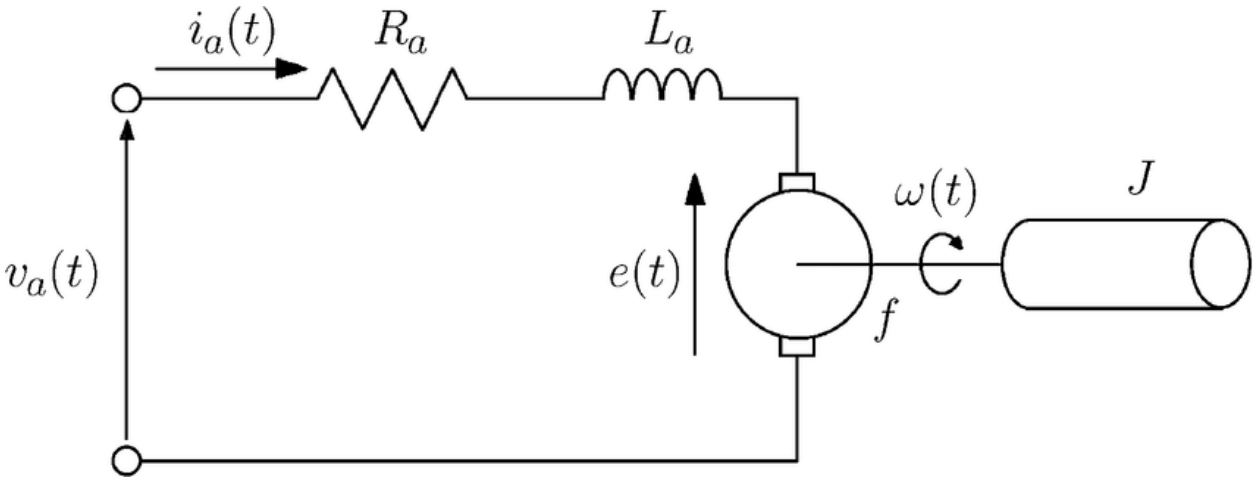

Figure 43: DC Motor Armature Circuit

If we apply Kirchhoff's Voltage Law (KVL) on the armature circuit:

$$Va(t) = Ra(Ia) + \dot{Ia}(La) + \varepsilon(t) \quad (3.1.1)$$

$$\varepsilon(t) = Back\ EMF \quad (3.1.2)$$

Where E is the back electromotive force (EMF), Va is the input voltage from the power supply, and I'a * La expresses the voltage over the inductor at any instant of time.

Assume initial conditions as zero, Laplace transform:

$$\begin{aligned} Va(s) &= RaIa(s) + SLa(s)\,La + \varepsilon(s) \\ Va(s) &= Ia(s)\,(Ra + SLa) + \varepsilon(s) \\ Ia(s) &= \frac{Va(s) - \varepsilon(s)}{SLa + Ra} \end{aligned} \tag{3.1.3}$$

Since most of the control system will be formulated later in the Euclidean state space, it is better to organize all of the upcoming mathematical equations to make them a function of the state variables, starting with the equation of the armature current in the armature circuit:

$$\dot{Ia} = \frac{Va(t) - RaIa - \varepsilon(t)}{La} \tag{3.1.4}$$

However, since both Va and E are not state variables, I'a is now a function of other variables other than the state variables. Therefore, the two linear relationships between the torque and armature current, and the back EMF and the angular velocity will be used to make the equation a function of only the state variables.

Current to torque:

$$\tau(t) = k_T\, Ia(t) \tag{3.1.5}$$

EMF to Angular velocity:

$$\varepsilon(t) = K_\varepsilon \dot{\theta}(t) \;\rightarrow\; \varepsilon(s) = K_\varepsilon S\theta(s) \tag{3.1.6}$$

In these relationships however, the gear ratio of the motor must not be forgotten.

$$\begin{aligned} \dot{\theta}_D &= G\dot{\theta} \\ \dot{\theta} &= \frac{\dot{\theta}_D}{G} \end{aligned} \tag{3.1.7}$$

$$\varepsilon(t) = \frac{K_{\varepsilon}\dot{\theta}_D}{G} \tag{3.1.8}$$

Resulting in:

$$\dot{Ia}(t) = \frac{1}{La}(Va(t)) - \frac{1}{La}(RaIa(t)) - \frac{1}{La}(\varepsilon(t))$$
$$\dot{Ia}(t) = \frac{-1}{La}(RaIa(t)) - \frac{K_{\varepsilon}}{GLa}\left(\dot{\theta}_D\right) + \frac{1}{La}(Va(t)) \tag{3.1.9}$$

3.3.2 Dynamic System Analysis

The dynamic system analysis of the bike was done by assuming the body to be an inverted pendulum, with its center of rotation being the point of contact of the wheel with the ground. In addition to the rotating reaction wheel, the system becomes a two degree of freedom system.

3.3.2.1 Mathematical Modelling

The mathematical model can be derived through the following three diagrams. Figure 44 represents the lengths, angles, and symbols of the two degrees of freedom. Figure 45is a free body diagram that portrays the external forces acting on the system. Finally, the third diagram, Figure 46, displays the effective forces acting on the system.

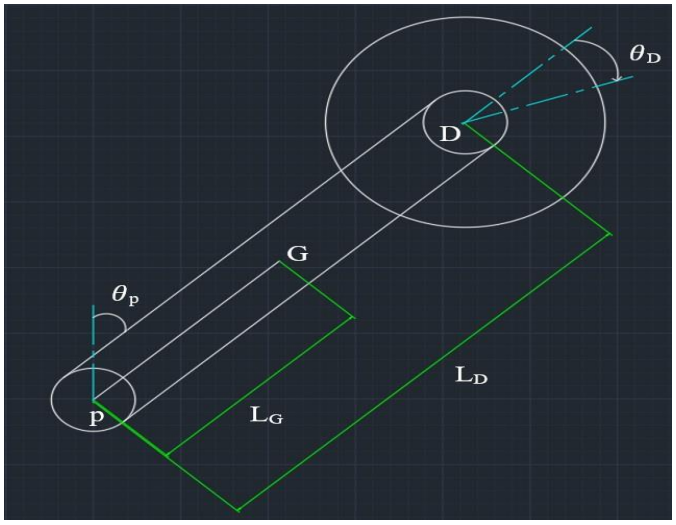

Figure 44: Free Body Diagram: Length and Angles

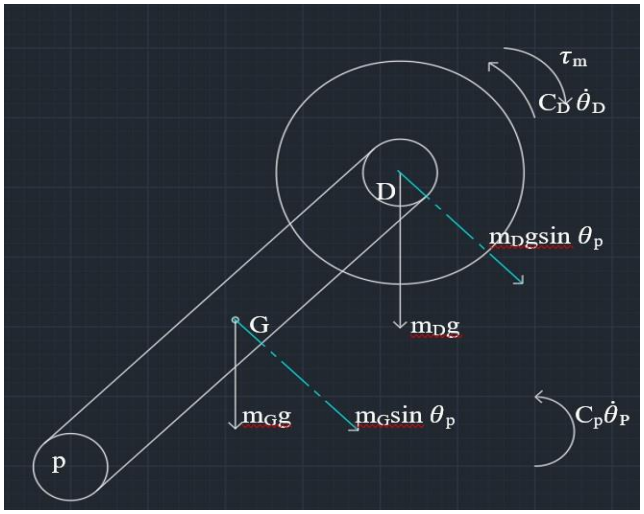

Figure 45: Free Body Diagram: External Forces

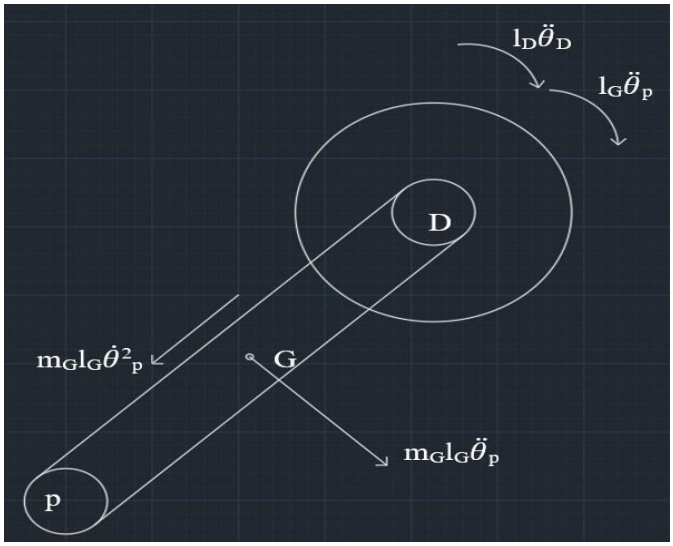

Figure 46: Free Body Diagram: Effective Forces

3.3.2.2 Derivation of Governing Equations

Applying Newton's Second Law to the two degrees of freedom:

$$+\uparrow \varepsilon M_{p\ external} = +\uparrow M_{p\ effective}. \tag{3.1.10}$$

$$+\uparrow \varepsilon M_{D\ external} = +\uparrow M_{D\ effective}.$$

$$\tau_m + m_D g l_D \sin\theta_p + m_G g l_G \sin\theta_p - C_D \dot{\theta}_D - C_p \dot{\theta}_p = I_D \ddot{\theta}_D + I_G \ddot{\theta}_p + m_G l_G^2 \ddot{\theta}_p \tag{3.1.11}$$

$$\tau_m - C_D \dot{\theta}_D - C_p \dot{\theta}_p + mag\left(l_D - l_G\right)\sin\theta_p = I_D \ddot{\theta}_D + I_G \ddot{\theta}_p + m_G l_G \left(l_D - l_G\right)\ddot{\theta}_p \tag{3.1.12}$$

Once the bike's governing equation 1.12 (first degree of freedom) is equated to zero, the result is equation 1.13, while equation 1.14 shows the disk's governing equation.

$$I_G \ddot{\theta}_p + I_D \ddot{\theta}_p + m_G l_G^2 \ddot{\theta}_p + m_D l_D^2 \ddot{\theta}_p + I_D \ddot{\theta}_D + m_G l_G g \sin\theta_p - m_D l_D g \sin\theta_p + C_p \dot{\theta}_P = 0 \tag{3.1.13}$$

(Pendulum/Bike)

$$I_D \ddot{\theta}_p + I_D \ddot{\theta}_D + C_D \dot{\theta}_D = \tau_m \quad \text{(Disk/Reaction Wheel)} \tag{3.1.14}$$

$$D_p = I_G + I_D + m_G l_G^2 + m_D l_D^2 \tag{3.1.15}$$

$$\ddot{\theta}_p\left(I_G+I_D+m_G l_G^2+m_D l_D^2\right)=-I_D\ddot{\theta}_D+m_G l_G g\sin\left(\theta_p\right)+m_D l_D g\sin\left(\theta_p\right)-C_p\dot{\theta}_p \tag{3.1.16}$$

$$\ddot{\theta}_p=\frac{m_G l_G g\sin\left(\theta_p\right)+m_D l_D g\sin\left(\theta_p\right)-C_p\dot{\theta}_p-I_D\ddot{\theta}_D}{I_G+I_D+m_G l_G^2+m_D l_D^2} \tag{3.1.17}$$

$$\ddot{\theta}_D=\frac{\tau_m-C_D\dot{\theta}_D-I_D\ddot{\theta}_p}{I_D} \tag{3.1.18}$$

Once equations 1.17 and 1.18 are obtained, an algebraic loop is formed where it is necessary to replace one of the equations into the other, as both are functions of each other. Therefore, it was decided to plug in equation 1.18 into 1.19, resulting in:

$$\ddot{\theta}_p=\frac{1}{\left(D_p\right)}\left(m_G l_G g\sin\left(\theta_p\right)+m_D l_D g\sin\left(\theta_p\right)-C_p\dot{\theta}_p+C_D\dot{\theta}_D+I_D\ddot{\theta}_p-\tau_m\right) \tag{3.1.19}$$

$$\ddot{\theta}_p=\frac{1}{\left(D_p-I_D\right)}\left(m_G l_G g\sin\left(\theta_p\right)+m_D l_D g\sin\left(\theta_p\right)-C_p\dot{\theta}_p+C_D\dot{\theta}_D-\tau_m\right) \tag{3.1.20}$$

$$\ddot{\theta}_D=\frac{1}{I_D}\left(\tau_m-C_D\dot{\theta}_D\right)-\frac{1}{D_p}\left(m_G l_G g\sin\left(\theta_p\right)+m_D l_D g\sin\left(\theta_p\right)-C_p\dot{\theta}_p-I_D\ddot{\theta}_D\right) \tag{3.1.21}$$

$$\ddot{\theta}_D=\frac{1}{I_D\left(1-\frac{I_D}{D_p}\right)}\left(\tau_m-C_D\dot{\theta}_D\right)-\frac{1}{D_p-I_D}\left(m_G l_G g\sin\left(\theta_p\right)+m_D l_D g\sin\left(\theta_p\right)-C_p\dot{\theta}_p\right) \tag{3.1.22}$$

After resulting in the two governing equations (1.20 and 1.22) of the system comes the crucial step of linearization. As previously mentioned in the beginning of this chapter, the

inverted pendulum is a highly nonlinear, unstable system. In addition, nonlinear control is a very complex field of control engineering that requires higher education and applying machine learning. Therefore, a form of linearization had to be done to eliminate sin(Θ), and make the state variables multiplied by only constants [11]. This form of linearization is small angle approximation, where

$$\sin\theta = \theta$$

By substituting this approximation into the governing equations and making them a function of the state variables as previously done with the DC motor, the result is equations 1.23 and 1.24.

$$\ddot{\theta}_p = \frac{1}{D_p - I_D}\left(g\left(m_G l_G + m_D l_D \right)\left(\theta_p \right) - C_p\left(\dot{\theta}_p \right) + C_D\left(\dot{\theta}_D \right) - K_\tau\left(l_a \right) \right) \tag{3.1.23}$$

$$\ddot{\theta}_D = \frac{1}{I_D\left(1 - \frac{I_D}{D_p} \right)}\left(K_\tau\left(l_a \right) - C_D\left(\dot{\theta}_D \right) \right) - \frac{1}{D_p - I_D}\left(g\left(m_G l_G + m_D l_D \right)\left(\theta_p \right) - C_p\left(\dot{\theta}_p \right) \right) \tag{3.1.24}$$

After deriving these 3 governing equations for the entire system, these equations must be transferred into the state space domain for solution.

3.3.2.3 Solution of the Governing Equations

As previously mentioned, the Euclidean space relies on the state variables to control the system, and transferring the governing equations to the state space follows the subsequent rules.

$$\ddot{\theta}_p = f\left(\theta_p, \dot{\theta}_p, \theta_D, \dot{\theta}_D \right) \tag{3.1.25}$$

$$\ddot{\theta}_D = f\left(\theta_p, \dot{\theta}_p, \theta_D, \dot{\theta}_D \right) \tag{3.1.26}$$

$$\dot{x} = f\left(x, u \right) \tag{3.1.27}$$

$$\dot{x} = Ax + Bu \tag{3.1.28}$$

$$y = h(x, u) \tag{3.1.29}$$

$$y = Cx + Du \tag{3.1.30}$$

Where A is the dynamics matrix, B is the input/actuator matrix, C is the output/sensor matrix, and D is neglected in this case of a pendulum (D=0).

Next are the definitions of the input vector u and the output vector y. Since the ultimate input of the system is the voltage provided by the battery, Va is the only input that concerns the control system. Furthermore, y will only assume the value of Θp because that is the angle of the bike and is the only state variable we wish to control.

$$x = \begin{vmatrix} Ia \\ \theta_p \\ \dot{\theta}_p \\ \theta_D \\ \dot{\theta}_D \end{vmatrix} \tag{3.1.31}$$

$$\dot{x} = \begin{vmatrix} \dot{Ia} \\ \dot{\theta}_p \\ \ddot{\theta}_p \\ \dot{\theta}_D \\ \ddot{\theta}_D \end{vmatrix} \tag{3.1.32}$$

$$y = \begin{vmatrix} \theta_p \end{vmatrix} \tag{3.1.33}$$

$$u = \begin{vmatrix} Va \end{vmatrix} \tag{3.1.34}$$

The dynamics matrix A will be constructed by taking the coefficients of each of the state variables in the governing equations and placing them in the 5*5 matrix.

$$A=\begin{vmatrix} \frac{-Ra}{La} & 0 & 0 & 0 & \frac{-K_{\varepsilon}}{GLa} \\ 0 & 0 & 1 & 0 & 0 \\ \frac{-K_{\varepsilon}}{G\left(D_p-I_D\right)} & \frac{g\left(m_G l_G+m_D l_D\right)}{D_p-I_D} & \frac{-C_p}{D_p-I_D} & 0 & \frac{C_D}{D_p-I_D} \\ 0 & 0 & 0 & 0 & 1 \\ \frac{K_{\tau}}{GI_D\left(1-\frac{I_D}{D_p}\right)} & \frac{-g\left(m_G l_G+m_D l_D\right)}{D_p-I_D} & \frac{C_p}{D_p-I_D} & 0 & \frac{-C_D}{I_D\left(1-\frac{I_D}{D_p}\right)} \end{vmatrix} \quad (3.1.35)$$

$$B=\begin{vmatrix} \frac{1}{La} \\ 0 \\ 0 \\ 0 \\ 0 \end{vmatrix} \quad (3.1.36)$$

Matrix C is constructed by placing a value of 1 that corresponds to the state variable Θp during matrix multiplication.

$$C=\begin{vmatrix} 0 & 1 & 0 & 0 & 0 \end{vmatrix} \quad (3.1.37)$$

$$y=\begin{vmatrix} 0 & 1 & 0 & 0 & 0 \end{vmatrix}\begin{vmatrix} Ia \\ \theta_p \\ \dot{\theta}_p \\ \theta_D \\ \dot{\theta}_D \end{vmatrix} \quad (3.1.38)$$

Finally, these values and matrices are taken to Matlab to start designing the different controllers tested on this inverted pendulum.

3.3.3 Proportional and PID Controllers

The initial plan was to design a P controller with a specific gain K that would stabilize the highly unstable system, and then later add differential and integral controllers to aid the response time and overshoot [12]. After setting the input constants and matrices into the Matlab code (which can be observed in detail in Appendix A), the system's transfer function G(s) was as follows in Figure 47.

```
G =

                  -348.1 s - 1.313e-12
  ---------------------------------------------------
  s^4 + 6675 s^3 + 5.982e04 s^2 - 3.641e05 s - 3.25e06
```

Figure 47: Transfer Function G(s)

Transfer function G(s) has the following poles in Figure 48.

```
>> sys_polesG

sys_polesG =

   1.0e+03 *

  -6.6657
   0.0074
  -0.0091
  -0.0073
```

Figure 48: Poles of G(s)

As it was expected, one of the system's poles, s=7.4, is in the right hand side of the complex plane, making the system instantaneously unstable without adding a controller. The step response of the system in Figure 49 also clearly indicates it diverges to infinity.

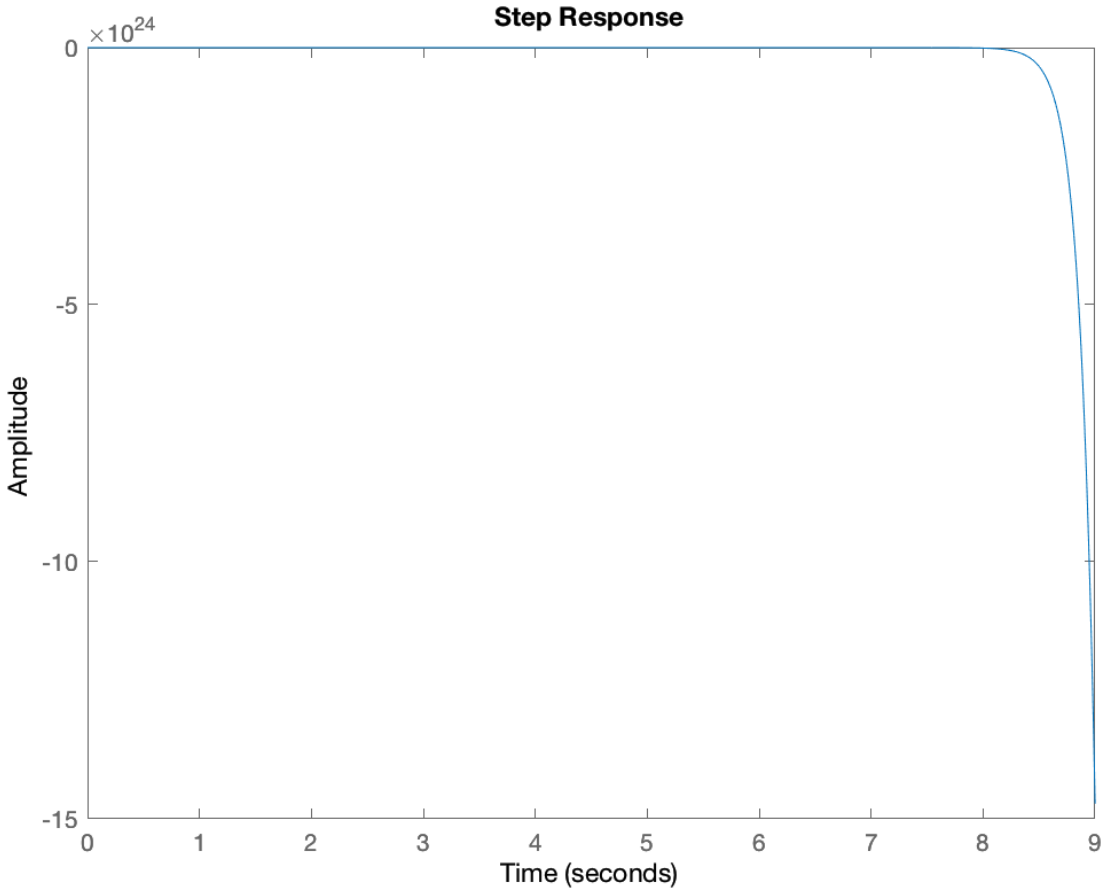

Figure 49: Step Response of System Without Control

After proving the system unstable comes the step of adding the controller and rechecking for stability. The P controller would result in the following block diagram of the system in Figure 50, with proportional gain Kp.

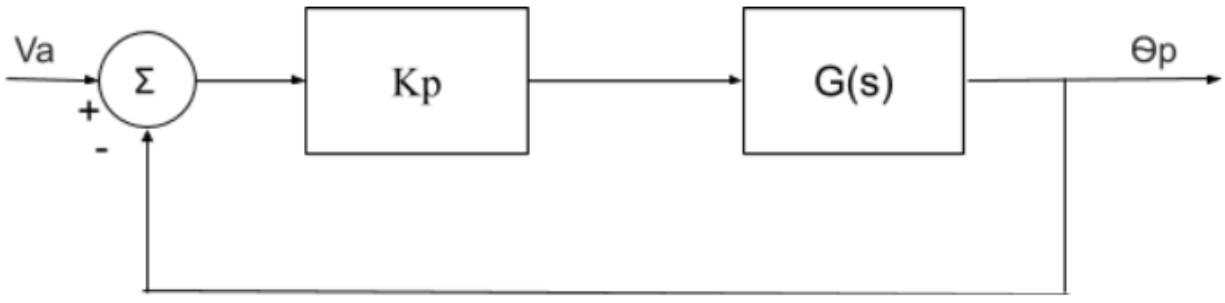

Figure 50: Block Diagram After Adding Controller

The root locus of G displayed in Figure 51.

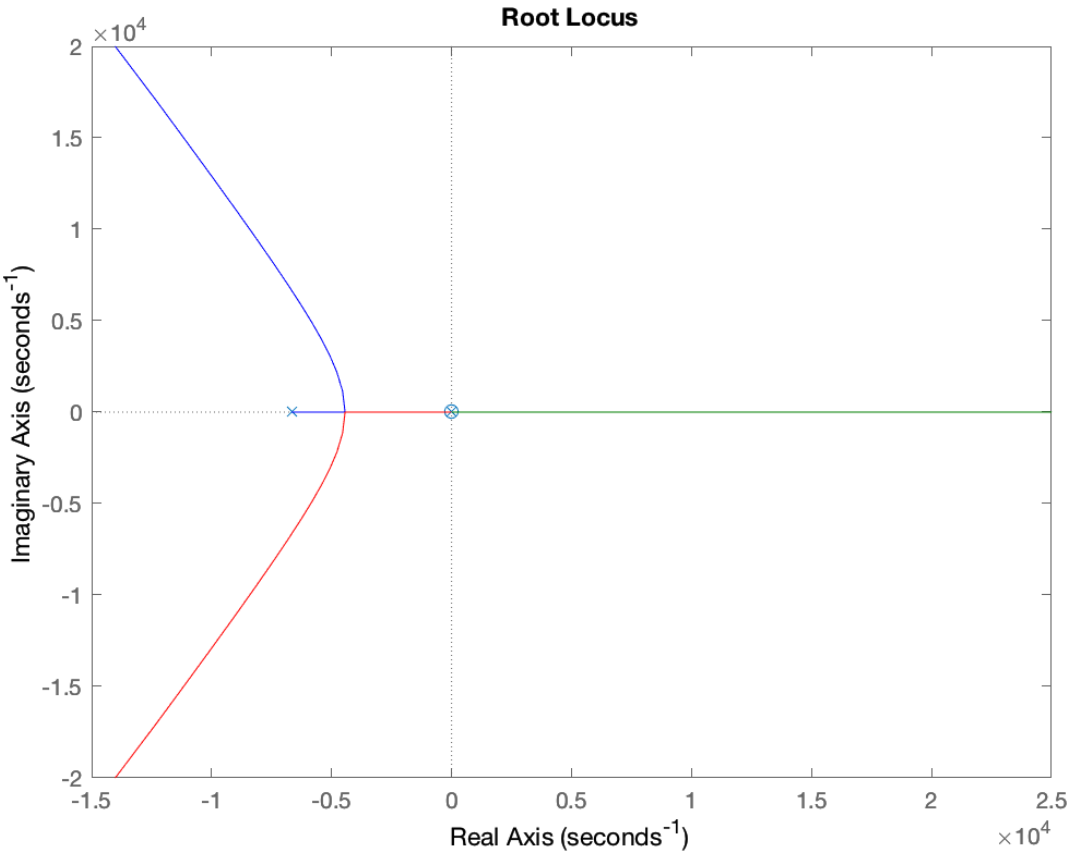

Figure 51: Root locus of G(s)

The problem with the P and PID controllers arises at the step of the transfer function and finds the poles in Figure 52. The root locus graph indicates that there is no value of gain K that would completely stabilize the system. In fact, some values of K such as K>100 would move the second pole out of the right-hand side to the left-hand side of the complex plane, but would immediately declare another pole unstable, as displayed in Figure 53.

```
TF =

                  -3.133e06 s^5 - 2.091e10 s^4 - 1.874e11 s^3 + 1.141e12 s^2 + 1.018e13 s + 0.03841
  ------------------------------------------------------------------------------------------------------------------
  s^8 + 1.335e04 s^7 + 4.467e07 s^6 + 7.947e08 s^5 - 2.22e10 s^4 - 2.744e11 s^3 + 8.844e11 s^2 + 1.255e13 s + 1.056e13

Continuous-time transfer function.
```

Figure 52: Transfer Function After Adding Controller

```
sys_polesTF =

   1.0e+03 *

  -6.6657
  -6.6657
  -0.0275
   0.0194
   0.0074
  -0.0091
  -0.0073
  -0.0009
```

Figure 53: System Poles with Controller

Therefore, the design of a P controller for such a system is impossible while considering negative feedback, and the system must rely on the full-state feedback controller for stability.

3.3.4 Full-State Feedback Controller

The full-state feedback controller is both designed and tested in the state space, meaning that there is no practical use for Laplace transformation while using such a controller. After declaring all the matrices and constants in MATLAB, the controller allows us to indicate where we wish to place the five poles on the complex plane. The placement of the poles along the z-plane is absolutely crucial. The specified location must not be too far away from the original pole location in transfer function G, but should also move all RHS poles to the LHS of the plane. Therefore, the only two poles that are to be adjusted in matrix p are the first pole (originally at s=0), and the third unstable pole (originally at s=7.4).

p = [-0.1 -6666 -0.16 -9.1 -7.3]

After applying the full-state feedback controller functions:

K = place(A,B,p);

A_ctrl = A-B*K;

B_ctrl = B*K;

```
C_ctrl = C;

D_ctrl = 0*C;

GyroBike_ctrl = ss(A_ctrl,B_ctrl,C_ctrl,D_ctrl);
```

The system has the following step response in Figure 52.

The step response of the second and third state variables of Figure 54(Θp,Θp'), which govern the angle and angular velocity of the bike, clearly converge to 0. This is precisely what is expected from the control system. Most importantly, the angle of the bike, which was considered highly unstable and would not stabilize through the P controller, now converges to 0 after a considerable percentage of overshoot.

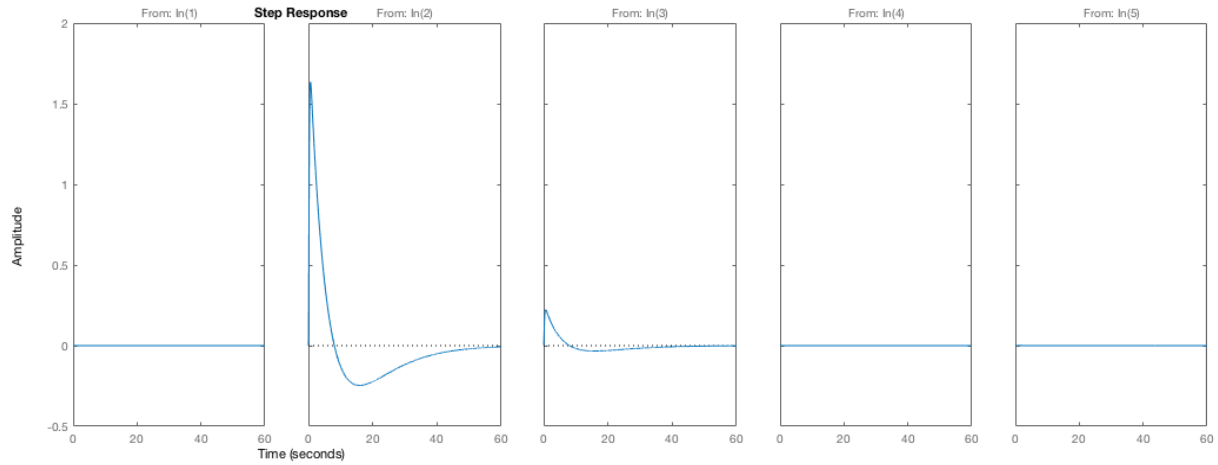

Figure 54: Step Response with Full State Feedback Controller

Even though the system is now stable and the angle of the bike converges to 0, the system still takes an unacceptable amount of time in order to do so. The transient state is about 50 seconds and must be minimized for the system to be deemed useful in further applications of balancing. This transient state can be minimized by manipulating the 'place' function on

MATLAB, which in turn affects the controller. By setting the poles at the given values of p, the system yields a much better settling time of approximately 2 seconds, as shown in Figure 55.

p = [-4 -6666 -3 -9.1 -7.3]

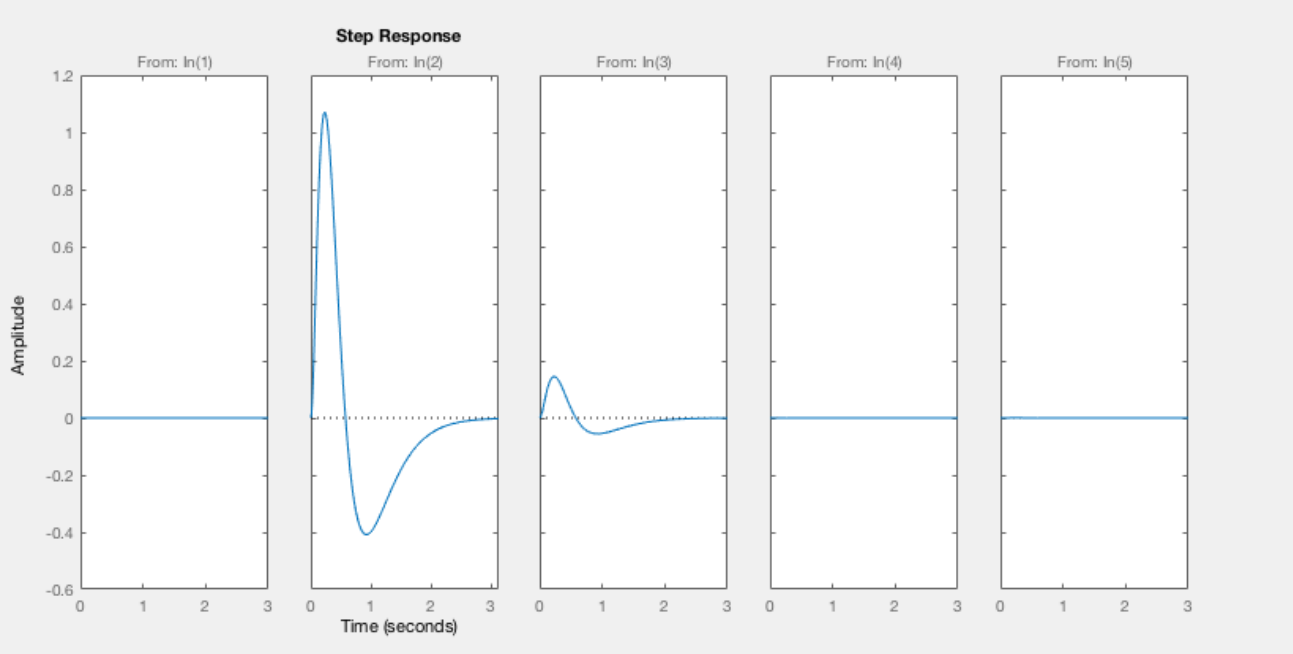

Figure 55: Step Response After Controller Optimization

3.3.5 Drag Calculations

The force resisting the motion of the gyrobike F_{total} consists of the sum of rolling friction F_{roll}, aerodynamic drag F_{wind}, the force needed to accelerate F_{accel}, the upward slope resistance F_{slope}, bearing friction resistance and loss due to the drivetrain efficiency factor η (Greek letter eta) [13]. However, considering that this is a prototype of the Gyrobike and would not be moving at high speeds, the more logical calculation would be to determine the drag force acting on the sides of the bike. Since the reaction wheel along with the top motor would be rotating at relatively high speeds and would abruptly change the position of the bike at high speeds, calculating the drag acting on the bike's sides is necessary. Furthermore, some aspects of the total force equation would be neglected. Since the speed and acceleration of the Gyrobike are

variables, the velocity and acceleration of the bike as well as the wind's velocity were taken as functions of angular velocity omega (ω) and angular acceleration (α).

$$F_{total} = (F_{roll} + F_{slope} + F_{accel} + F_{wind})/\eta \quad (3.2.1)$$

Where η : Drivetrain efficiency, dimensionless.

The drivetrain efficiency is taken as 97% since the system is gearless.

The individual retarding forces are described as follows:

1- **Rolling friction**: is the force resisting the motion when a wheel rolls on a surface. It is mainly caused by non-elastic effects; that is, not all the energy needed for deformation (or movement) of the wheel is recovered when the pressure is removed. In the gyrobike, the rolling friction will be zero because there is no sliding or slipping while the bike balances in its location.

2- **Force based on wind**: Calculating the force of wind requires the mass of air and acceleration of wind. The mass of air hitting a surface then equals air density times the area. The acceleration equals the square of the wind speed in meters per second (m/s).

$$F_{roll} = c_r\, m\, g = 0 \quad (3.2.2)$$

Where c_r : coefficient of rolling resistance, dimensionless

m : total mass of the vehicle in kg (m = 9.9 kg)

g : acceleration due to gravity (g = 9.81 m/s^2)

$F_{slope} = smg = 0$ (3.2.3)

Where s : upward slope, dimensionless

$F_{accel} = a\ m$ (3.2.4)

Where a : acceleration in m/s^2

$F_{accel} = (\alpha * R) *\ m$ (3.2.5)

$F_{accel} = \alpha * 0.4 * 9.9$

$F_{accel} = 3.96 * \alpha$

$F_{wind} = (r\ c_w\ A\ v_{wind}^2)/2$ (3.2.6)

Where r : density of air in kg/m^3

c_w : coefficient of wind resistance, dimensionless ($c_w = 1.8$)

A : side area in m^2 ($A = 0.66\ m^2$)

v_{wind} : wind velocity in m/s

$F_{wind} = (1.225 * 1.8 * 0.66 * (\omega * 0.4)^2) / 2$

$F_{wind} = 0.1164241 * \omega$

The power required to overcome the total drag is:

$$P = F_{total}\, v \quad (3.2.7)$$

Where v : velocity in m/s

$$F_{total}=(F_{accel} + F_{wind})/ \eta \quad (3.2.8)$$

$$F_{total}= (3.96*\alpha + 0.1164241*\omega) / 0.97$$

$$F_{total}= 4.08*\alpha + 0.12*\omega \text{ N}$$

After determining the total drag force acting on the bike as it balances, the power to overcome this force must be calculated, which is determined by:

$$P = F_{total}\, v \quad (3.2.9)$$

$$P = (4.08*\alpha + 0.12*\omega)*(0.4*\omega) \text{ W}$$

This final equation can be calculated with the microcontroller consistently through software interrupts in the C code. It is an important part of the control system as the only forces that must be overcame by the reaction wheel are the drag, gravity, and additional disturbances caused by asymmetry and impact forces.

3.4 Cost Analysis

Before indulging in the Gyrobike's manufacturing and supplies costs, the team had to first invest in some tools that would serve as a capital investment for this project and possibly future projects, which is all detailed in Table 2.

Table 2: Capital Investment

Capital investment			
Part Name	Quantity	UNIT Price	Total
Vernier Caliper	1	6$	6$
Safety equipments	4	12$	48$
Files	2	7$	14$
Wrenches	3	6$	18$
Screw driver	2	5$	10$
Tap for tapping	1	25$	25$
Tap wrench	1	15$	15$
Total			136$

Furthermore, table 3 shows some indirect costs that were not as easy to predict were also included in the total cost. Some of these spendings were on shipping of materials and transportation of team members to the nearby city of Lefkoşa in order to acquire supplies.

Table 3: Indirect and Additional Cost

Other expenses	
Category	Cost
Transportation	50$
Shipping	100$
Meetings	50$
Tickets	112$
Total	312$

Table 4: Bill of Materials

Bill of Material Details

Date : 2/6/2021

Assembly Name :	Gyrobike
Assembly Number :	

Approval Date :	7/6/2021
Part Count :	3
Total Cost :	453$

Item No.	Part No.	Part Name	Producer	Quantity	Unit of Measur	Source	Unit Cost	Total Cost	Notes
0	10-001	MPU 92250 Gyroscope	INVENSENSE	1		Invoice	12$	12$	
1	10-002	Arduino Mega 2560	ELEGOO	2		Invoice	15$	30$	
2	10-003	Arduino Bluetooth Module	ELEGOO	1		Invoice	8.3$	8.3$	
3	10-004	Breadboard	Hwayeh	2		Invoice	1.25$	2.5$	
4	10-005	Wire Set	PCB Solder Cable	1	mm	Robotistan	5.4$	5.4$	
5	10-006	Arduino motor shield L293D	ROBOTIS INC	1		Invoice	3$	3$	
6	20-001	12V(330rpm) DC Motor	Pololu	1	RPM	Robotistan	52$	52$	
7	20-002	Nema 23 Hybrid stepper motor	Pololu	1	A	Invoice	47$	47$	
8	20-003	Nema 14 Hybrid stepper motor	Pololu	2	A	Invoice	16.3$	16.3$	
9	20-004	Timing poly and belt	Unbranded	1		Robotistan	28$	28$	
10	20-005	Volt regulator	Unbranded	2		Robotistan	3$	6$	
11	20-006	Current sensor	Unbranded	1	A	Robotistan	3$	3$	
12	30-001	3D Printing	Invoice	3	Kg	Invoice	121.3$	121.3$	
13	30-002	Aluminuim sheet	Unbranded	0.5	mm	steel store	15$	15$	
14	30-003	Lipo 14.8V 3000mAh	Li-po battery	1	V	Robotistan	103$	103$	

Checked By / Authorised Signatory : _____ Date : 2/6/2021

The provided bill of materials in table 4 includes all of the required mechanical and electrical components in order to manufacture and assemble the Gyrobike. Even though the bill of materials includes all the costs related to direct production, some indirect costs are not directly related to the bike, and were listed in tables 2 and 3. Even though the total costs exceed the $1000 mark by a small amount, some of the indirect costs are estimated and might not reach such prices, which would decrease the total amount by a considerable quantity.

Chapter 4

Manufacturing Plan

4.1 Manufacturing Process Selection

Table 5: Pugh criteria matrix for material selection

Material	Availability	Cost	Weight	Manufacturing	Yield Strength	Total
PLA	+	+	+	++	++	7
ABS	+	-	++	++	+	5
7075 Aluminum	--	--	--	--	+++	-5
MDF Wood	++	++	+	-	++	6

Table 5 portrayed above shows the comparison between the materials that were considered for the manufacturing of the Gyrobike. The criteria were based on the availability in Northern Cyprus, the cost, the weight, the manufacturability, and the yield strength. As the table indicates the best material to use is PLA that is manufactured through 3D printing which has become a popular material due to it being economically produced from renewable resources [14], as it is available in Cyprus, considerably economical, lightweight, and has sufficient yield strength to hold the bike together. Most importantly it can be used to manufacture all the complex parts (such as the front and back wheel connectors) in the bike. However, not all the bike's parts have a complex design (like the support beams), which calls for using MDF wood or aluminum as it also fills the criteria necessary for the bike while being cheaper than 3D printing. Figure 56 portrays the process of manufacturing the support beams and the wheels' shafts on the turning machine.

Figure 56: 3D Support Beams and Shafts on Turning Machine

Due to the graph presented, it was finally decided it was best to use PLA 3D printing for most of the complex parts. Its manufacturability allows for more complex shapes like the wheels, the wheel holders, and the front wheel connector while it could also be easily replaced during maintenance. Since the Gyrobike design is unique compared to traditional bikes, finding these shapes in the market will be exceedingly difficult. PLA is also easily modifiable post-manufacturing since it supports threaded inserts. For instance, if the team needed to screw support bolts into the bike after it had already been printed, PLA's mechanical properties allowed it to persist cracks to a certain extent. Figure 57 shows the 3D printing process of the front and back wheels connectors of the gyrobike.

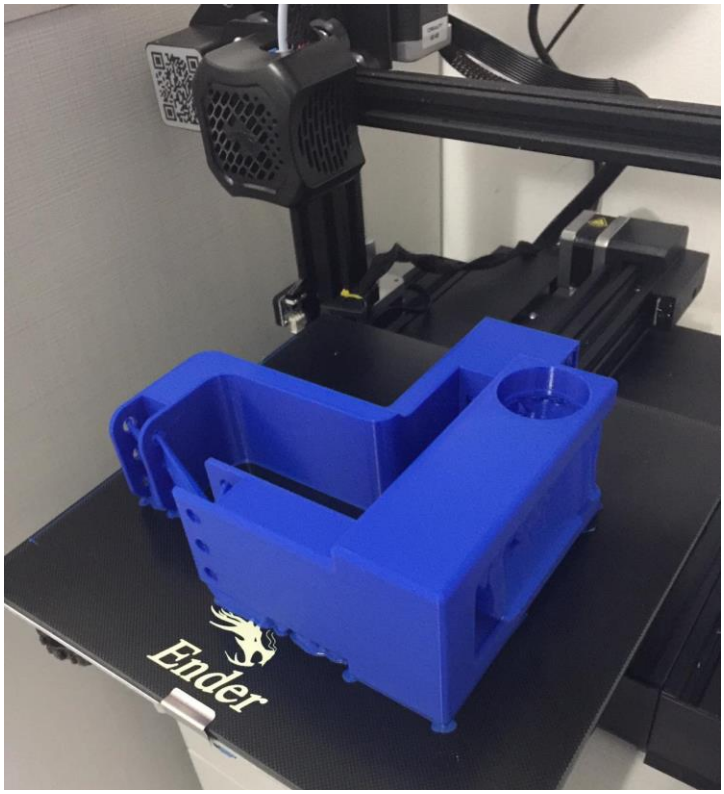

Figure 57: 3D Printed PLA – Front and Back Connectors

Since PLA printing isn't that cheap for a student lead project, it was decided that it is best to not have all the parts 3D printed. Furthermore, all the gyrobike's parts were roughly separated into complex and simple parts. Simple structures like the support beams that don't have many grooves and are easily manufactured would be made out of medium-density fiberboard wood (MDF). Instead of 3D printing those parts, using MDF which is an engineered wood product made by breaking down hardwood or softwood residuals into wood fibers, often in a defibrator, combining it with wax and a resin binder, and forming it into panels by applying high temperature and pressure [15]. So, it reduces the cost of the overall project without heavily affecting the efficiency of the entire vehicle. However, the wheels of the bike had to be 3D printed in order to get a near-circular shape, which would not be possible with wood machining. Figure 58 illustrates the final product of the gyrobike's wheels after printing.

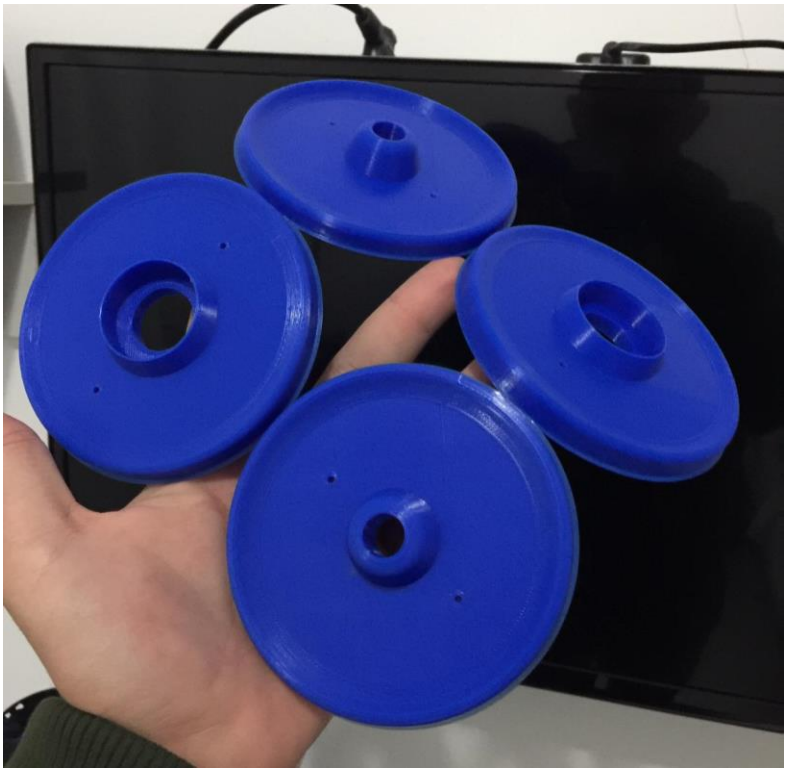

Figure 58: 3D Printed Wheels of the Gyrobike

4.2 Detailed Manufacturing Process

Firstly, the manufacturing process will start with 3D printing the parts that cannot be bought or manufactured economically. These include the three batteries, breadboard, and motor shelves along with the front connector, the front and back wheel, and the balance wheel. After that, the MDF wood would be turned and set to the required dimensions for the construction of the support beams. Next, the screws would be used to connect the back wheel to the rear connector, and the entire part to the middle of the breadboard shelf. Next, the front connector must be fastened tightly by screws to the center of the battery plank. These joints must be properly joined as the wheels should be sturdy during the bike's operation. After that, the battery, breadboards, and the motor must all be placed on top of their respective brackets, and the stepper motor must fit into the pocket at the end of the front connector.

Regarding the 3D printing process, ABS was used for its flexible machining properties. The turning machine within the workshop in the university was used to manufacture the shafts of both wheels. The next step included modifying the balancing wheel connectors and fixing the front stepper motor for the steering connectors so the wheel can turn right and left. The aluminum shelf was used to support the back and front connectors by cutting out and using 0.5mm thickness from the sheet. Next, the aluminum beams were fitted into the upper and lower shelves as the connector between the two of them, while the balance wheel and the DC motor were fitted together using a set screw and a special connector to compensate for the DC motor's smaller shaft. Finally, the motor's shelf was designed for more stability and two bearings were used for each of the back and front wheels (front wheel 600 RS bearing, back wheel 6201 bearing). Figure 59 shows the general assembly of the chassis of the gyrobike.

Figure 59: Assembly of Gyrobike Chassis

Chapter 5

Product Testing Plan

This chapter is mainly concerned with the testing plan for both the expected performance of the bike and the engineering standards specified in Chapter 3.

5.1 Verification Plan for Product Objectives

As previously mentioned in Chapter 1, the Gyrobike is still a foreign concept to the engineering world, and relies on non-traditional control techniques to stabilize the moving pendulum. Therefore, the project's main objective is to prove that the performance and balance of such a bike is actually possible, and the validation of this theory is a challenging task. The plan is to use MATLAB's simulation tools to create a virtual world with similar physics to that of our own, and embed the bike's geometric shape into that world. Even though the mathematics in the project verifies the project's success, it is crucial to rely on different computer software such as ANSYS and MATLAB in order to properly validate all calculations before initiating the step of manufacturing and purchasing materials.

Even after manufacturing and assembling the bike, the vehicle's performance depends on a series of trial and error tests to determine the location of the IMU. Because the gyroscope and the geomagnetic sensor inside the IMU are affected by magnetic fields, placing the IMU near either the top or rear motors might lead to a lot of noise and error in the calculations. Finally, it was decided that it was best the IMU is placed under the DC motor's shelf, where it is clear from both the magnetic fields of the driving stepper motor and the operation of the DC motor above it. Figure 60 displays the IMU position on the gyrobike.

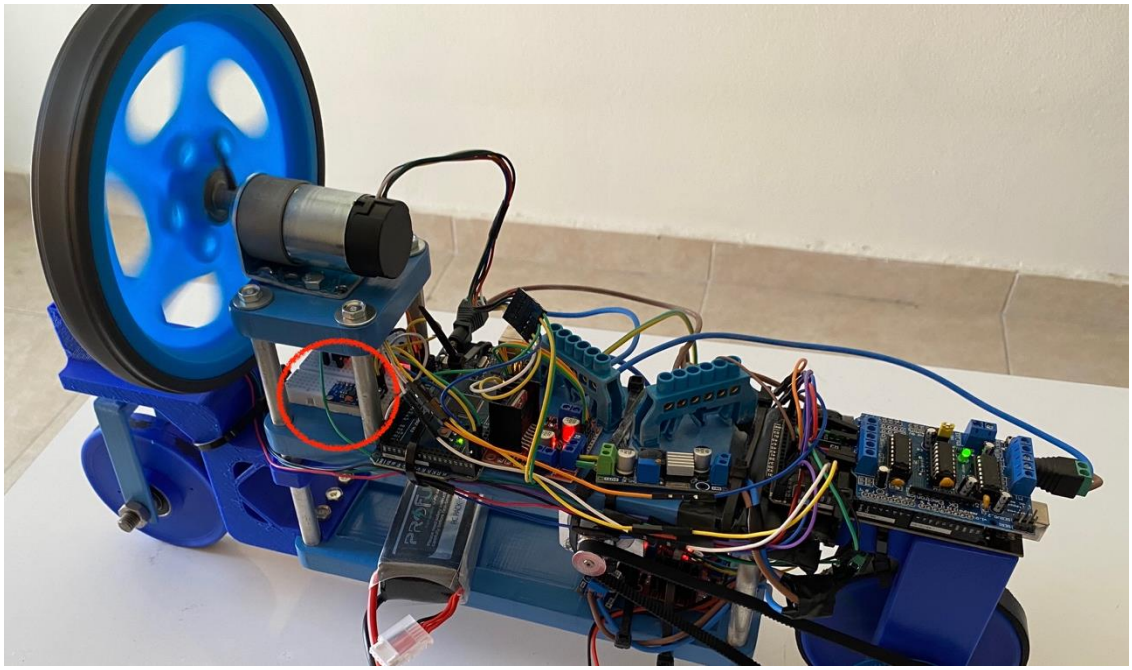

Figure 60: IMU Placement to Avoid Noise

Another expected obstacle during the testing of the product would be the shift in the bike's center of gravity. When the mechanical design was finalized on Solidworks, it was extremely difficult to account for every single component that would be placed on the bike. This is due to the fact that different electrical as well as mechanical parts would be added later to solve issues that arise during testing. Therefore, one of the ideas was to use a small, steel beam to compensate for whichever side the center of gravity leans to. However, the better, executed idea was to use the battery's own weight in order to do that correction, which is best summarized in Figure 61.

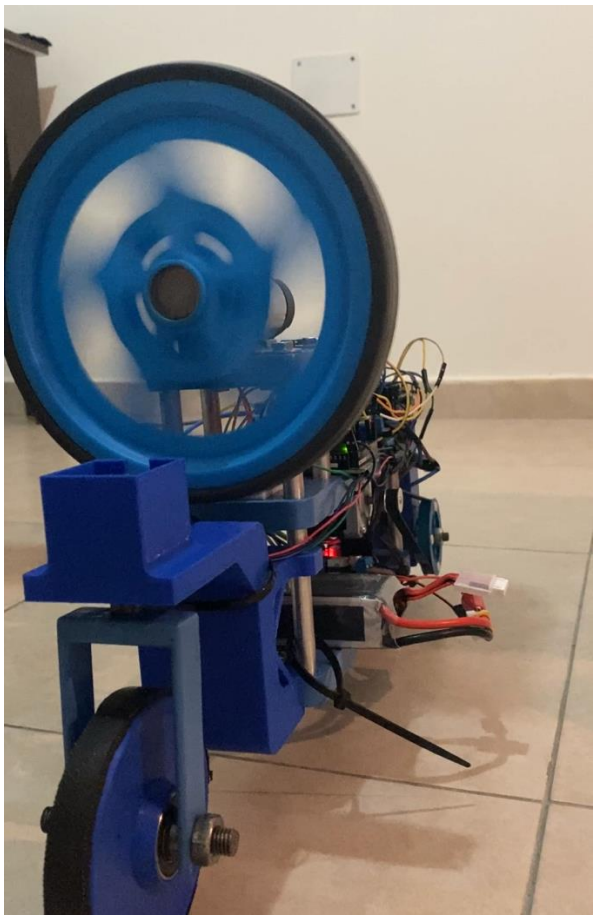

Figure 61: Using Battery's Orientation for Center Correction

5.2 Verification Plan for Applied Engineering Standards

In order to ensure that the proper engineering standards have been followed in this project, multiple tests have to be conducted in the future after manufacturing.

1. The vehicle is battery powered and the industrial DC motors require a high current to deliver maximum torque. The wires that this current will flow through must be high gauge in order to resist factors such as melting that might be a safety hazard.
2. The Bluetooth communication system must be reliable and the delay should not exceed a certain extent.
3. Batteries in general have multiple serious depletion-related problems [16]. Lithium ion batteries specifically provide high energy density, and can be recharged time after time.

These batteries contain lithium ions and highly flammable electrolytes, which makes regular battery maintenance and check-ups a very important aspect in applying standards.

4. All electrical components and circuits must be properly concealed and secured if the vehicle was to pass the research phase and reach customer use. The proper road vehicle standards must also be applied for the Gyrobike to roam the streets, which includes a reliable braking system and appropriate lights.

Chapter 6

Results and Discussion

This chapter revolves around the results of the project once the testing of the prototype was completed. It also discusses the engineering standards used in the testing stage of the project and explores the different shortcomings and constraints of the bike due to inaccuracies in the design of the system. The final assembly of the Gyrobike is displayed as it is in motion in Figure 62.

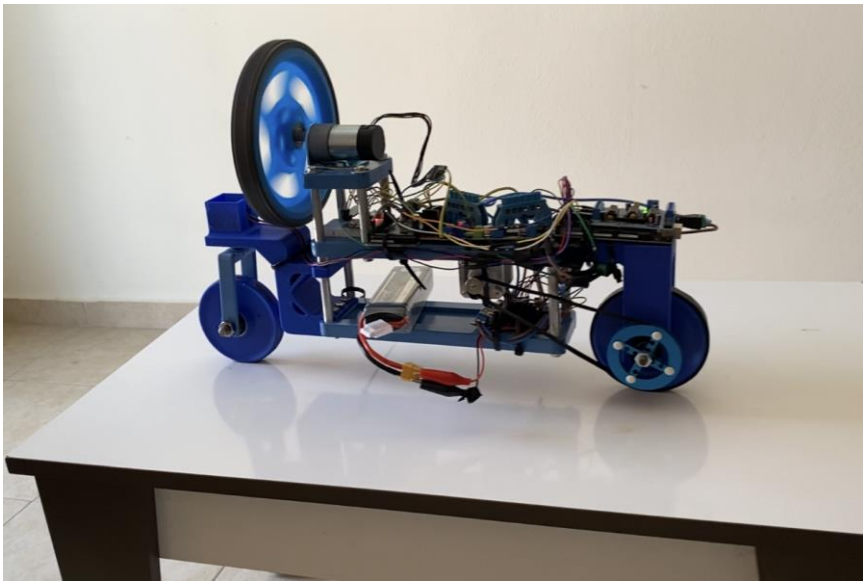

Figure 62: Final Assembly of the Gyrobike

6.1 The Results

The results regarding the testing of the bike were satisfactory to say the least. The operation of the bike included the following properties:

- The bike managed to stay balanced, even though the sideways movement was not as smooth as predicted.

- The bike successfully steered and moved forward and backward while maintaining upright posture, but could not do both steering and driving simultaneously.
- The control system successfully resisted minor disturbances caused by hands and disruptions to the center of gravity caused by adding weights. However, the system could only resist lightweight disturbances, as any powerful interference caused the vehicle to fall over.

6.2 The Engineering Standards

The following engineering standards are those that are applied on the testing of the Gyrobike if it were to ever become a produced product used by consumers:

- ISO 8856:2014: lays down test methods and general requirements for the determination of the electrical characteristics of DC starter motors intended to start internal combustion engines of road vehicles.
- ISO 11452-1:2015: specifies general conditions, defines terms, gives practical guidelines, and establishes the basic principles of the component tests used in the other parts of ISO 11452 for determining the immunity of electronic components of passenger cars and commercial vehicles to electrical disturbances from narrowband radiated electromagnetic energy, regardless of the vehicle propulsion system.

- IEEE 1561: this guide is applicable to lead-acid batteries that are used as the energy storage component in remote hybrid power supplies. The remote hybrid application, with its dual generator option, i.e., both renewable and dispatch-able generation, is advantageous in that the battery can usually be charged at will and

under circumstances that may also be advantageous for the dispatch-able generator.

- DIN ISO 6727:2013-12: this standard specifies the symbols used to identify certain controls, indicators and tell-tales on a motorcycle and to facilitate their usage. This standard also indicates the colors of possible optical tell-tales which warn the driver of the operation or malfunctioning of the related devices and equipment.

6.3 The Constraints

As discussed previously in the results subsection, the system could not withstand abundant disturbances due to multiple inaccuracies and imperfections with the design of both the mechanical and mathematical designs of the Gyrobike. Some of these limitations are:

- The mechanical design that was followed did not include all the electrical components that would be added later in the final stages of assembly, which caused a slight shift in the bike's center of gravity that was not accounted for.
- The wheel used as the reaction, or balance, wheel was not perfectly symmetric. However, the calculations which the control system was based on were done according to a symmetric reaction wheel. This caused an unaccounted change in the dynamics of the system.
- Economic constraints as well as the lockdown caused by COVID-19 lead to the team settling for a less powerful DC motor to control the reaction wheel. Perhaps a more powerful motor with higher torque would have helped the system resist more intense disturbances.

- The linearization process used while designing the control system was small angle approximation, meaning that all the functions sin(θ) were approximated as θ. This linearization process is suitable if the system would stay in a small angle range that is smaller than 1 degree. However, as the angle of the bike increases, the inaccuracies the control system would face increase as well.
- The contact points with the ground were assumed to be a single point in the mathematical model of the system. However, the mechanical design turned out to have wheels that have more than a single contact point with the ground, which further complicated the dynamics of the system.

Chapter 7

Conclusion and Future Work

This chapter summarizes the work done on the Gyrobike throughout the previous 18 months and reviews the future work that can be done in order to further improve the system.

7.1 The Conclusion

The Gyrobike's concept was created in order to test the corresponding linear quadratic regulator (LQR) controller on a system in motion. Therefore, the main idea behind the project was never to turn this bike into a future product that can be sold and one that people would ride on the road. However, the bike sets the path for the control of nonlinear, underactuated mechanical systems that take the form of inverted pendulums as they operate. Such systems include satellites, submarines, drones, and even humanoid robots.

The reaction wheel has proved successful in the control of the bike, even though the system could not handle major disturbances. However, a student budget can only take a team so far in a research-based project. Perhaps with a bigger and more flexible budget, the inaccuracies and constraints would decrease and make way for turning the system into a promising controller that would be embedded into inverted pendulums that humans use and rely on every single day.

7.2 The Future Work

The first and foremost scheme that must be considered in the near future is testing the controller on systems different from the Gyrobike. For instance, satellites in space face smaller forces in magnitude than a bike would on Earth, meaning that a controller with a less powerful motor might not be an issue in such an environment. As for the Gyrobike itself, the simple steps taken to minimize the constraints and shortcomings discussed in chapter 6 would improve the

system drastically. Simply embedding a more powerful motor in the system, adjusting the bike's center of gravity, and following a more reasonable linearization method would take the system forward to maybe one day becoming a product that consumers use on a daily basis.

REFERENCES

1. Embedded Artistry LLC. (2019, October 8). *Inertial Measurement Unit*. Embedded Artistry. https://embeddedartistry.com/fieldmanual-terms/inertial-measurement-unit/
2. Wikipedia contributors. (2021a, April 16). *Polylactic acid*. Wikipedia. https://en.wikipedia.org/wiki/Polylactic_acid
3. Wikipedia contributors. (2021a, April 16). *Polylactic acid*. Wikipedia. https://en.wikipedia.org/wiki/Polylactic_acid
4. *PID Controller: Types, What It Is & How It Works | Omega*. (n.d.). PID CONTROLLER. https://www.omega.co.uk/prodinfo/pid-controllers.html#:%7E:text=A%20PID%20controller%20is%20an,most%20accurate%20and%20stable%20controller.
5. Chen, M. L. (2012, June 1). *Analysis and Design of Robust Feedback Control Systems for a Nonlinear Two-Wheel Inverted Pendulum System - IEEE Conference Publication*. IEEE. https://ieeexplore.ieee.org/document/6228229
6. Murata, M., Moran, M., & Hayase, H. (1995, August). *Control of Inverted Pendulum - Wheeled Cart Systems Using Nonlinear Observers.* Research Gate. https://www.researchgate.net/publication/3664959_Control_of_inverted_pendulum-wheeled_cart_systems_using_nonlinear_observers
7. Huang, R. I., Wang, J., & Tao, Y. (2014). *Dynamic Surface Control of Mobile Wheeled Inverted Pendulum Systems with Nonlinear Disturbance Observer*. IFAC. https://www.sciencedirect.com/science/article/pii/S1474667016423086
8. Cazzolato, B. and Prime, Z., (2011). *On the Dynamics of the Furuta Pendulum*. Journal of Control Science and Engineering.

https://www.researchgate.net/publication/228421122_On_the_Dynamics_of_the_Furuta_Pendulum

9. Wikipedia contributors. (2021a, April 2). *Furuta pendulum*. Wikipedia. https://en.wikipedia.org/wiki/Furuta_pendulum#cite_note-1
10. Arduino Project Hub. 2020. Arduino Bluetooth Basic Tutorial. [online] Available at: <https://create.arduino.cc/projecthub/mayooghgirish/arduino-bluetooth-basic-tutorial-d8b737>.
11. Enev, F., (2014). F*eedback Linearization Control of the Inertia Wheel Pendulum. Cybernetics and Information Technologies*. https://www.researchgate.net/publication/285276762_Feedback_Linearization_Control_of_the_Inertia_Wheel_Pendulum
12. Mathworks.com. (2020). *MATLAB Based PID Controller. [online]* Available at: <https://www.mathworks.com/matlabcentral/fileexchange/35163-matlab-based-pid-controller>.
13. Rainer, P. R. (1990, May). *Bicycle Drag Force Formulas*. SheldonBrown. https://www.sheldonbrown.com/rinard/aero/formulas.htmlPeople.ucalgary.ca. Available at: <https://people.ucalgary.ca/~aknigh/electrical_machines/fundamentals/f_dc_armature.html#:~:text=DC%20Armature,armature%20is%20the%20rotating%20circuit.>.
14. Wikipedia contributors. (2021a, April 16). *Polylactic acid*. Wikipedia. https://en.wikipedia.org/wiki/Polylactic_acid
15. Wikipedia contributors. (2021, April 17). *Medium-density fibreboard*. Wikipedia. https://en.wikipedia.org/wiki/Medium-density_fibreboard#cite_note-1

16. Boyer, E., (2020). *Lithium-Ion Safety Concerns – Battery University*. [online] Batteryuniversity.com. Available at: <https://batteryuniversity.com/learn/archive/lithium_ion_safety_concerns>.
17. Moreno-Valenzuela, J. and Aguilar-Avelar, C. (2017). *Motion Control Of Underactuated Mechanical Systems*. Cham: Springer International Publishing.
18. Awrejcewicz, J., (2014). *Applied Non-Linear Dynamical Systems*. Cham: Springer International Publishing.
19. Qu, Z., (2012). *Robust Control Of Nonlinear Uncertain Systems*. Weinheim: Wiley-VCH.
20. "Free CAD Designs, Files & 3D Models | The GrabCAD Community Library." Grabcad.Com, grabcad.com/library/wheels-cars-bikes-1. Accessed 3 June 2020.
21. ISO. (2014). *ISO 8856:2014*. [online] Available at: <https://www.iso.org/standard/61337.html>.
22. Knight, A., (2020). *Electrical Machines - DC Machine Armature*. [online] People.ucalgary.ca. Available at: <https://people.ucalgary.ca/~aknigh/electrical_machines/fundamentals/f_dc_armature.html#:~:text=DC%20Armature,armature%20is%20the%20rotating%20circuit.>.
23. Sae.org. (2002). *J1739: Potential Failure Mode And Effects Analysis In Design (Design FMEA) And Potential Failure Mode And Effects Analysis In Manufacturing And Assembly Processes (Process FMEA) And Effects Analysis For Machinery (Machinery FMEA) - SAE International*. [online] Available at: <https://www.sae.org/standards/content/j1739_200208/>.
24. Ullman, D., n.d (1991). *The Mechanical Design Process*. 4th ed. McGraw-Hill.

APPENDIX A: Electronic Media

All related electronic media, including the Gyrobike's poster, Bluetooth Arduino Code, MATLAB codes and simulations, design stages and the final design, etc, are all uploaded to the provided link along with this report. All rights are reserved concerning the media on the website. None of the codes or designs were obtained through any third parties and all the contents belong to their respective owners in the team.

Link:

https://drive.google.com/drive/folders/1lXTFORdJNkEJ96mMHep0K0WU9FsGLbz?usp=sharing

APPENDIX B: Constraints

Table 6: Project Constraints

Constraints	Yes	No
Economical	X	
Environmental	X	
Availability	X	
Manufacturability	X	
Reliability		X
Ethical	X	
Health & Safety		X
Efficiency	X	

APPENDIX C: Standards

Table 7: Engineering Standards - Product

Standards	**Definition**
ISO 11992	Electrical Connectors and Electrical Towing Connections
IEC 61851-21 Ed. 1.0 b:2001	Electric vehicle conductive charging system connection to an a.c./d.c. supply
ISO 13064-2:2012	Battery-electric mopeds and motorcycles
ISO 21940-31:2013	Mechanical Vibration - Rotor Balancing
SAE J 2561:2016-11-08	Bluetooth TM Wireless Protocol for Automotive Applications
ISO 2953:1985	Balancing Machines - Description and Evaluation
ISO 17409	Electrical Propelled road vehicles – Connection to an external electric power supply – Safety requirements
ISO/TS 16949	Automotive Quality Management
DIN ISO 6727:2013-12	Road vehicles - Motorcycles - Symbols for controls

ISO 885:2000	General purpose bolts and screws — Metric series — Radii under the head
DIN 75303:2019-06	Rear Load Carrier for Wheeled Vehicle

Table 8: Engineering Standards - Manufacturing

Standards	Definition
SAE J 1739:2009-01-15	Potential Failure Mode and Effects Analysis in Design (Design FMEA), Potential Failure Mode and Effects Analysis in Manufacturing and Assembly Processes (Process FMEA)
ISO/IEC CD 23510	Information Technology - 3D Printing and Scanning - Framework for Additive Manufacturing Service Platform (AMSP)
ISO 14001:2015	Environmental management systems
ISO 45001:2018	Occupational Health and Safety Management Systems

Table 9: Engineering Standards - Testing

Standards	Definition
ISO 8856:2014	Road vehicles - Electrical performance of starter motors - Test methods and general requirements
ISO 11452-1:2015	Road vehicles - Component Test Methods for Electrical Disturbances from Narrowband Radiated Electromagnetic Energy
IEEE 1561-2019	Guide for Optimizing the Performance and Life of Lead-Acid Batteries in Remote Hybrid Power Systems
DIN ISO 6727:2013-12	Rear load carrier for wheeled vehicle and its trailer

APPENDIX D: Logbook

Team Meeting Minutes

Design Organization:	**Date: 3/3/2021**

Agenda:

1. General discussion about project.
2. General overview of
3. Sharing opinions about distributing project parts to members.
4. Distributing parts of project.

Discussion: Chapters of report has been distributed between team members to start research immediately.

Decisions Made:

Ahmad and Mahmoud will work on chapter 1. (Literature Review)

Rayan and Mohammad will work on chapter 3. (Mechanical Design)

Hamza Katout and Mahmoud Zamel will work on chapter 2. (RC)

Mohammad Said and Ahmad Hammouda will work on chapter 4. (The Control System)

Action Items	Person Responsible	Deadline
First draft of Literature Review	Ahmad and Mahmoud	10/3/2021
Research about RC applications and functions	Hamza and Mahmoud	10/3/2021
Research about the general structured design of Gyrobike	Rayan and Mohammad	10/3/2021
Research about the mechanism of control system	Mohammad and Ahmad	10/3/2021
Team member: Ahmed Hammouda	Date for next meeting: 10/3/2021	
Team member: Hamza Katout		
Team member: Mohammad Said		
Team member: Mahmoud Zamel		
Team member: Rayan Darwiche		

The Mechanical Design Process Designed by Professor David G. Ullman

 Form # 3.0

Team Meeting Minutes

Design Organization:	**Date: 10/3/2020**

Agenda:

5. Literature review
6. General mechanism
7. General structured mechanism design
8. Ordering the requirements parts.

Discussion: applications, functions, mechanism, general structure, control systems and functional requirements has been discussed.

Decisions Made: Important information about has been noted and shared among the members of team and each member should do research on the part that is going to work on for designing the.

Action Items	Person Responsible	Deadline
First draft of Literature Review	Ahmad and Mahmoud	17/3/2021
Research about RC applications and functions	Hamza and Mahmoud	17/3/2021
Research about the general structured design of Gyrobike	Rayan and Mohammad	17/3/2021
Research about the mechanism of control system	Mohammad and Ahmad	17/3/2021

Team member: Ahmed Hammouda	Date for next meeting: 17/3/2021
Team member: Hamza Katout	
Team member: Mohammad Said	
Team member: Mahmoud Zamel	
Team member: Rayan Darwiche	

Team Meeting Minutes

Design Organization:	**Date:** 17/3/2021

Agenda:

9. Mechanism of power transfer
10. Modify the mechanical design of Gyrobike.
11. Design the first part of control system.
12. Design the first part of RC system.

Discussion:

Start dealing with the control system equations.

The required components and material of the mechanism have been studied.

Decisions Made:

The necessary dimensions and design to deal with and selecting the required parts of RC.

Action Items	Person Responsible	Deadline
Do research about Pendulum.	Ahmad	24/3/2021
Continue with mechanism design	Rayan and Mohammad	24/3/2021
Research about the control system equations	Mohammad	24/3/2021
Continue with RC system calculations and design	Hamza and Mahmoud	24/3/2021
Team member: Ahmed Hammouda	Date for next meeting: 24/3/2021	
Team member: Hamza Katout		
Team member: Mohammad Said		
Team member: Mahmoud Zamel		
Team member: Rayan Darwiche		

Team Meeting Minutes

Design Organization:	**Date:** 24/3/2021

Agenda:

13. Finalize the mechanism of power transfer
14. Finalize the mechanical design
15. Design the second part of RC system.

Discussion:

The required product for designing the mechanism has been studied and figured out.
Approximately half of the mechanism design and RC system has been done.

Decisions Made:

Add some more parts to the design of mechanism.
Start researching about the required standards.

Action Items	Person Responsible	Deadline
Do research for standards	Mohammad and Mahmoud	7/4/2021
Start chapter 1 of the report	Ahmad	7/4/2021
Continue with RC system calculations and design	Hamza and Mahmoud	7/4/2021
Team member: Ahmed Hammouda	Date for next meeting: 7/4/2021	
Team member: Hamza Katout		
Team member: Mohammad Said		
Team member: Mahmoud Zamel		
Team member: Rayan Darwiche		

Team Meeting Minutes

Design Organization:	**Date:** 7/4/2021

Agenda:

16. Finalize chapter 1 and 2 of the report.
17. Design the second part of control system.
18. Preparing the Gantt chart

Discussion:

Gantt chart has been prepared.

Chassis has been discussed.

Starting the manufacturing.

Decisions Made:

Design of control system.

Design the chassis.

Action Items	Person Responsible	Deadline
Decide the material	Rayan and Mohammad	14/4/2021
Continue with the chapter 4	Ahmad	14/4/2021
Gantt chart	Mohammad	14/4/2021
Manufacturing	Mohammad	14/4/2021
Continue with the chapter 2	Mahmoud	14/4/2021

Team member: Ahmed Hammouda	Date for next meeting: 14/4/2021
Team member: Hamza Katout	
Team member: Mohammad Said	
Team member: Mahmoud Zamel	
Team member: Rayan Darwiche	

Team Meeting Minutes

Design Organization:	**Date:** 14/4/2021

Agenda:

19. Design the chassis

Discussion:

The mechanism has been placed in the chassis.

Decisions Made: Start working on differential and chain.

Action Items	Person Responsible	Deadline
Chain, steering system and manufacturing	Mohammad	21/4/2021
Derivation of Governing Equations	Ahmad	21/4/2021
Do calculations of drag and strength	Rayan	21/4/2021
Team member: Ahmed Hammouda	Date for next meeting: 21/4/2021	
Team member: Hamza Katout		
Team member: Mohammad Said		
Team member: Mahmoud Zamel		
Team member: Rayan Darwiche		

Team Meeting Minutes

Design Organization:	**Date:** 21/4/2021

Agenda:

20. Research about steering system.
21. Research about balancing system.
22. Research about the required balancing system's components.
23. Calculate strength and drag measurements.

Discussion:

Type of steering system has been discussed and the relation of it to the mechanism.

Decisions Made: Pick the right component for balancing system according to mechanism design.

Action Items	Person Responsible	Deadline
Finalize manufacturing parts	Mohammad	28/4/2021
Derivation of Governing Equations	Ahmad	28/4/2021
Finalize strength calculations	Rayan	28/4/2021
Team member: Ahmed Hammouda	Date for next meeting: 28/4/2021	
Team member: Hamza Katout		
Team member: Mohammad Said		
Team member: Mahmoud Zamel		
Team member: Rayan Darwiche		

Team Meeting Minutes

Design Organization:	**Date:** 28/4/2021

Agenda:

24. Report.
25. Finalize design of differential
26. Finalize manufacturing parts.
27. Finalize steering system.
28. Finalize mechanism system.
29. Finalize strength calculations.

Discussion:

Final design after manufacturing, differential, steering and mechanism is done and added to the report.

Decisions Made:

Start assembling the DC and stepper motors, gears of balancing wheel, chains, battery.

Action Items	Person Responsible	Deadline
Assembling and electric connections	Mohammad	5/5/2021
Continue the control programming	Ahmad	5/5/2021
Team member: Ahmed Hammouda	Date for next meeting: 5/5/2021	
Team member: Hamza Katout		
Team member: Mohammad Said		
Team member: Mahmoud Zamel		
Team member: Rayan Darwiche		

Team Meeting Minutes

Design Organization:	**Date:** 5/5/2021

Agenda:

30. Finalize the mechanism system.
31. Finalize gears of balancing wheel.
32. Finalize the batteries and electric motors.

Discussion:

Mechanism system has been finished. Balancing wheel and batteries and electric motors have been added to the mechanism.

Decisions Made:

Mechanism system has been finalized and steering system and gear set will be finalized for the next meeting.

Finalize assembly design.

Action Items	Person Responsible	Deadline
Continue with balancing system	Ahmad	12/5/2021
Steering system	Mohammad and Rayan	12/5/2021
Continue with the report and RC system	Hamza and Mahmoud	12/5/2021

Team member: Ahmed Hammouda	Date for next meeting: 12/5/2021
Team member: Hamza Katout	
Team member: Mohammad Said	
Team member: Mahmoud Zamel	
Team member: Rayan Darwiche	

Team Meeting Minutes

Design Organization:	**Date:** 12/5/2020

Agenda:

33. Finalize the steering system and power system.
34. Finalize the control system.

Discussion:

Power system and steering system has been placed.

Decisions Made:

Start working on report, standards and components.

Action Items	Person Responsible	Deadline
Research about required standards.	Mohammad	19/5/2021
Continue with report	Rayan	19/5/2021
Modify the control system	Ahmad	19/5/2021
Continue with report	Hamza	19/5/2021
Continue with report	Mahmoud	19/5/2021

Team member: Ahmed Hammouda	Date for next meeting: 19/5/2021
Team member: Hamza Katout	
Team member: Mohammad Said	
Team member: Mahmoud Zamel	
Team member: Rayan Darwiche	

Team Meeting Minutes

Design Organization:	**Date:** 19/5/2021

Agenda:

35. Modify mechanism system.
36. Finalize the chassis of Gyrobike.

Discussion:

Working on report.

Start testing.

Decisions Made:

Continue with report

Find the required standards and components.

Action Items	Person Responsible	Deadline
Research about standards	Rayan	23/5/2021
Start testing	Ahmad and Mohammad	23/5/2021
Continue with report	Hamza and Mahmoud	23/5/2021
Team member: Ahmed Hammouda	Date for next meeting: 23/5/2021	
Team member: Hamza Katout		
Team member: Mohammad Said		
Team member: Mahmoud Zamel		
Team member: Rayan Darwiche		

Team Meeting Minutes

Design Organization:	**Date:** 23/5/2021

Agenda:

37. Modify the whole design.
38. Finalize the calculations and engineering standards.

Discussion:

Working on the final calculations.

Working on report.

Decisions Made:

Continue with report.

Continue with testing.

Action Items	Person Responsible	Deadline
Continue with testing	Mohammad and Ahmad	26/5/2021
Design the presentation template	Rayan	26/5/2021
Continue with report (chapter 6)	Hamza	26/5/2021
Continue with report (chapter 7)	Mahmoud	26/5/2021

Team member: Ahmed Hammouda	Date for next meeting: 26/5/2021
Team member: Hamza Katout	
Team member: Mohammad Said	
Team member: Mahmoud Zamel	
Team member: Rayan Darwiche	

Team Meeting Minutes

Design Organization:	**Date:** 26/5/2021

Agenda:

39. Testing and simulation.

Discussion:

Checking the efficiency of the project.

Working on report.

Decisions Made:

Continue with report and finalize it.

Action Items	Person Responsible	Deadline
Continue with report and presentation	Rayan	2/6/2021
Testing and simulation	Ahmad and Mohammad	2/6/2021
Continue with report (chapter 6)	Hamza	2/6/2021
Continue with report (chapter 7)	Mahmoud	2/6/2021

Team member: Ahmed Hammouda	Date for next meeting: 2/6/2021
Team member: Hamza Katout	
Team member: Mohammad Said	
Team member: Mahmoud Zamel	
Team member: Rayan Darwiche	

APPENDIX E: Timeline/Gantt Chart

APPENDIX F: Engineering Drawings

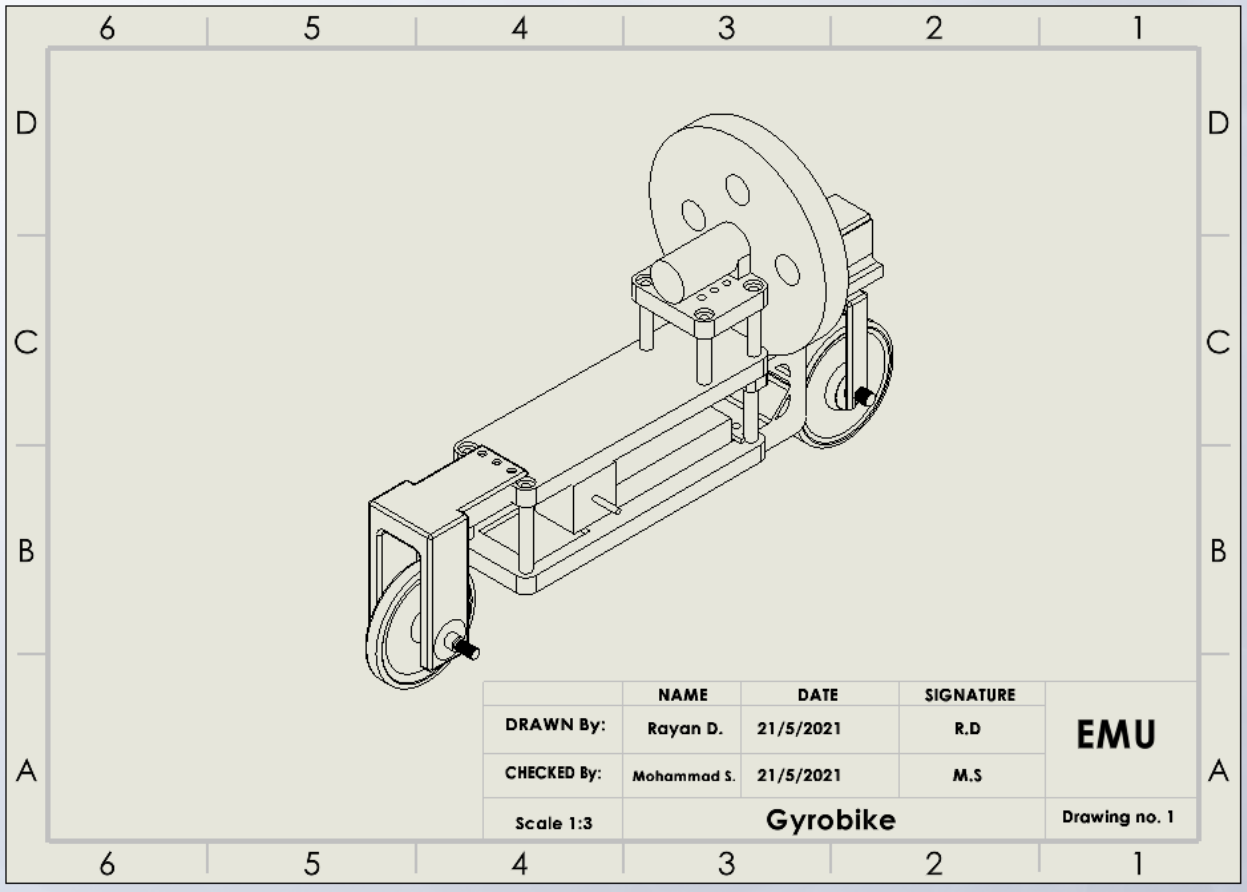

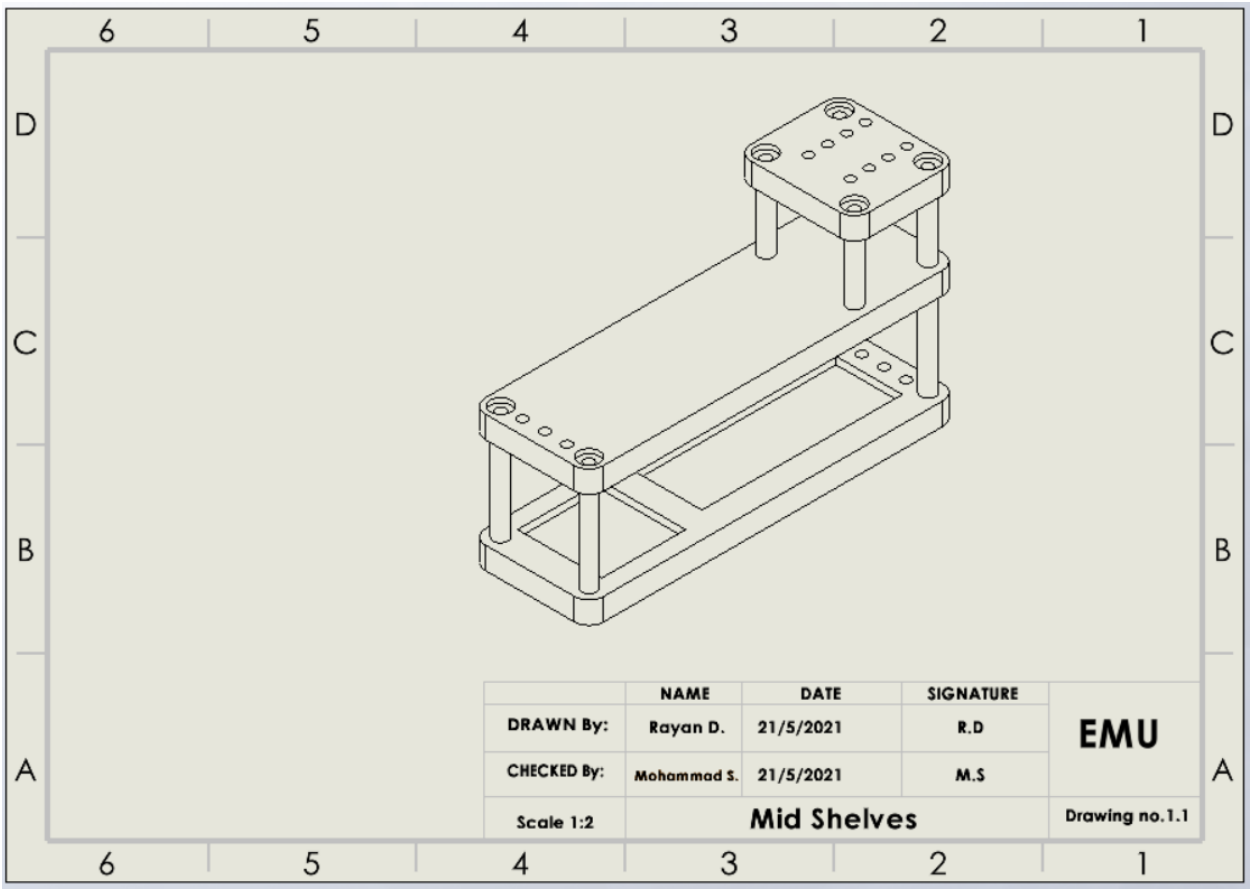
6
5
4
3
2
1
D
C
B
A
NAME
DATE
SIGNATURE
DRAWN By:
Rayan D.
21/5/2021
R.D
CHECKED By:
Mohammad S.
21/5/2021
M.S
EMU
Scale 1:2
Mid Shelves
Drawing no.1.1

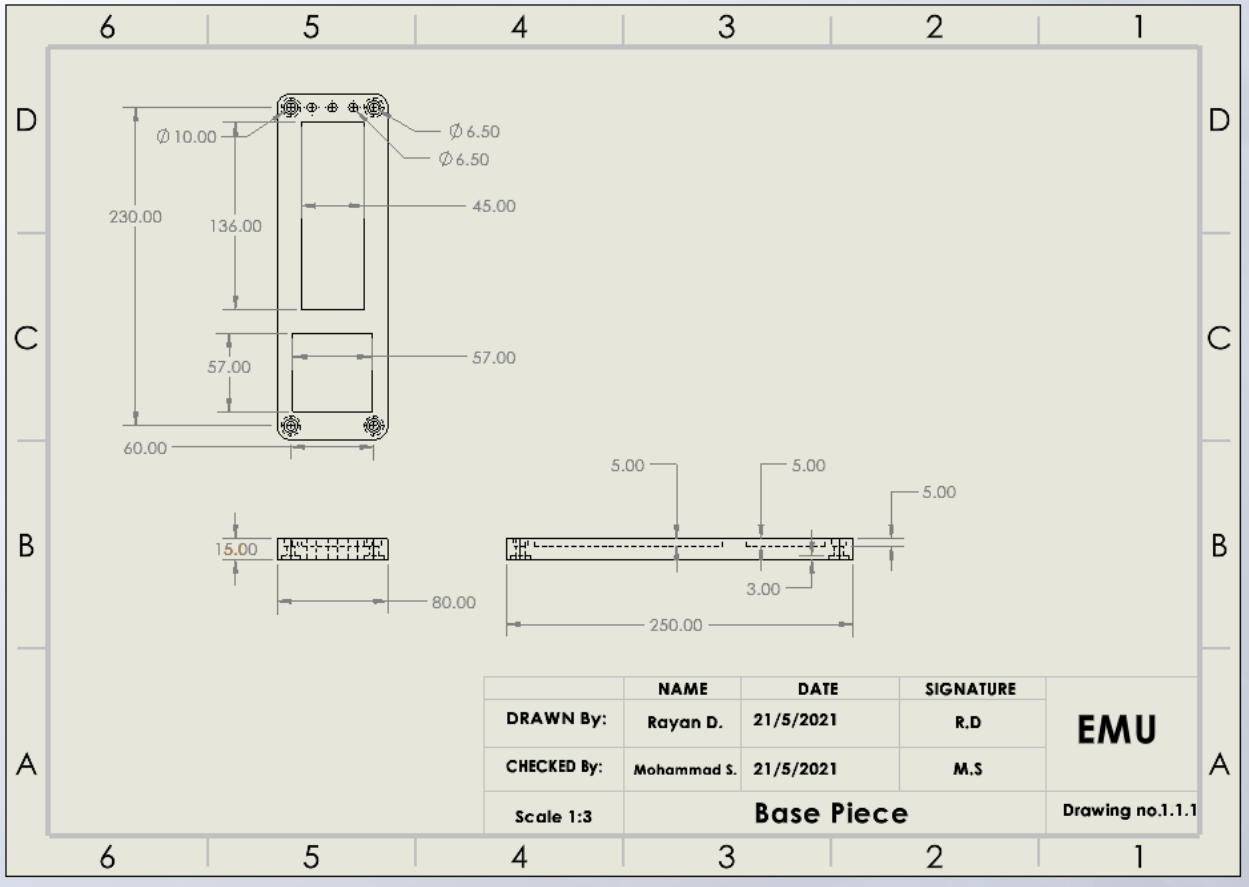
6
5
4
3
2
1
D
C
B
A
Ø 10.00
Ø 6.50
Ø 6.50
230.00
136.00
45.00
57.00
57.00
60.00
5.00
5.00
5.00
15.00
80.00
3.00
250.00
NAME
DATE
SIGNATURE
DRAWN By:
Rayan D.
21/5/2021
R.D
CHECKED By:
Mohammad S.
21/5/2021
M.S
EMU
Scale 1:3
Base Piece
Drawing no.1.1.1

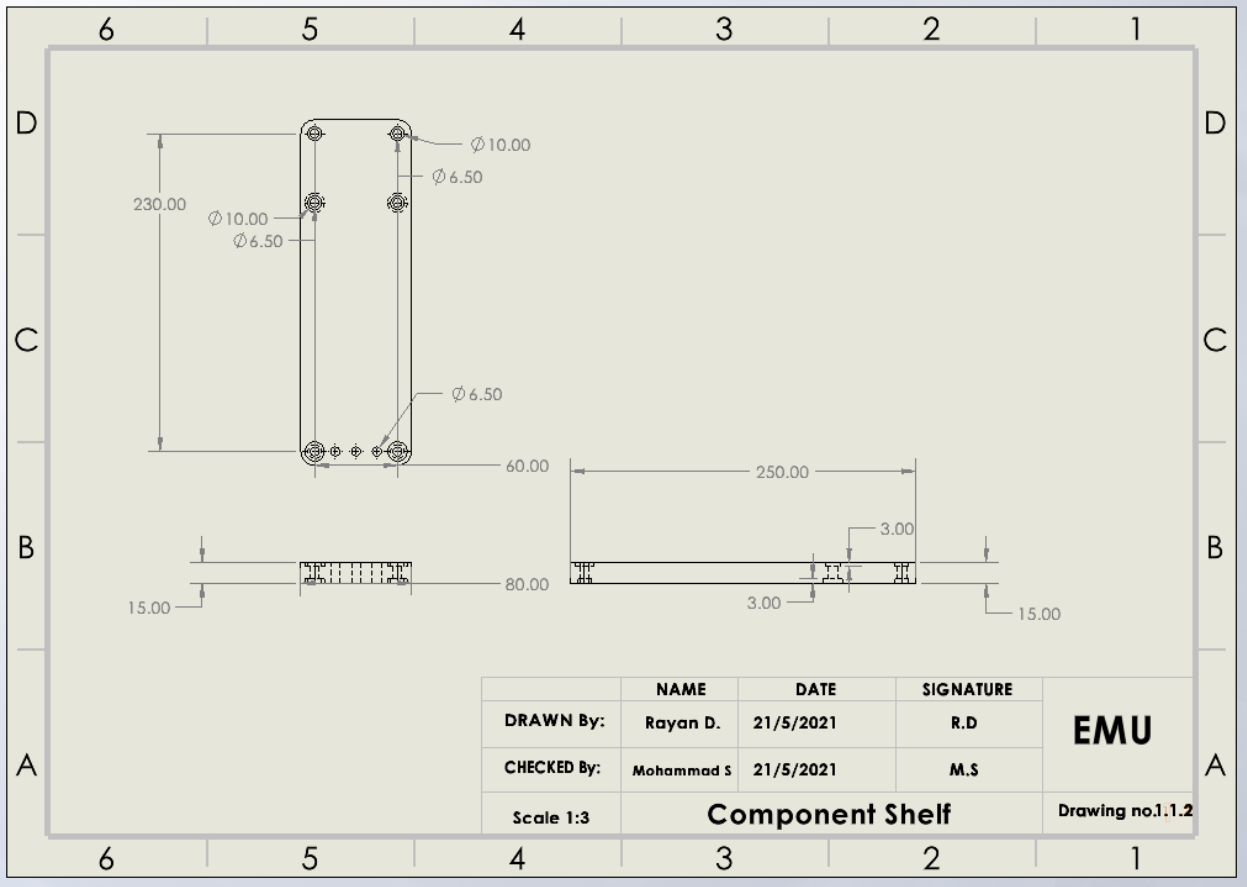
6
5
4
3
2
1
D
C
B
A
Ø10.00
Ø6.50
230.00
Ø10.00
Ø6.50
Ø6.50
60.00
250.00
3.00
80.00
15.00
3.00
15.00
NAME
DATE
SIGNATURE
DRAWN By:
Rayan D.
21/5/2021
R.D
CHECKED By:
Mohammad S
21/5/2021
M.S
EMU
Scale 1:3
Component Shelf
Drawing no.1.1.2

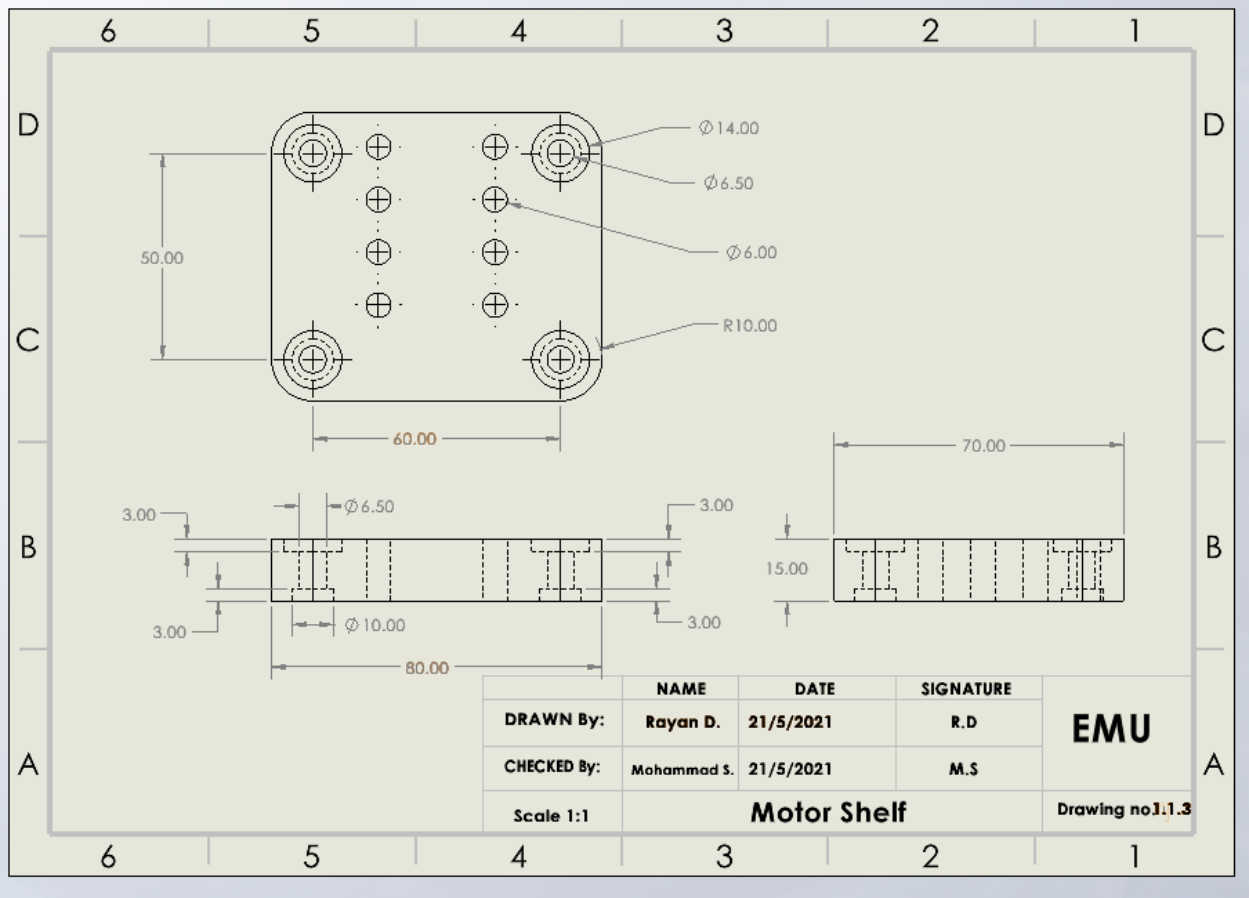
6
5
4
3
2
1
D
C
B
A
Ø14.00
Ø6.50
Ø6.00
R10.00
50.00
60.00
70.00
3.00
Ø6.50
3.00
15.00
3.00
Ø10.00
3.00
80.00
NAME
DATE
SIGNATURE
DRAWN By:
Rayan D.
21/5/2021
R.D
EMU
CHECKED By:
Mohammad S.
21/5/2021
M.S
Scale 1:1
Motor Shelf
Drawing no1.1.3

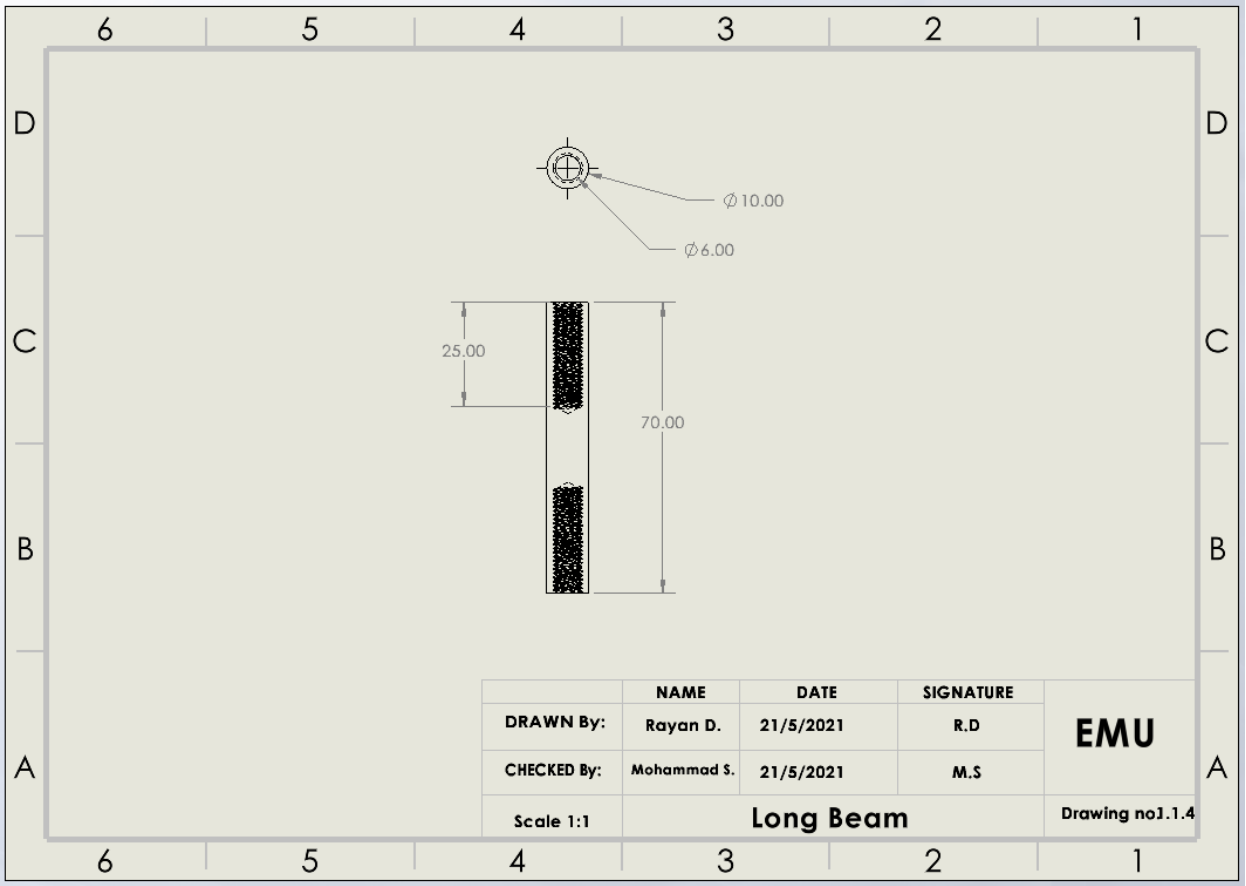
6
5
4
3
2
1
D
C
B
A
Ø10.00
Ø6.00
25.00
70.00
NAME
DATE
SIGNATURE
DRAWN By:
Rayan D.
21/5/2021
R.D
CHECKED By:
Mohammad S.
21/5/2021
M.S
EMU
Scale 1:1
Long Beam
Drawing no1.1.4

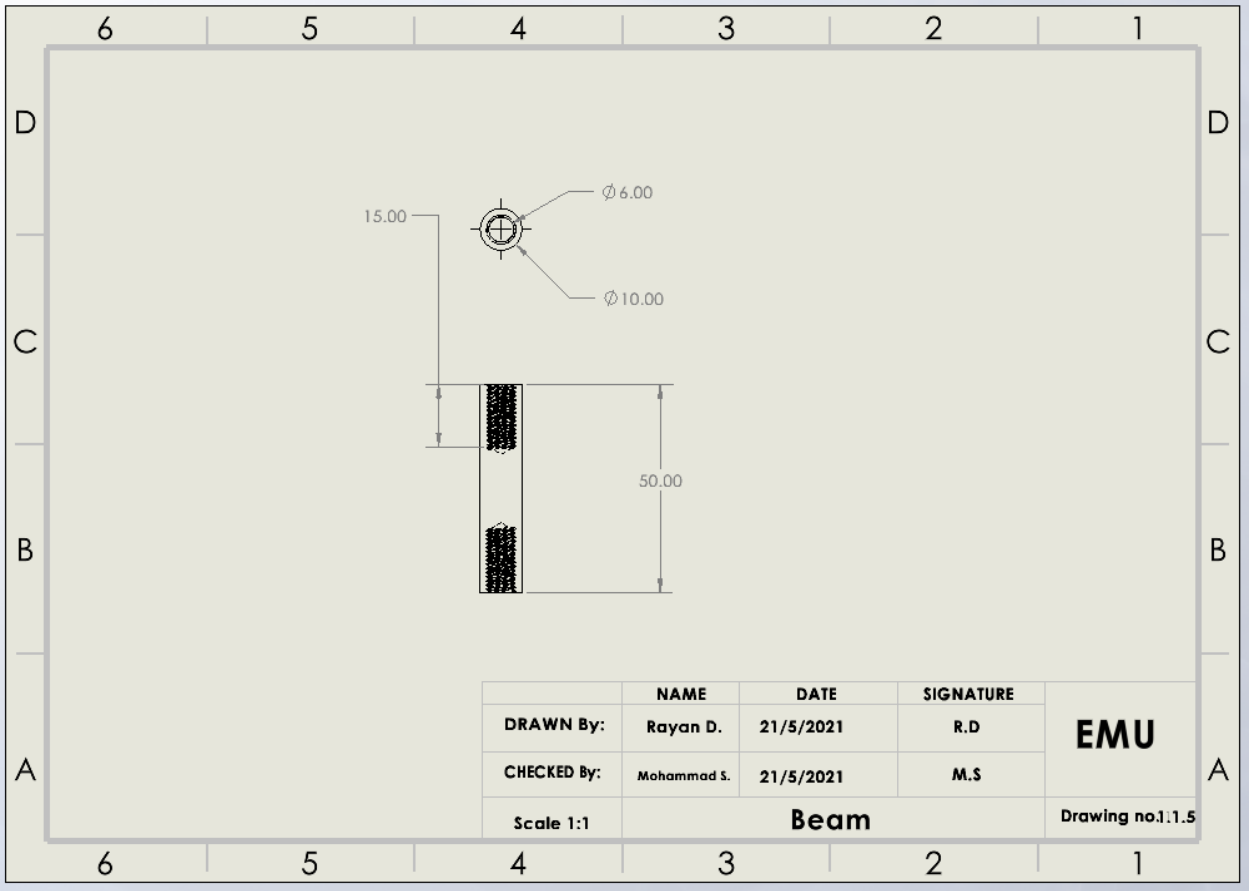
6
5
4
3
2
1
D
C
B
A
15.00
Ø6.00
Ø10.00
50.00
NAME
DATE
SIGNATURE
DRAWN By:
Rayan D.
21/5/2021
R.D
CHECKED By:
Mohammad S.
21/5/2021
M.S
EMU
Scale 1:1
Beam
Drawing no.1.1.5

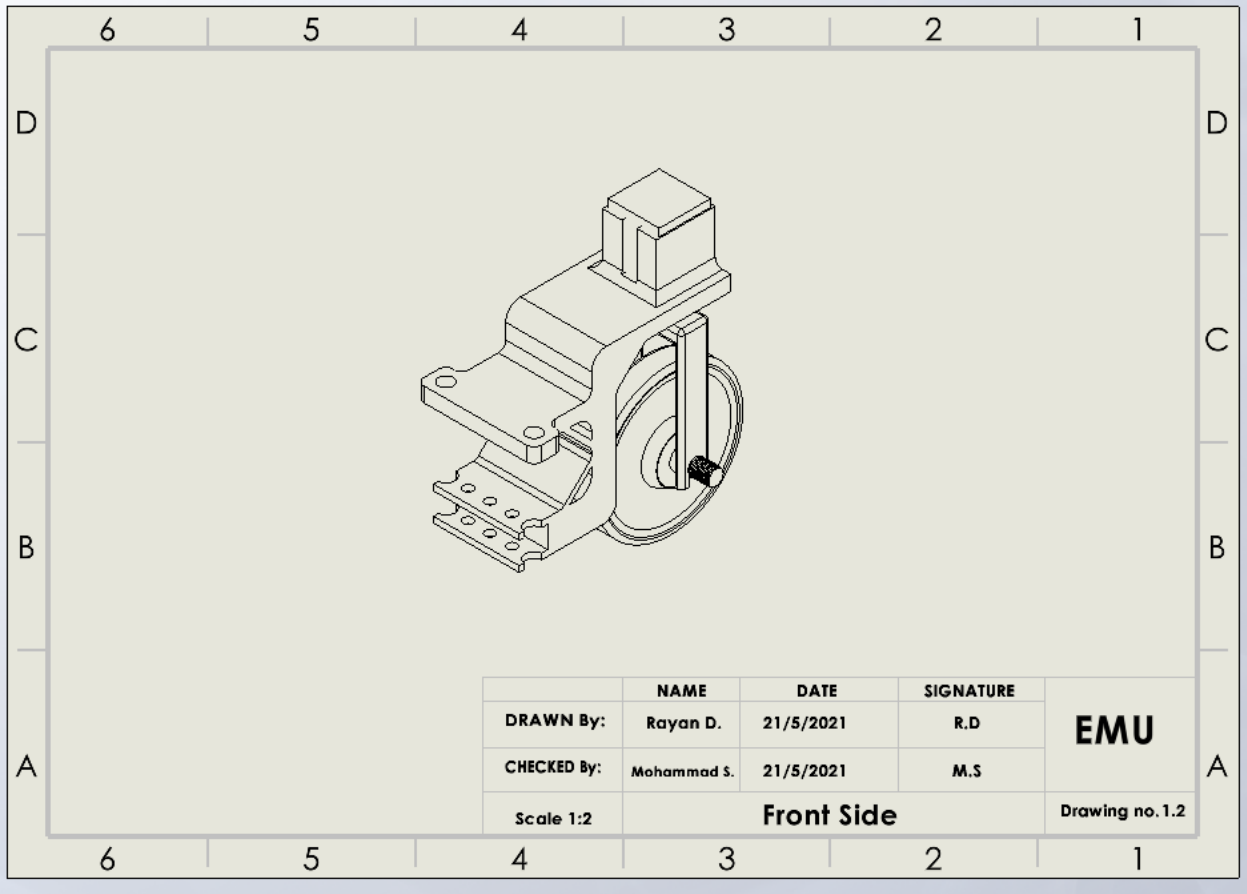
6
5
4
3
2
1
D
C
B
A
NAME
DATE
SIGNATURE
DRAWN By:
Rayan D.
21/5/2021
R.D
CHECKED By:
Mohammad S.
21/5/2021
M.S
EMU
Scale 1:2
Front Side
Drawing no. 1.2

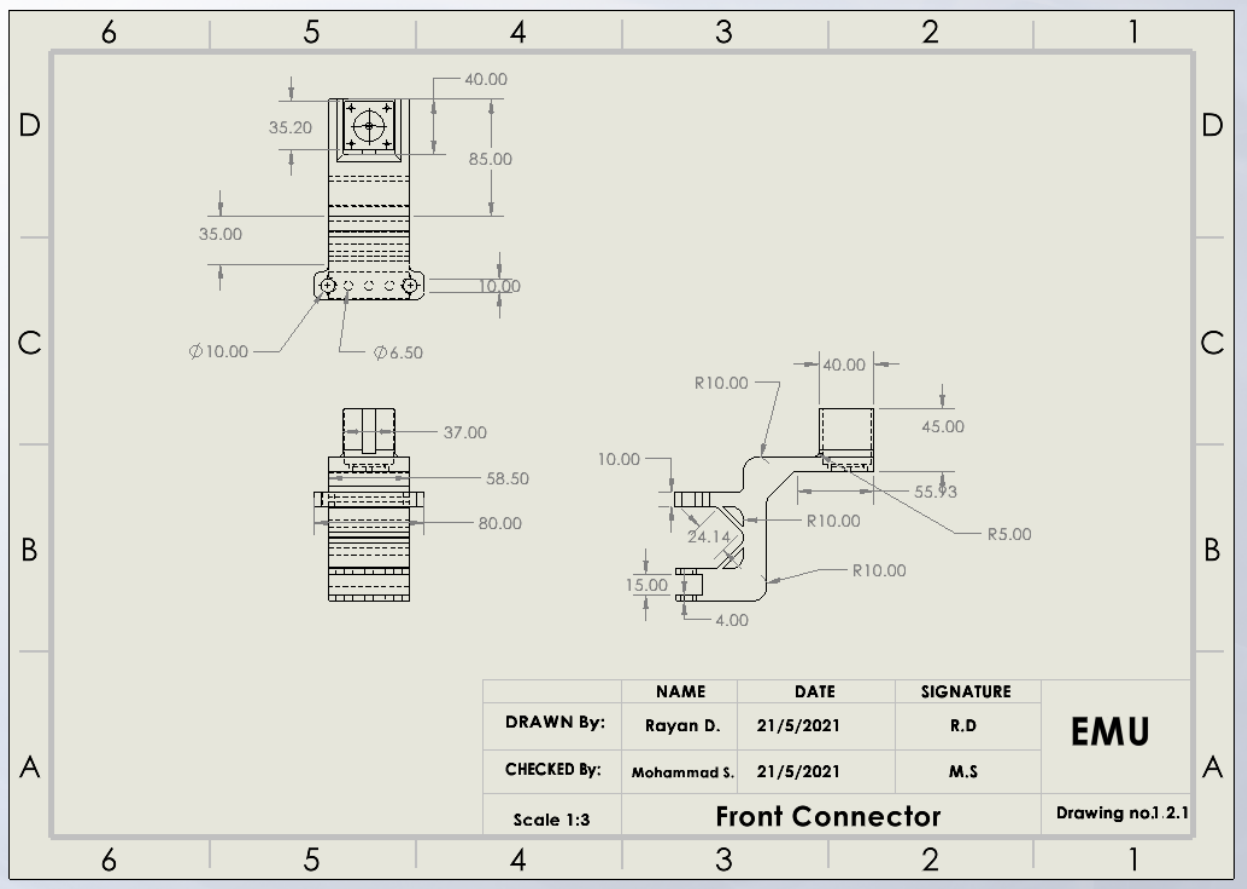
6
5
4
3
2
1
D
C
B
A
40.00
35.20
85.00
35.00
10.00
Ø10.00
Ø6.50
37.00
58.50
80.00
40.00
R10.00
45.00
10.00
55.93
R10.00
R5.00
24.14
R10.00
15.00
4.00
NAME
DATE
SIGNATURE
DRAWN By:
Rayan D.
21/5/2021
R.D
CHECKED By:
Mohammad S.
21/5/2021
M.S
EMU
Scale 1:3
Front Connector
Drawing no.1.2.1

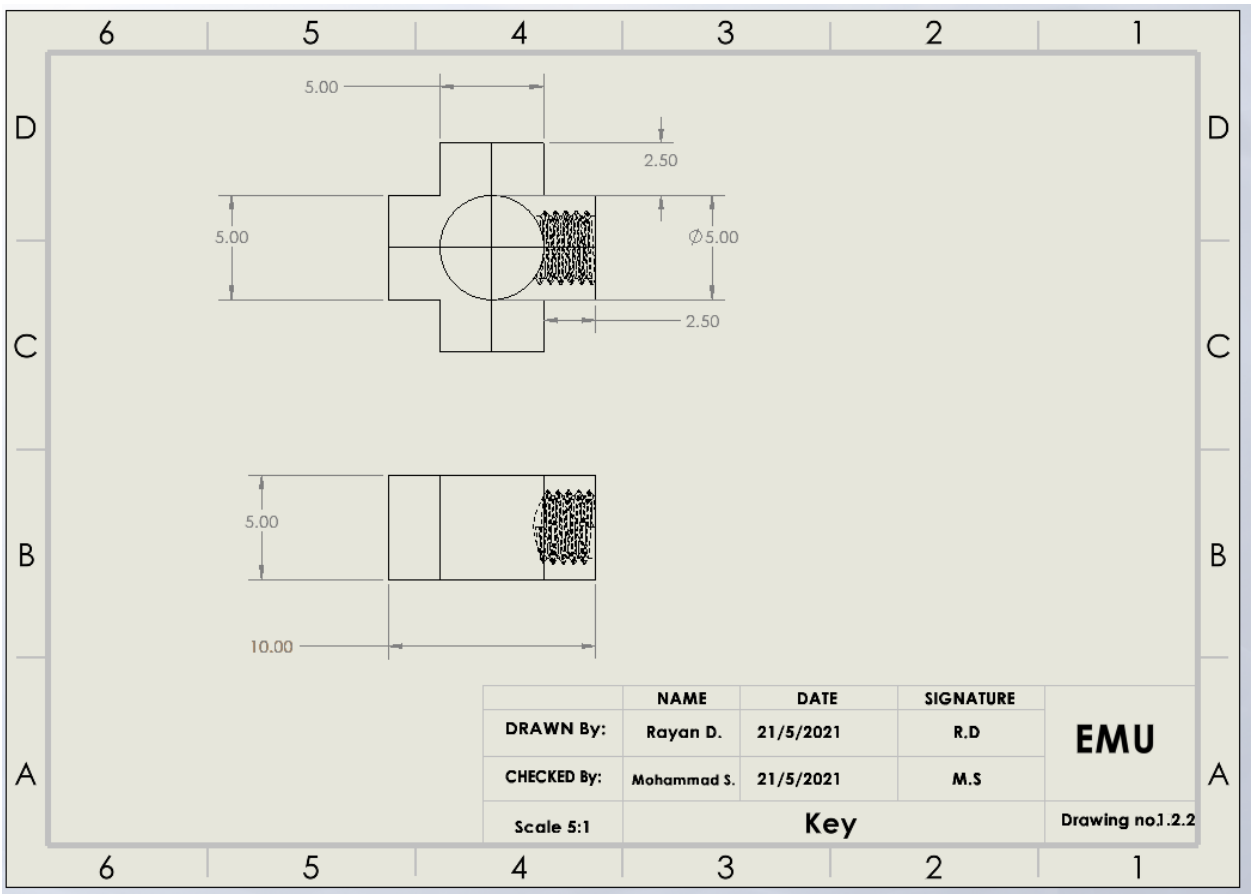
6
5
4
3
2
1
D
C
B
A
5.00
2.50
5.00
∅5.00
2.50
5.00
10.00
NAME
DATE
SIGNATURE
DRAWN By:
Rayan D.
21/5/2021
R.D
CHECKED By:
Mohammad S.
21/5/2021
M.S
Scale 5:1
Key
EMU
Drawing no.1.2.2

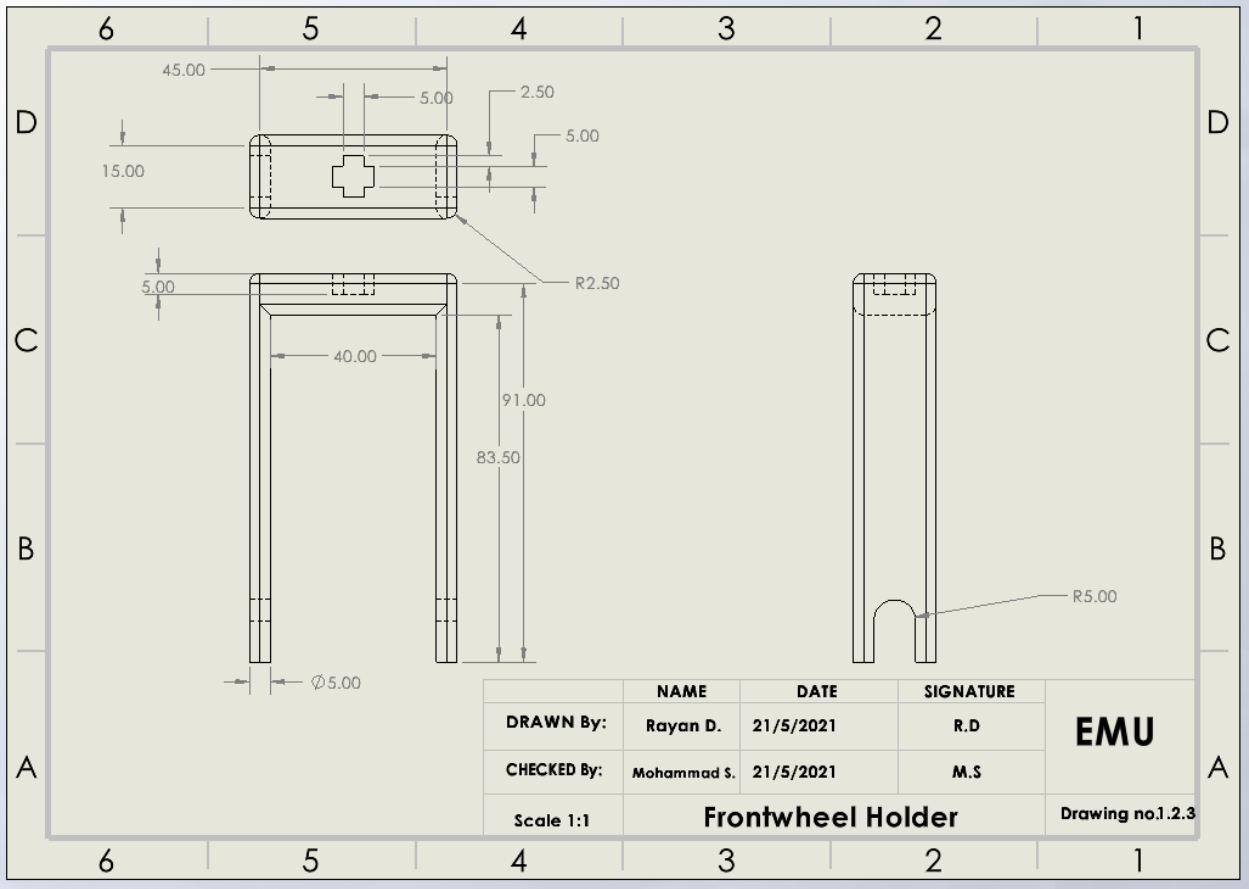
45.00
5.00
2.50
5.00
15.00
R2.50
5.00
40.00
91.00
83.50
Ø5.00
R5.00
NAME
DATE
SIGNATURE
DRAWN By:
Rayan D.
21/5/2021
R.D
CHECKED By:
Mohammad S.
21/5/2021
M.S
EMU
Scale 1:1
Frontwheel Holder
Drawing no.1.2.3

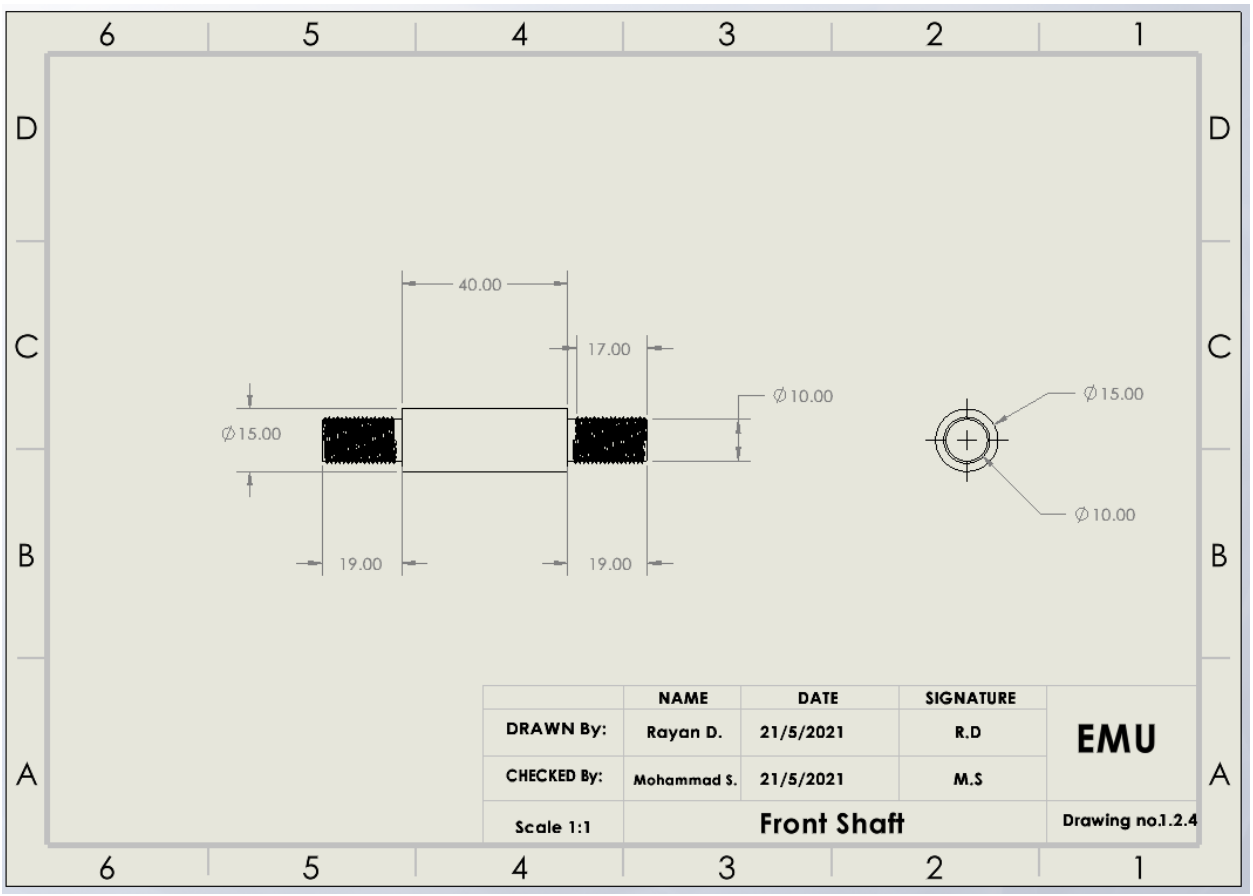
6
5
4
3
2
1
D
C
B
A
40.00
17.00
Ø10.00
Ø15.00
19.00
19.00
Ø15.00
Ø10.00
NAME
DATE
SIGNATURE
DRAWN By:
Rayan D.
21/5/2021
R.D
CHECKED By:
Mohammad S.
21/5/2021
M.S
EMU
Scale 1:1
Front Shaft
Drawing no.1.2.4

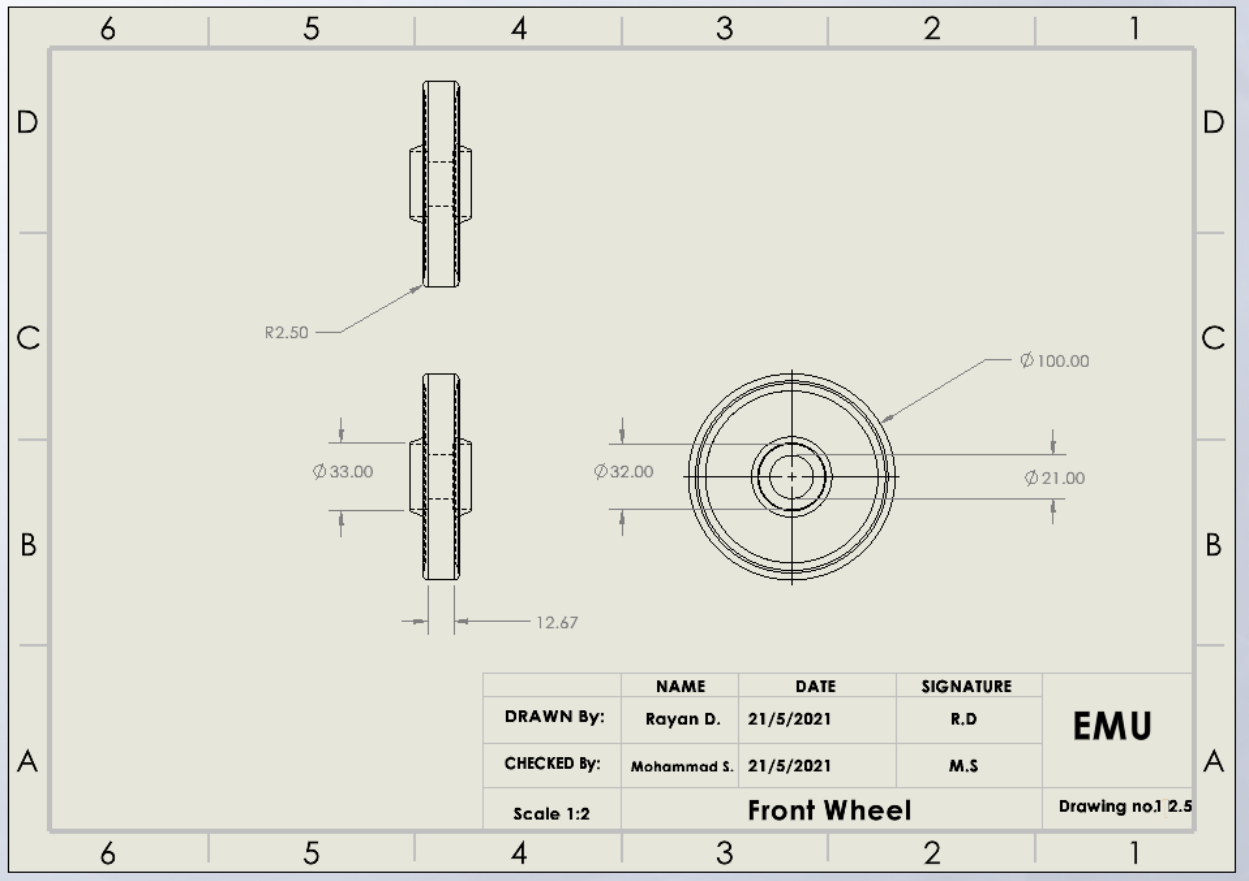
R2.50
Ø33.00
12.67
Ø100.00
Ø32.00
Ø21.00
NAME
DATE
SIGNATURE
DRAWN By:
Rayan D.
21/5/2021
R.D
CHECKED By:
Mohammad S.
21/5/2021
M.S
EMU
Scale 1:2
Front Wheel
Drawing no.1 2.5

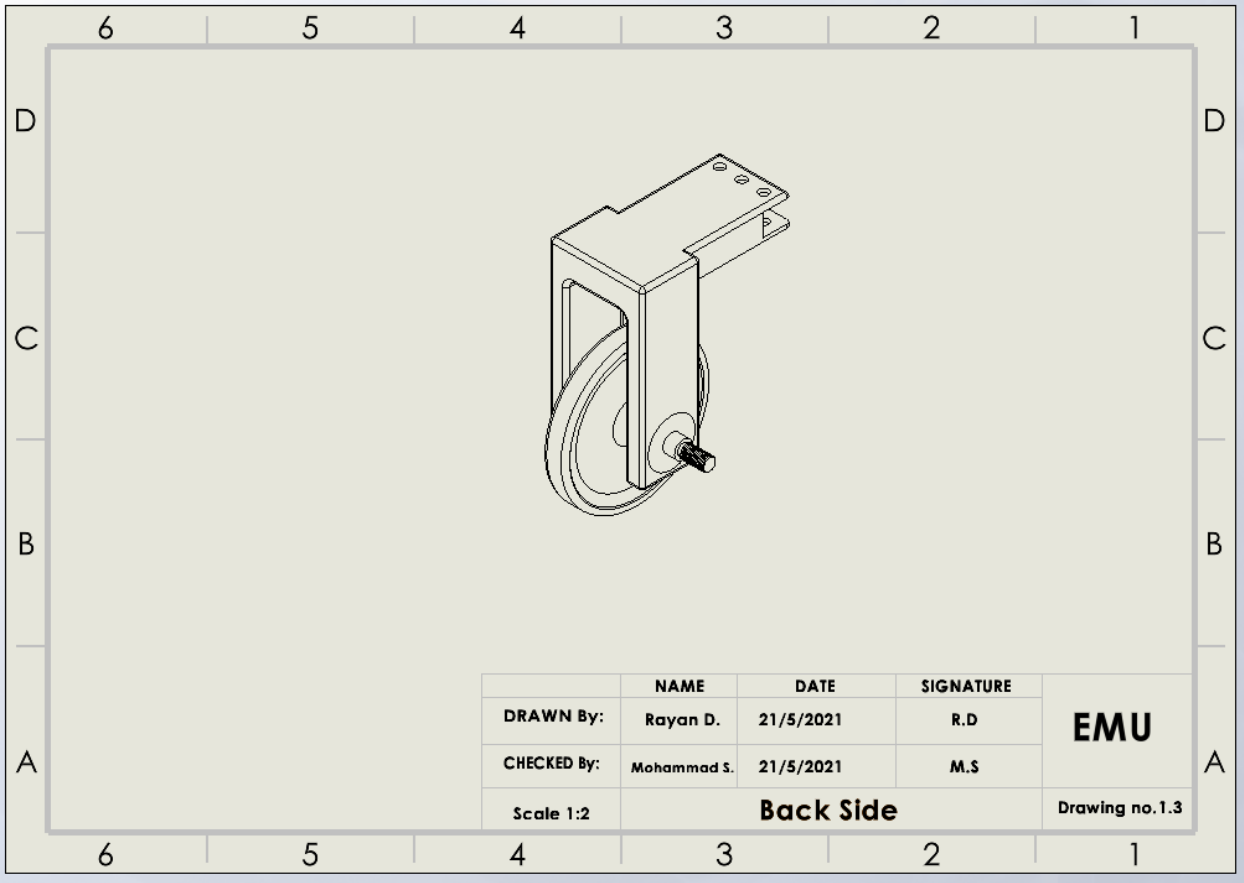
6
5
4
3
2
1
D
C
B
A
NAME
DATE
SIGNATURE
DRAWN By:
Rayan D.
21/5/2021
R.D
CHECKED By:
Mohammad S.
21/5/2021
M.S
EMU
Scale 1:2
Back Side
Drawing no.1.3

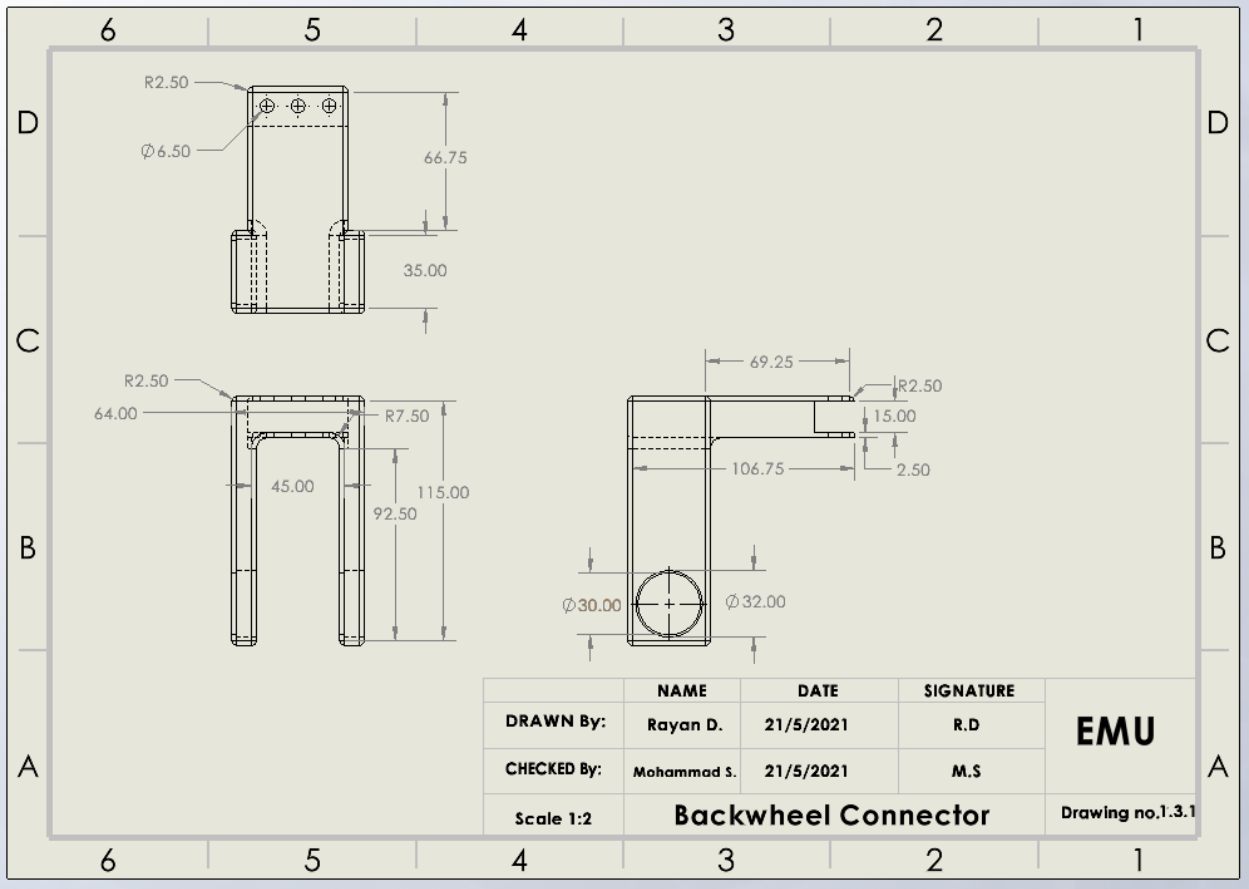
R2.50
Ø6.50
66.75
35.00
R2.50
64.00
R7.50
45.00
115.00
92.50
69.25
R2.50
15.00
106.75
2.50
Ø30.00
Ø32.00
NAME
DATE
SIGNATURE
DRAWN By:
Rayan D.
21/5/2021
R.D
CHECKED By:
Mohammad S.
21/5/2021
M.S
EMU
Scale 1:2
Backwheel Connector
Drawing no.1.3.1

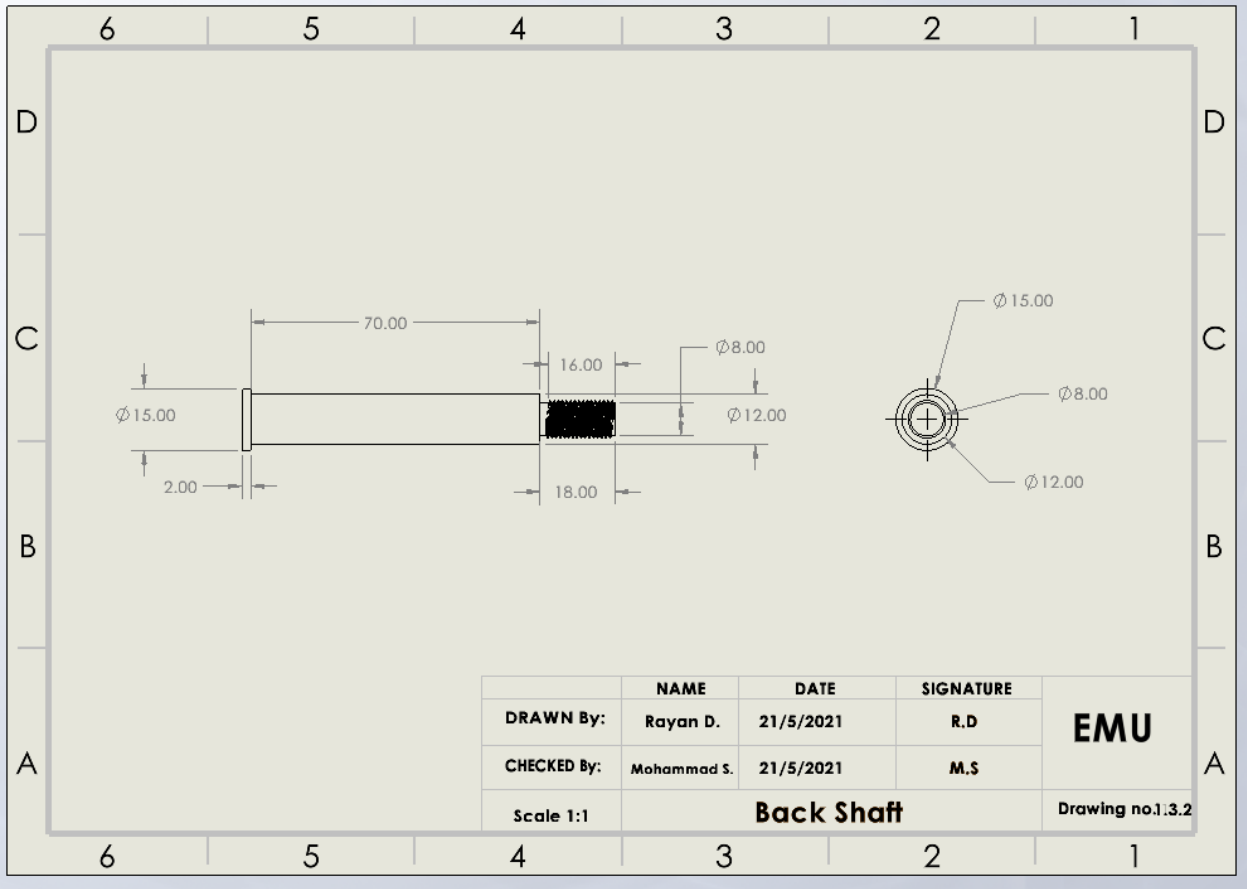
6
5
4
3
2
1
D
C
B
A
70.00
16.00
Ø8.00
Ø15.00
Ø12.00
2.00
18.00
Ø15.00
Ø8.00
Ø12.00
NAME
DATE
SIGNATURE
DRAWN By:
Rayan D.
21/5/2021
R.D
CHECKED By:
Mohammad S.
21/5/2021
M.S
EMU
Scale 1:1
Back Shaft
Drawing no.1.3.2

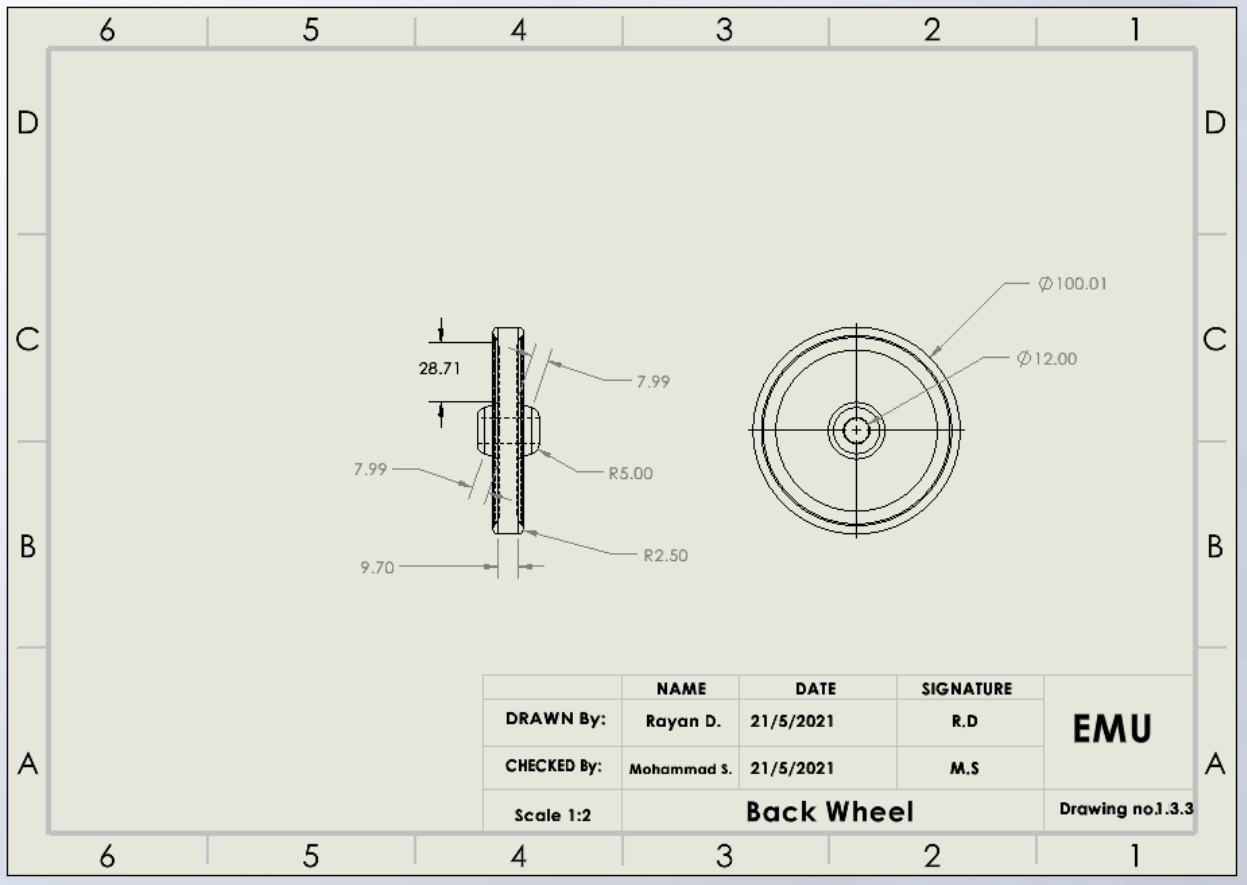
6
5
4
3
2
1
D
C
B
A
28.71
7.99
7.99
R5.00
9.70
R2.50
∅100.01
∅12.00
NAME
DATE
SIGNATURE
DRAWN By:
Rayan D.
21/5/2021
R.D
CHECKED By:
Mohammad S.
21/5/2021
M.S
EMU
Scale 1:2
Back Wheel
Drawing no.1.3.3

APPENDIX G: Structural Breakdown